SOUFIANE BOUCETTA

MODULATION OF INTRINSIC AND SYNAPTIC EXCITABILITY DURING SLEEP OSCILLATIONS AND ELECTROGRAPHIC SEIZURES

Mémoire présenté
à la Faculté des études supérieures de l'Université Laval
dans le cadre du programme de maîtrise en neurobiologie
pour l'obtention du grade de maître ès sciences (M.Sc.)

FACULTÉ DE MÉDECINE
UNIVERSITÉ LAVAL
QUÉBEC

AVRIL, 2005

Résumé

Le présente mémoire fournit des nouvelles évidences montrant la modulation de l'excitabilité neuronale intrinsèque et synaptique, et la conséquence de cette modulation sur l'activité neuronale durant à la fois, les oscillations lentes du sommeil, et les crises électrographiques *in vivo* chez des animaux anesthésiés. Nous effectuons des enregistrements intracellulaires simultanés de neurones corticaux et des potentiels de champs locaux au niveau du gyrus suprasylvien à l'intérieur du cortex associatif pariétal (aires : 5, 7 et 21). Nous suggérons que la fluctuation de la concentration extracellulaire du calcium durant les oscillations lentes du sommeil module à la fois, l'excitabilité intrinsèque et synaptique des neurones corticaux, ainsi par conséquent, elle module affecte la relation d'input-output de ces neurones.

L'apparition durant les oscillations lentes du sommeil, des crises de type Lennex-Gastaut qui sont générées corticalement, nous a permet d'étudier les propriétés spatio-temporelles des ondes paroxysmiques rapides associées avec ce type de crises. Nous suggérons que les ondes paroxysmiques rapides apparaissent comme des oscillations quasi-indépendantes même dans les localisations corticales voisines, suggérant leur origine focal.

Abstract

The present memoir provides new evidences showing the modulation of intrinsic and synaptic excitability of cortical neurons, and the consequence of this modulation on neuronal activity during both slow sleep oscillations and electrographic seizures in vivo in anaesthetized animals. We performed simultaneous recordings of cortical neurons with local field potentials in suprasylvian gyrus within parietal associative cortex (area 5, 7 and 21). We suggest that the fluctuation of extacellular calcium concentration during slow sleep oscillations, modulates both intrinsic and synaptic excitability cortical neurons, thus by consequence modulates the input-output relationship of these neurons.

The occurrence during slow-wave sleep of cortically generated Lennox-Gastaut type of seizures admits us to study the spatio-temporal properties of paroxysmal fast runs associated with this type of seizures. We suggest that fast runs appeared as quasi-independent oscillations even in neighbouring cortical locations suggesting their focal origin.

Foreword

The following memoir is presented in the form of two principal scientific articles. One of them is submitted for publication in Journal of Physiology and the other one is submitted to the Journal of Neurophysiology. The articles are precedes by a general introduction, which describes the theoretical context and experimental strategies of the studies described in the articles including one part of an article to which I contributed as coauthor and which is published in European Journal of Neuroscience titled: *Modulation of synaptic transmission in neocortex by network activities.* A general conclusion finalizes the memoir with the presentation of a communes concepts linked the results of these articles. The bibliography used for both introduction and conclusion, is presented at the very end of the memoir. Since the articles have been submitted to different scientifics journals, the format of bibliographical citations changes from one to another.

I would like to use this occasion to express my gratitude to my memoir supervisor Dr. Igor Timofeev for the opportunity of working in his laboratory. Without his critics, discussions, corrections and support the present study would not have been possible.

I also would like to thank my colleagues Sylvain Crochet, who in parallel with my superviser, teached me to do electrophysiological experiments and analysis, Sylvan Chauvette for his unvaluable contribution to our common publications and Josée Seigneur for her general help.

Finally, I would like to thank Mr. Pierre Guiguère, Denis Drolet and all my colleagues for their technical and moral support in every moment.

Dedication

I dedicate this thesis to my mother Khadidja
for her love and tenderness,
to my father Mohamed for his endorser,
in the same, to my family and my country, Algeria.

TABLE OF CONTENTS

LIST OF ABBREVIATIONS

$[Ca^{2+}]_i$	intracellular calcium concentration
$[Ca^{2+}]_o$	extacellular calcium concentration
$[K^+]_o$	extacellular potassium concentration
Ach	acetylcholine
AHP	afterhyperpolarization
AMPA	alpha-amino-3-hydroxy-5-methyl-4-isoxazole propionate
BK	big conductance Ca^{2+} activated K^+ channels
Ca^{2+}	calcium
CX	cortex
DC	direct current
EEG	electroencephalogram
EPSP	excitatory postsynaptic potential
FRB	fast-rhythmic-bursting
FS	fast-spiking
GABA	gamma-amino butyric acid
Hz	Hertz
IN	interneuron
$I_{Na(p)}$	persistent sodium current
$I_{K(Ca)}$	calcium activated potassium current
IB	intrinsically-bursting
IPSP	inhibitory postsynaptic potential
K^+	potassium
LTS	low-threshold spike
Na^+	sodium
NMDA	N-methyl-D-aspartate
PDS	paroxysmal depolarizing shifte
PPS	paired-pulse stimulation
PSW	polyspike-wave
PY	pyramidal neuron

REM	rapid eye mouvement
R_{in}	apparent input resistance
RS	regular-spiking
SK	small conductance Ca^{2+} activated K^{+} channels
SW	spike-wave
SWS	slow-wave sleep
TC	thalamocortical
TEA	tetraethylammonium
V_m	membrane potential

LIST OF FIGURES

1. INTRODUCTION

RESULTS

2. Extracellular Ca^{2+} modulation affects AHP and modifies firing properties of cortical neurons.

3. Focal generation of paroxysmal fast runs during electrographic seizures

1. Introduction

In the brain the interneuronal communications mediate behavior, perception, and thought. The properties of a neuronal population depend on the properties of individual neurons and the feed-back mechanisms that can affect individual neurons (Johnston and Brown 1986). These feedback mechanisms include synaptic connections, ephaptic interactions, and changes in extracellular space and ion concentrations. Many of the interactions are nonlinear and can lead to an output that is unstable and characterized by oscillations (Rutecki 1992). The important point to be made is that the behavior of individual neurons is defined by intrinsic ion conductances. Synaptic input will be amplified or dumped by these conductances and an output will be generated. The intrinsic currents generated by these conductances are affected by synaptic activities or changes in extracellular ion concentrations. The synaptic interactions between local neuronal constellations will influence other neurons and can result in coordinated activity of many neurons contributing to a functional output. Thus, change in either individual neuronal properties or feedback mechanisms of a neural network result in a change in the network output. These underlying changes may be rather small, but when processed in neural network, a small change may result in more dramatic network changes.

The Ca^{2+} as an endogenous ion plays a major role in modulation of both intrinsic neuronal excitability and synaptic activity (Crochet et al. 2005; Hille 2001; Katz 1969). However, the action of Ca^{2+} in these two phenomena is opposite. Extracellular calcium concentration ($[Ca^{2+}]_o$) is not fixed and fluctuate during both slow-wave sleep (Crochet et al. 2005; Massimini and Amzica 2001) and paroxysmal sleep oscillations (Amzica et al. 2002; Heinemann et al. 1977). As the consequence of this modulation the synaptic excitability decreases when $[Ca^{2+}]_o$ decreases (Crochet et al. 2005; Katz 1969), but in the same time the intrinsic excitability increases (see below).

The following sections of this introduction describe the electrophysiological properties of cortical neurons; the modulation of these properties by network activity during both slow-wave sleep and paroxysmal activity.

1.1 Electrophysiological properties of cortical neurons

Cortical neurons generate complicated patterns of activity during various network states, which depend on the interaction of very large numbers of interconnected neurons, their intrinsic properties and the state levels of neuromodulator activities. They display a heterogeneous distribution of electrophysiological properties that correlate with their morphology, anatomical connections and perhaps even neurotransmitter content (Connors and Gutnick 1990; McCormick et al. 1985).

1.1.1 Intrinsic properties

The intrinsic properties of a neuron depend on unique sets of ionic channels, specific to a given neuron and on their distribution in different compartments of the neuron. The diversity of channels in neurons is large and results in a variety of patterns of action potential generation induced by a constant input. In the neocortex, four basic electrophysiological firing patterns of neuron have been identified: (a) Regular-spiking (RS) neurons constitute the majority of cortical neurons. They display trains of single spikes that adapt quickly or slowly to maintained stimulation. (b) Fast-rhythmic-bursting (FRB) neurons give rise to high-frequency (300-600 Hz) spike-bursts recurring at fast rates (30-50 Hz). (c) Intrinsically bursting (IB) neurons generate clusters of action potentials, with spike inactivation, followed by hyperpolarization and neuronal silence. (d) Fast-spiking (FS) neurons fire thin action potential and sustain tonically very high firing rates (up to 800 Hz) without frequency adaptation (Gray and McCormick 1996; McCormick et al. 1985; Steriade et al. 1998b). The duration of intracellularly recorded action potentials at half amplitude, measured during the state of natural waking in chronically implanted cats, shows modes between 0.6 and 1 ms in RS neurons. Slightly longer spikes are fired by IB neurons. In contrast, both FRB and FS neurons demonstrate much shorter action potentials, with modes at about 0.3 ms (fig. 1.1) (Steriade et al. 2001). Generally, RS, FRB and IB neurons are pyramidal-shaped neurons, while FS firing patterns are conventionally regarded as defining local GABAergic cells (GABA is γ-aminobutyric acid). However, in addition to pyramidal-shaped FRB neurons, other neurons, with the same FRB firing patterns, are local-circuit, sparsely spiny or aspiny interneurons (Steriade et al. 1998b). Some local inhibitory interneurons discharge like RS or bursting cells (Thomson et al. 1996). Thus, each of the aforementioned four firing patterns

does not necessarily apply to a single of morphological class of neurons. Furthermore, the electrophysiological characteristics of different cortical neurons are flexible and a same neuron can change its firing pattern as a function of membrane potential, network activity and state of vigilance (Steriade et al. 1998b; Steriade et al. 2001; Timofeev et al. 2000a) and modulation of $[Ca^{2+}]_o$ (see chapter 2). Intrinsic firing patterns enable a neuron to modify the input signal to a structured output pattern. Only fast-spiking neurons possess linear input-output characteristic. Below (see chapter 2) we will demonstrate that changes in $[Ca^{2+}]_o$ affect intrinsic neuronal discharges.

1.1.2 Impact of network activity on neuronal excitability

In intact brain, the neuron receives several thousand synaptic contacts located throughout the dendrite and soma. The postsynaptic conductance change produced by neurotransmitters will act upon the many different voltage-gated channels in the dendrite and soma, and results in either postsynaptic subthreshold potential, or to different patterns of action potential generation (Pare and Lang 1998). The synaptic connectivity in the neocortex is very dense. Each pyramidal cell receives 5000 to 60000 synapses (Cragg 1967; DeFelipe and Farinas 1992). Local-circuit synapses have been estimated to account for as many as 70 % of the synapses present in some areas of the cortex (Gruner et al. 1974; Szentagothai 1965). Thus, this robust input influx should create tremendous synaptic bombardment onto postsynaptic neurons, affecting reliability of unitary responses (Crochet et al. 2005) or modulating theirs intrinsic properties, the rate of intrinsic bursting firing is much higher in isolated cortical territory compared to isolated large gyrus or intact cortex (Timofeev et al. 2000a; Timofeev et al. 2000b). Network activity during various functional states modifies the firing patterns generated by intrinsic neuronal properties (Steriade et al. 2001; Timofeev et al. 2000a). The long-lasting changes in activity influence the intrinsic excitability of cortical neurons (Topolnik et al. 2003a), this regulation is consistent with a role in stabilizing firing rates. Recent experimental work proves that preventing cortical neurons from firing for two days dramatically increased their intrinsic excitability (Cudmore and Turrigiano 2004; Desai et al. 1999). In response to injected current, activity-deprived neurons fired much more rapidly and did so in response to smaller current injections. This increase in excitability was

mediated by selective regulation of the magnitudes of persistent sodium and potassium currents; the former increased, whereas the latter decreased. These findings demonstrate that the history of activity of a cortical neuron helps to determine its intrinsic excitability. This may allow a neuron to adjust the way it modifies synaptic input efficiency to maintain its responsiveness during periods of intense change in synapse number and strength (Desai et al. 1999)

1.1.3 Neuronal oscillations during slow-wave sleep

The slow wave sleep is dominant by slow oscillations of EEG less than 1 Hz (generally 0.5-1 Hz). The slow oscillations are observed during the natural sleep in cat (Amzica and Steriade 1998a; Steriade et al. 1996; Steriade et al. 2001) and in human (Achermann and Borbely 1997; Amzica and Steriade 1997; Simon et al. 2000), just like under anesthesia with urethane, ketamine-xylazine, or nitrogen oxide (Contreras and Steriade 1995; Steriade et al. 1994a; Steriade et al. 1993a, b). The slow oscillation groups other sleep rhythms such as spindles and delta waves (Amzica and Steriade 1995b, 1998b; Contreras and Steriade 1995; Steriade and Amzica 1998). The cortical origin of slow oscillations was demonstrated by (a) its survival in the cerebral cortex after thalamectomy (Steriade et al. 1993a); (b) its absence in the thalamus of decorticated animals (Timofeev and Steriade 1996); (c) the disruption of its long-range synchronization after disconnection of intracortical synaptic linkages (Amzica and Steriade 1995a) and (d) its presence in isolated cortical preparations (Sanchez-Vives and McCormick 2000; Timofeev et al. 2000a). The sleeping cortex appears as an oscillator master imposing the slow rhythm to the thalamus and modulating activity originating in the thalamus (Steriade et al. 1994b). During slow oscillations, the membrane potential of cortical neuron alternates between depolarizing and hyperpolarizing phases (Steriade et al. 1993b). The neuronal depolarization is associated with a depth-negative EEG deflection, and the neuronal hyperpolarization is associated with a depth-positive EEG deflection (Contreras and Steriade 1995). The depolarizing phase corresponds to a general excitation of cortical neurons associated with excitatory postsynaptic potentials (EPSPs), inhibitory postsynaptic potentials (IPSPs), and action potentials (Steriade et al. 1993a, b). The long-lasting hyperpolarizing phase of the slow

oscillation is associated with absence of firing of all cortical neurons, inducing a generalized disfacilitation in the cortical network (Contreras et al. 1996; Timofeev et al. 2001). The slow oscillation is accompanied: (1) by a progressive decrease of $[Ca^{2+}]_o$ during the depolarizing phase with run down of synaptic efficacy (Crochet et al. 2005; Massimini and Amzica 2001), and (2) by the glial regulation of $[K^+]_o$, which likely modulates neuronal excitability (Amzica and Massimini 2002).

1.2 Role of Ca^{2+} in intrinsic neuronal excitability

Calcium influx into cells or release of calcium from intracellular stores has a variety of consequences including mediator release from synaptic vesicles, activation of second messenger systems, gene transcription, and opening of calcium dependent ion channels. Important currents that control firing properties of neurons are calcium dependent potassium currents (I_C and I_{AHP}). They are largely activated following Ca^{2+} influx via voltage gated Ca^{2+}channels during the action potentials and generating the afterhyperpolarization that follows action potentials.

1.2.1 Effect of Ca^{2+}-activated K^+ currents on spike afterhyperpolarization (AHP)

In neurons, action potentials are followed by an afterhyperpolarization that may have three components. These have been called the fast afterhyperpolarization (fAHP), the medium AHP (mAHP), and the slow AHP (sAHP) (Sah and Faber 2002). The fAHP is activated immediately after the action potential and lasts several tens of milliseconds. The mAHP is also activated rapidly following the action potential (<5 ms) but decays with a time course of several hundred milliseconds. Finally, the third component of the AHP is the slow AHP, which rises to a peak over several hundred milliseconds; and can last up to 5 s following an action potential (Sah and Faber 2002). While in some neurons slow AHPs have been described following a single action potential (Hirst et al. 1985; Sah and McLachlan 1991), it is more commonly seen following a train (4–10) of spikes (Faber et al. 2001; Lancaster and Nicoll 1987; Schwindt et al. 1988). All three types of AHP are known to be mediated by calcium-activated potassium channels, which are activated in response to calcium influx via voltage dependent calcium channels that open during the action potential

(Lancaster and Nicoll 1987; Storm 1987, 1990). The current underlying the fAHP has been named I_c. This current is voltage dependent (Adams et al. 1982) and is blocked by low concentrations of TEA, iberiotoxin, and paxilline indicating that the underlying channels are BK-type channels (Adams et al. 1982; Lancaster and Nicoll 1987; Shao et al. 1999). The exact identity of these channels, however, has not been determined. In contrast, the mAHP is unaffected by BK channel blockers but is blocked by apamin indicating that it is due to the activation of SK-type channels (Pennefather et al. 1985; Sah and McLachlan 1991, 1992; Schwindt et al. 1988). The current that underlies the mAHP has been called I_{AHP} (Adams et al. 1982). It peaks rapidly following calcium influx (<5 ms) and decays with a time constant of 50 to several hundred milliseconds (Pennefather 1988; Sah 1992). It is notable that while activation of BK channels generates the fAHP, these channels also contribute to action potential repolarisation. In contrast, activation of SK channels does not contribute to action potential repolarisation (Lancaster and Nicoll 1987; Sah 1996; Storm 1987, 1990). The current that underlies the slow AHP was first described in neurons in the myenteric plexus (Hirst et al. 1985). Following calcium influx, this current has a time to peak on the order of hundreds of milliseconds, and decays to baseline with a time constant of 1–2 s at 30 °C. To distinguish it from I_{AHP}, this current has been designated I_{sAHP} (Sah 1996). As with I_{AHP}, this current requires a rise in cytosolic calcium for activation and is voltage insensitive. I_{sAHP} is not blocked by apamin or TEA. However, I_{sAHP} is modulated by a range of neurotransmitters including noradrenaline, serotonin, glutamate, and acetylcholine all of which block the current (Nicoll 1988).

1.2.2 Ca^{2+} can modulate neuronal firing pattern

The spike AHP, which is mediated by activation of Ca^{2+}-activated K^+ currents has two functions: (*a*) it limits the firing frequency of the neuron and (*b*) is responsible for generating the phenomenon of spike-frequency adaptation. Thus, the change in Ca^{2+} influx can modulate the AHP, and afterward the firing properties of the neuron. The firing pattern of cortical neurons is not fixed and it can change as discussed above. In chapter II we will demonstrate that the change in $[Ca^{2+}]_o$ can switch RS firing to FRB firing in some cortical neurons. This switching of firing pattern is also confirmed by in vitro experiments in rat layer 2/3 cortical neurons by buffering $[Ca^{2+}]_i$ (Brumberg et al. 2000). Furthermore, a model study

suggest that modulator-induced regulation of Ca^{2+} dynamics or of BK channel conductance, for example via protein kinase A, could play a role in determining the firing pattern of neocortical neurons (Traub et al. 2003).

1.3 Role of Ca^{2+} in synaptic activity

As known, Ca^{2+} is a key factor in synaptic activity; the release of neurotransmitter from vesicles is dependent on Ca^{2+} entry induced by arriving of an action potential to the presynaptic terminal (Katz 1969). Ca^{2+} enters through clusters of channels near docked synaptic vesicles in active zones. This Ca^{2+} acts at extremely short distance (tens of nanometers) in short time (200 μs) and at very high local concentration (~100 μM), in calcium microdomains, by binding cooperatively to a low-affinity receptor with fast kinetics to trigger exocytosis. When Ca^{2+} channels close, these microdomains of high Ca^{2+} return to near resting concentrations quickly and the evoked response is terminated. Speed, efficiency, and flexibility are the hallmarks of this process (Macleod et al. 2004)

1.3.1 Impact of $[Ca^{2+}]_o$ modulation on synaptic transmission

As mentioned above, the $[Ca^{2+}]_o$ fluctuates as a function of neuronal activity, it decreases by approximately 20% during active states of the cortical network (Massimini and Amzica 2001). In the study *Modulation of synaptic transmission in neocortex by network activities* (Crochet et al. 2005) we investigated the effects of fluctuations of $[Ca^{2+}]_o$ on synaptic transmission. We observed an increase in number of failures and a decrease in amplitude and duration of postsynaptic responses during active network states. To study the effects of fluctuations of $[Ca^{2+}]_o$ on synaptic transmission, we performed two types of experiments. *First*, in ketamine-xylazine anesthetized cats we measured the modulation of response amplitude elicited by microstimulation and the parallel changes of $[Ca^{2+}]_o$ (Fig. 1.2). The amplitude and the duration of responses during active network states were reduced as compared to the silent network states (Fig. 1.2, a). Measurements of individual responses demonstrated (a) a progressive increase in the amplitude of responses starting from the onset of silent state as estimated form the onset of depth-positive field potential and from the onset of neuronal hyperpolarization, (b) an abrupt decrease in the EPSPs' amplitude at the onset of active state and (c) a recovery of the response amplitude as network goes back to silent

states. The progressive increase in the EPSPs' amplitude occurred in parallel with an increase in the $[Ca^{2+}]_o$ (Fig. 1.2, b-c). The decrease in the EPSPs' amplitude at the onset of active state was likely due to the decrease in the input resistance of neuron and due to the decrease in the $[Ca^{2+}]_o$. Since the time constant of Ca^{2+} electrodes was long (hundreds of milliseconds) the exact changes of the $[Ca^{2+}]_o$ measured in these experiments were likely underestimated and the decrease in the $[Ca^{2+}]_o$ could occur immediately at the onset of active state. *Second*, in order to provide further evidences of Ca^{2+} nature of high failure rates during active network states, we combined microstimulation with microdialysis of artificial cerebrospinal fluid (ACSF) containing different $[Ca^{2+}]_o$, and direct $[Ca^{2+}]_o$ measurements with Ca^{2+} sensitive electrodes in barbiturate anesthetized cats (Fig.1.3a). Microdialysis of 1.0 mM of Ca^{2+} (control solution) yielded free $[Ca^{2+}]_o$ of 1.1-1.2 mM; using the high Ca^{2+} solution (5 mM) raised $[Ca^{2+}]_o$ to 2.5-3.0 mM and employment of Ca^{2+} free solution lowered $[Ca^{2+}]_o$ to 0.7-0.8 mM. Microstimulation evoked responses (n=7) were compared for the three conditions when $[Ca^{2+}]_o$ reached steady levels. The total averaged response was increased in high calcium condition and decreased in low calcium condition (Fig. 1.3b). As shown by histograms of response amplitude (Fig. 1.3c), both the amplitude of successful responses and the failure rate were affected by changes in $[Ca^{2+}]_o$. In control condition the mean amplitude of successful EPSPs was 0.83±0.14 mV and the overall failure rate was 54±12 %. Raising $[Ca^{2+}]_o$ increased the amplitude of EPSPs to 1.23±0.18 mV, and decreased failure rates to 29±11 %. Lowering $[Ca^{2+}]_o$ reduced the amplitude of EPSPs to 0.49±0.06 mV and increased failure rate to 76±6 %. Paired t-test revealed that these differences were significant at $p<0.05$. In addition, on some occasions (n=7) we observed bimodal distribution of histograms of successful responses (see control in Fig. 1.3c). Invariantly, the second peak of histogram increased in high $[Ca^{2+}]_o$ conditions and it was abolished in low $[Ca^{2+}]_o$ conditions. These data suggests that presynaptic stimuli in control conditions activated one or several release sites. Increase in $[Ca^{2+}]_o$ increased probability of simultaneous activation of two release sites and decrease in $[Ca^{2+}]_o$ allowed activation of maximum one release site per stimulus (Crochet et al. 2005).

1.4 From sleep to seizure

The adage “sleep and epilepsy are common bedfellow” is supported by much clinical and experimental evidence showing that epileptic seizures of different types preferentially occur during slow-wave sleep (SWS or non-REM). It is considered the possibility that many spontaneous electrographic seizures in "normal" subjects may not be recognized, and that those sleeping individuals pass in and out of seizures during slow sleep oscillations. Needless to say, these are *electrical seizures* and it is refrain from using the term *epilepsies* (Timofeev and Steriade 2004)

1.4.1 Normal oscillations during slow-wave sleep developing into seizures

Spontaneously occurring seizures consisting of Spike-Wave (SW) complexes at approximately 3–4 Hz, similar to those seen in absence epilepsy, or more compound patterns as in Lennox-Gastaut seizure, may develop without discontinuity from the slow (mainly 0.5-0.9 Hz) sleep-like, cortically generated oscillation (Steriade et al. 1998a; Timofeev and Steriade 2004). The rather high proportion of SW/PSW seizures that occur *spontaneously* under ketamine–xylazine anesthesia may be due to the highly synchronized activity in corticothalamic systems, which develop into grouped sleep-like oscillations that promote paroxysms. However, similar electrographic patterns of cortical seizures have been recorded during natural sleepiness and slow-wave sleep (Steriade 1974; Steriade et al. 1998a). The prevalence of paroxysmal activity during SWS is observed not only with full-blown seizures but also with interictal EEG “spiking”. Most patients show maximal EEG “spiking” in SWS stage 3 and 4; because of less frequent interictal “spikes” in waking and REM sleep, recordings during these states of vigilance provide better localization of these signs for the presurgical assessment of temporal lob epilepsy (Sammaritano et al. 1991)

1.4.2 Electrographic patterns of Lennox-Gastaut seizures

The electrographic pattern of seizures accompanying Lennox-Gastault syndrome as well as their occurrence during slow-wave sleep described below in animal model, resemble the clinical Lennox-Gastaut syndrome of humans (Halasz 1991; Kotagal 1995; Niedermeyer 1999a, b). These seizures are generated intracortically and spontaneously without discontinuity from the sleep-like slow oscillations, they are characterized by SW or spike-

wave/polyspike-wave (SW/PSW) complexes of 1.5-3 Hz, intermingled with episodes of fast runs at ~7-16 Hz (Fig.1.4) (Neckelmann et al. 1998; Steriade et al. 1998a; Steriade and Contreras 1998; Timofeev et al. 1998). The intracortical origin suggested because the majority of thalamocortical neurons do fire spikes during these seizures (Steriade and Contreras 1995; Timofeev et al. 1998) and similar seizures are recorded in cats with large with matter undercuts (Topolnik et al. 2003b) or could be elicited in isolated neocortical slabs (Timofeev et al. 1998). During the initial part of the seizure, SW/PSW complexes characterize the EEG recording, while, at neuronal level, the slope as well as the amplitude of the shift in the membrane potential from hyperpolarized to depolarized levels increased compared to the pre-seizure epoch. The action potentials were partially inactivated and AHP disappeared during paroxysmal depolarizing shift (PDS). The following period, with fast runs, was characterized by EEG "spikes", at the neuronal level, a tonically depolarized membrane potential, with smaller depolarization superimposed. The synchrony between cortical neuronal pools during fast runs is impaired that suggests their focal generation; (see chapter III). The end of the seizure was associated with a short period of hyperpolarization, followed by resumption of the sleep-like slow oscillation (Steriade et al. 1998a; Timofeev and Steriade 2004).

1.4.3 Neuronal mechanisms of seizures

The modulation of neuronal excitability by many factors is responsible of shift from normal to paroxysmal activity. Various neuronal ionic currents contribute to the increase in the susceptibility to seizures. The discovery of voltage-dependent Na^+ and Ca^{2+} channels in dendrites changed the model of dendrites with only passive properties and demonstrated that different intrinsic currents can amplify synaptic signals (Schwindt and Crill 1995), which may eventually lead to abnormal cellular excitation and paroxysmal discharges (Ward and Schmidt 1961). During cortically driven seizures (Timofeev and Steriade 2004), the persistent Na^+ current [$I_{Na(p)}$] and probably the high-threshold Ca^{2+} current contribute to the generation of paroxysmal depolarizing shifts (PDSs). Ca^{2+}-activated K^+ current [$I_{K(Ca)}$] take also part in the control of the amplitude and duration of PDSs. The hyperpolarizing components of seizures largely depended on Cs^+-sensitive K^+ currents. $I_{K(Ca)}$ plays a significant, while not exclusive, role in the mediation of hyperpolarizing potentials related to

EEG "waves" during spike-wave seizures (Timofeev et al. 2004). Recent intracellular studies of neocortical neurons *in vivo* (Timofeev et al. 2002b) as well as work on human and rat slices (Cohen et al. 2002; Fujiwara-Tsukamoto et al. 2003) demonstrate that PDSs contain an important inhibitory component. The hyperplarization activated depolarizing current plays a critical role in the generation of subsequential PDSs (Timofeev et al. 2002a). The intrinsic propensity of some neocortical neurons to bursting is also a factor that predisposes to seizures. The FRB neurons fire high-frequency (approximately 300–400 Hz) spike-bursts at fast rates (approximately 30–40 Hz), they have the highest propensity to drive seizures. This is coupled with the crucial role played by FRB neurons in the generation of ultra-fast oscillations, called ripples (80–200 Hz), which initiate seizures in both animal experiments (Grenier et al. 2003) and humans (Fisher et al. 1992). The firing frequency of IB (8 Hz) and number of theirs spikes fired during fast runs suggest their role in generation of fast runs (Fig. 3.6) (see chapter III). It is widely accepted that the development epileptiform activity results from a shift in the balance between excitation and inhibition toward excitation (Dichter and Ayala 1987; Galarreta and Hestrin 1998; Nelson and Turrigiano 1998; Tasker and Dudek 1991). Other two factors (increased inhibition and decreased excitation) also may lead to functional unbalance in cortical circuits; however, their role in seizure initiation was poorly explored. By increased "inhibition" we mean either increased number of IPSPs or disfacilitation, i.e. temporal absence of network activity. By decreased excitation we mean significantly decreased activity in afferent structures or decreased effectiveness of EPSPs. If one of the above factors occurs, it would create conditions that are favorable to seizure generation. One condition for seizure generation is the functional heterogeneity of cortical networks, such as the presence of two or more different cortical regions with relatively high and low levels of synaptic activity. Transitory or persistent reduction in synaptic activity within some cortical foci would increase the sensitivity of cortical neurons in those foci and in surrounding areas (Abbott et al. 1997; Desai et al. 1999) and the synaptic inputs from cortical regions exhibiting moderate or high levels of activity would lead to an increased responsiveness in those cortical areas.

Thus, a mosaic of intrinsic cell properties, changes in extracellular ion concentrations (K^+, Ca^{2+}) (Heinemann et al. 1977), as well as intracellular acidification (Xiong et al. 2000), may play a role in the induction and/or duration of seizures. Since seizure activities are

regarded as hypersynchronous states, but the synaptic transmission during seizures is impaired due to low $[Ca^{2+}]_o$, we hypothesized that (a) the low $[Ca^{2+}]_o$ enhance intrinsic neuronal responsiveness and (b) the local synchronization during seizures is also impaired. These issues were investigated experimentally and the results are presented in chapters 2 & 3.

1.5. Figures

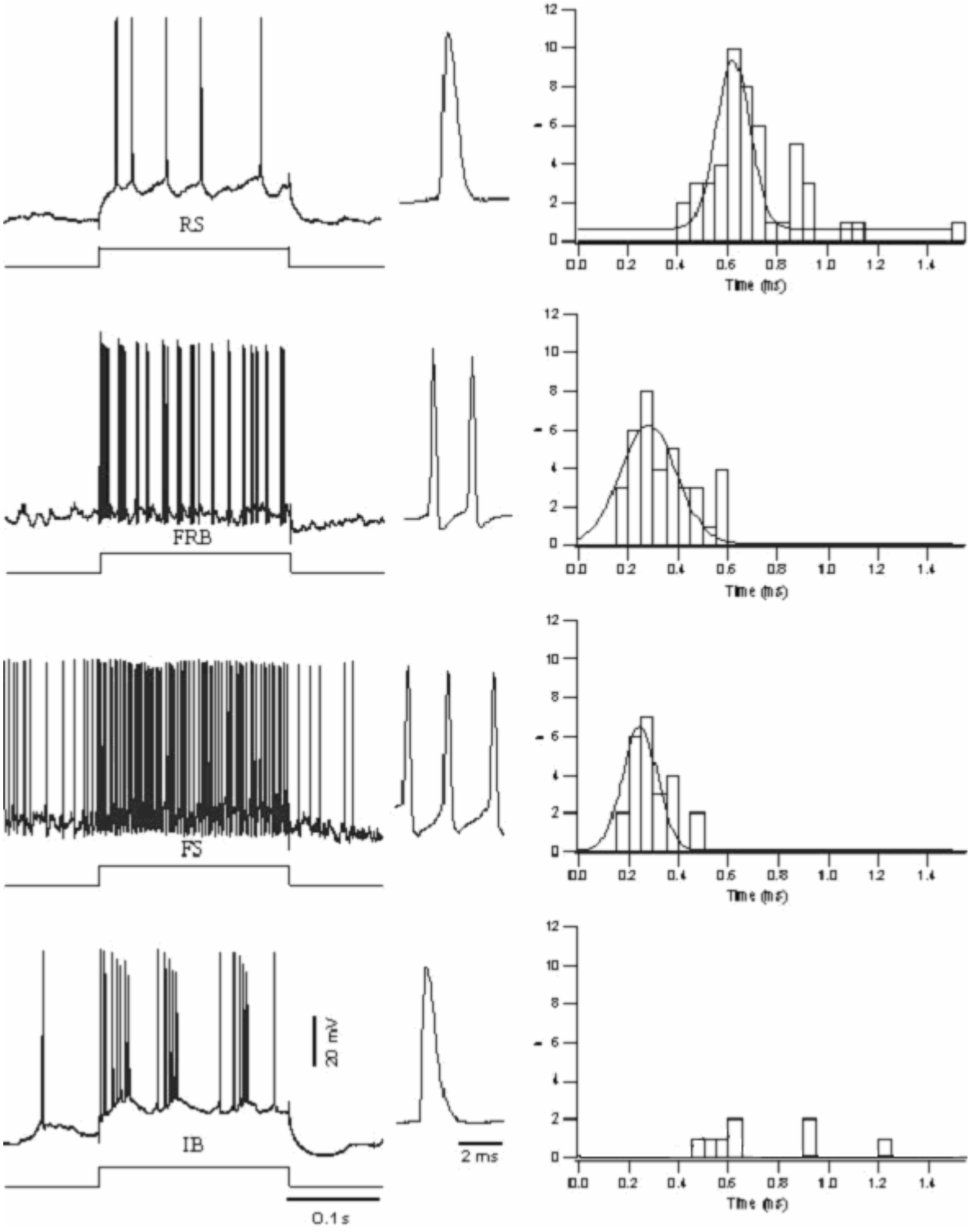

Figure 1.1

Figure 1.1: Electrophysiological identification of different cell classes in neocortex. Chronically implanted, awake cat. Left column depicts responses of regular-spiking (RS), fast-rhythmic-bursting (FRB), fast-spiking (FS) and intrinsically bursting (IB) neurons from area 4 to depolarizing current pulses p(0.2s, 0.8 nA). At the right of each depolarizing current pulse, action potentials of each cell are shown; note thin spikes of FRB and FS neurons, compared to those of RS and IB neurons. Right column illustrates the width of action potentials (at half amplitude) in a sample of 117 neurons (48 RS, 37 FRB, 24 FS and 8 IB, corresponding to patterns depicted on the left). (Steriade et al. 2001).

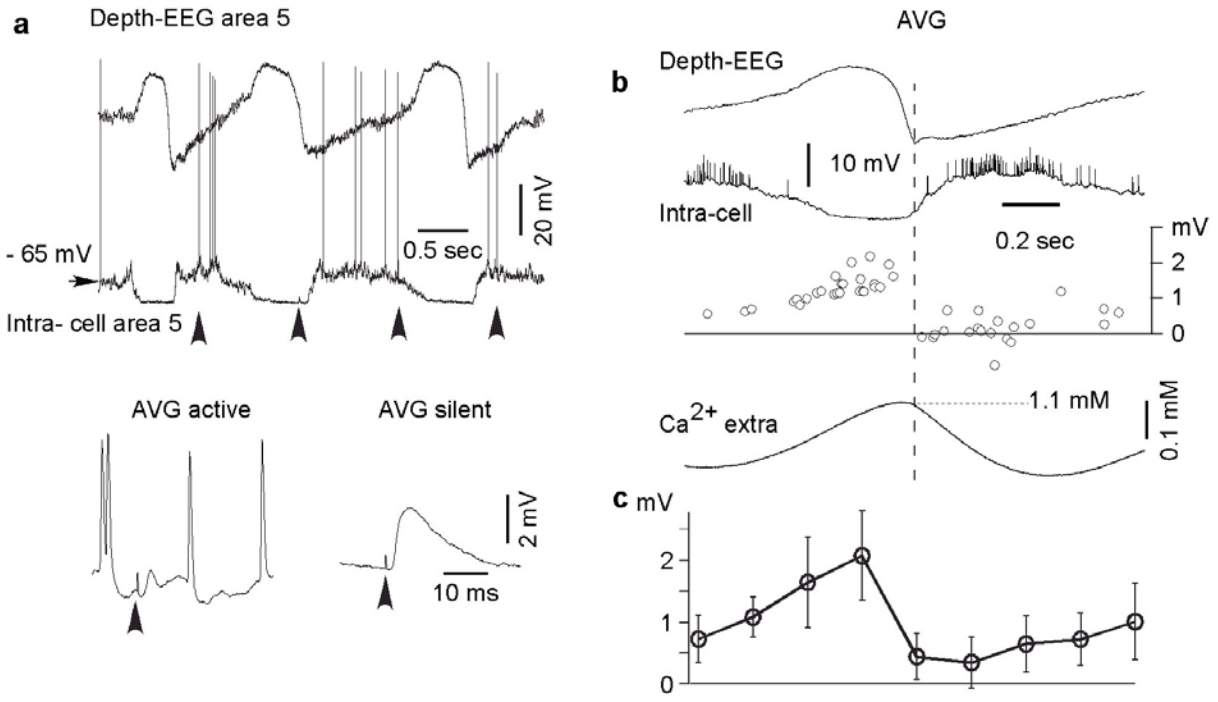
a
Depth-EEG area 5
- 65 mV
0.5 sec
20 mV
Intra- cell area 5
AVG active
AVG silent
2 mV
10 ms
AVG
b
Depth-EEG
10 mV
Intra-cell
0.2 sec
mV
2
1
0
Ca2+ extra
1.1 mM
0.1 mM
c mV
2
1
0

Figure 1.2

Figure 1.2: Activity dependent modulation of responses elicited by microstimulation.

a. A period of spontaneous activity in neocortex in ketamine-xylazine unesthetized cat (upper panel) and averaged responses to microstimulation during active and silent network states (lower panel). Arrowheads indicate the time of stimulation. **b**. Wave-triggered average of EEG, intracellular activities and $[Ca^{2+}]_o$ as well as amplitude of intracellular response to microstimuli applied during different phases of slow oscillation. The first maximum of EEG-depth negativity was taken as 0 time. **c.** Averaged amplitude of responses to microstimuli from 9 neurons during different phases of slow oscillation. The amplitude was averaged in following time windows: -800 to -600 ms, -600 to -400 ms, -400 to -200 ms, -200 to 0 ms, 0 to 200 ms, 200 to 400 ms, 400 to 600 ms and 600 to 800 ms. The time base in **b** and **c** is the same. (Crochet et al. 2005).

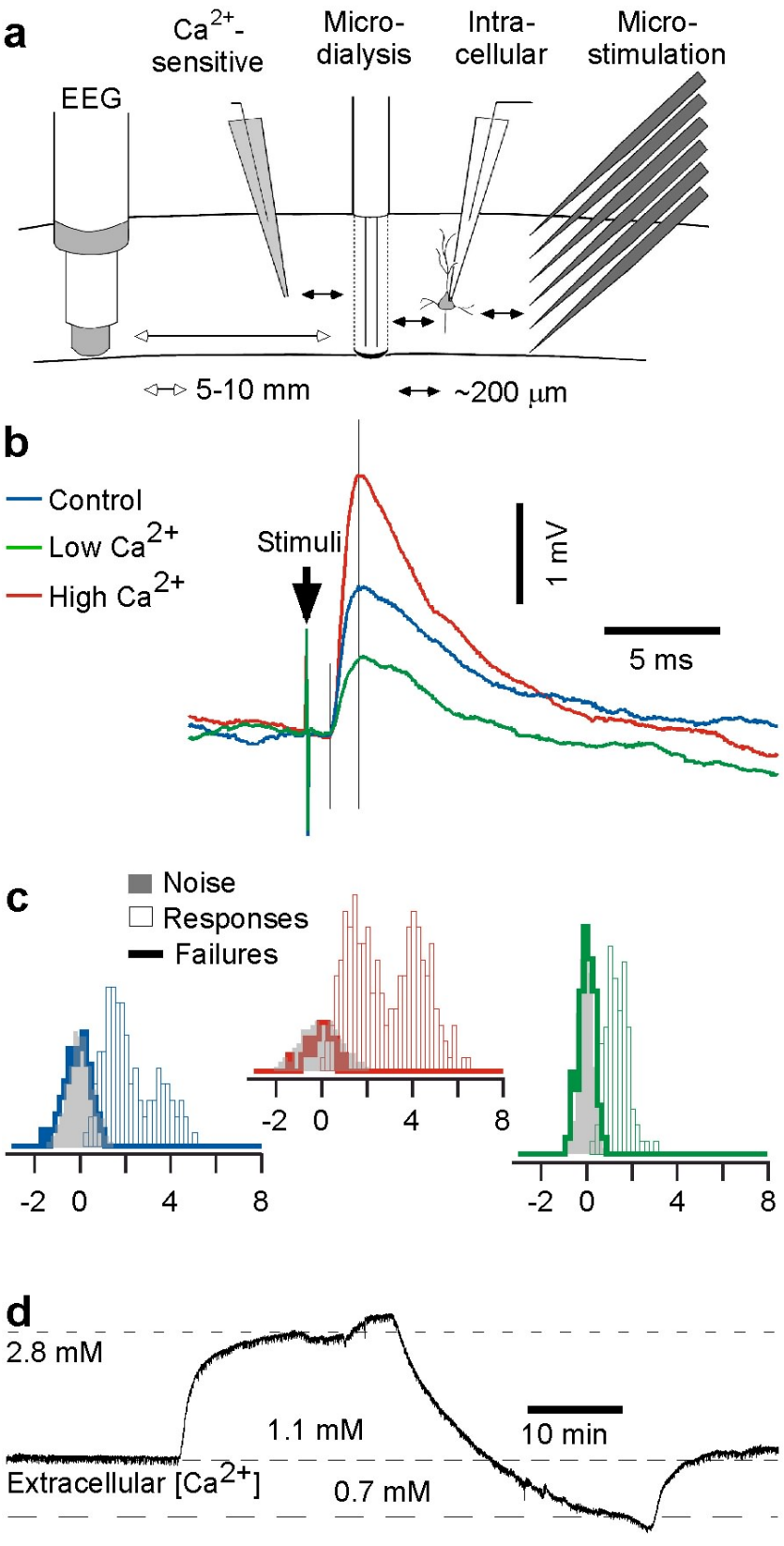
a
Ca2+-sensitive
Micro-dialysis
Intra-cellular
Micro-stimulation
EEG
5-10 mm
~200 μm
b
Control
Low Ca2+
High Ca2+
Stimuli
1 mV
5 ms
c
Noise
Responses
Failures
-2 0 4 8
-2 0 4 8
-2 0 4 8
d
2.8 mM
1.1 mM
10 min
Extracellular [Ca2+]
0.7 mM

Figure 1.3

Figure 1.3: Modulation of microstimulation induced EPSPs by changes in $[Ca^{2+}]_o$.

a. Set up for intracellular recordings, microstimulation, microdialysis, direct Ca^{2+} and EEG measurements. **b**. Averaged responses in the conditions of different $[Ca^{2+}]_o$. Red, high $[Ca^{2+}]_o$; blue normal $[Ca^{2+}]_o$ and green low $[Ca^{2+}]_o$. Microstimuli induced a single EPSP. High $[Ca^{2+}]_o$ resulted in increased amplitude of the response, whereas low $[Ca^{2+}]_o$ decreased the response. **c.** Histograms showing for each condition the distribution of the amplitude of the background synaptic noise (filled gray), the responses (failure excluded, open bars) and the failures (thick line). Color-code same as part b. Note the distribution of noise that become wider in high $[Ca^{2+}]_o$ and narrower in low $[Ca^{2+}]_o$. **d**. Measured changes in the $[Ca^{2+}]_o$. (Crochet et al. 2005).

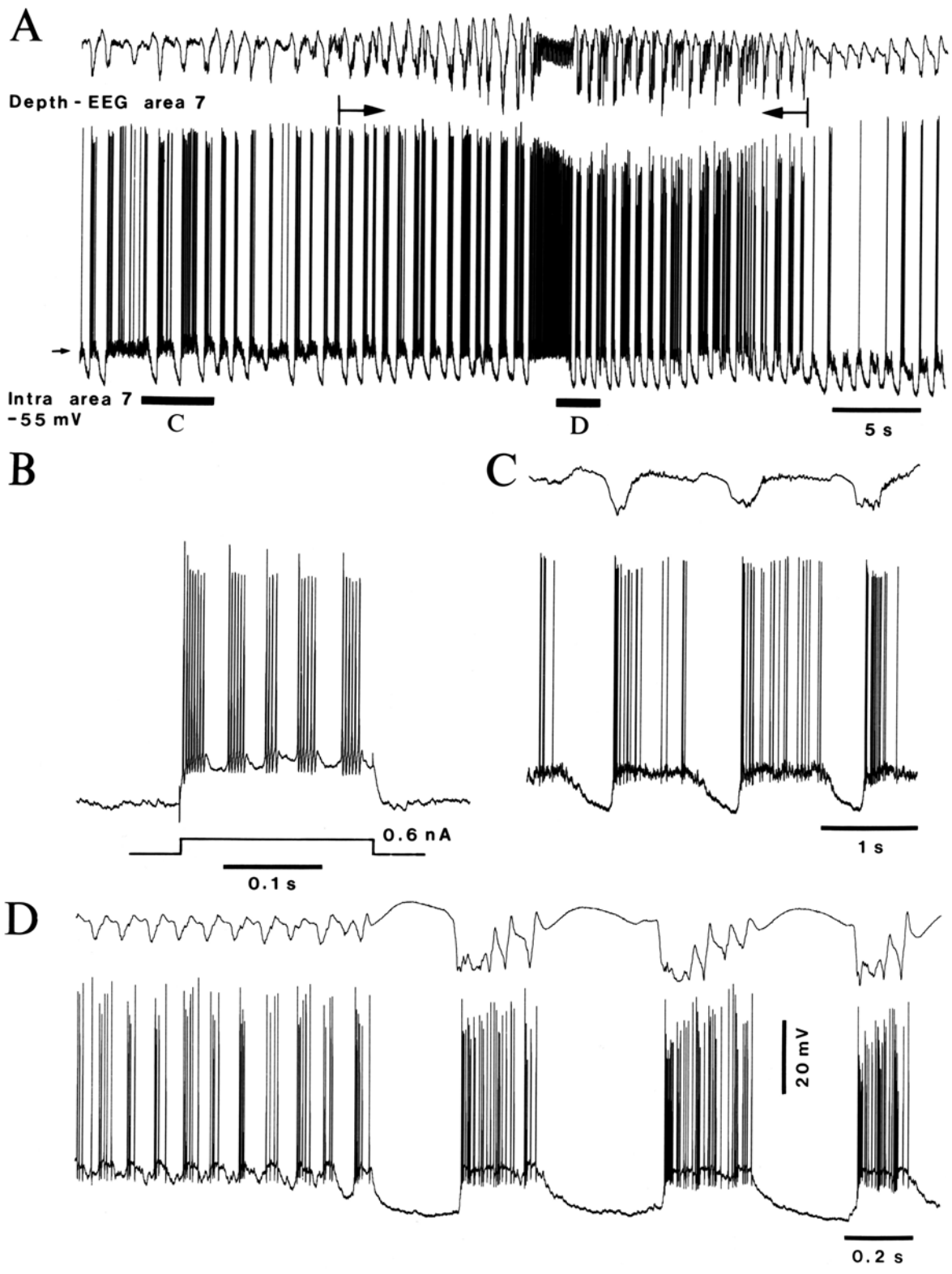
A
Depth - EEG area 7
Intra area 7
-55 mV
C
D
5 s
B
0.6 nA
0.1 s
C
1 s
D
20 mV
0.2 s

Figure 1.4

Figure 1.4: Fast-rhythmic-bursting (FRB) cortical neuron during SW and fast seizure developing spontaneously from slow sleep oscillation.

A: intracellular and depth-EEG recording from area 7. Seizure is indicated by arrows (below the EEG trace) and lasted for ~26 s. **B:** electrophysiological identification by depolarizing current pulse (0.2 s). See text. Epochs *C* and *D* in *A* are expanded below. **C:** slow oscillation before the seizure. **D:** both fast runs (~12 Hz) and PSW complexes (~2 Hz). (Steriade et al. 1998a)

RESULTS

Chapter II

2. Extracellular Ca^{2+} modulation affects AHP and modifies firing properties of cortical neurons.

Sofiane Boucetta, Sylvain Chauvette and Igor Timofeev. *Submitted to the Journal of Physiology (2005).*

2.1 Résumé

Généralement, les neurones corticaux sont classés selon leur mode de décharge en quatre types : décharge régulière avec adaptation du taux de décharge (RS), décharge en bouffées de potentiel d'action (IB), décharge en bouffées rapides et rythmiques (FRB) et 4) décharge rapide et sans adaptation (FS). Précédemment, nous avons montré que les patrons de décharge intrinsèque ne sont pas fixes et changent en fonction du potentiel de membrane des neurones ou de l'état de vigilance. D'autres données montrent que la concentration extracellulaire du calcium $[Ca^{2+}]_o$ change en fonction de la phase des ondes EEG corticales. Dans cette présente étude, nous avons investigué comment les changements de la $[Ca^{2+}]_o$ affectent les paramètres des potentiels d'action et les patrons de décharge. Les activités intracellulaires des neurones corticaux ont été enregistrées chez des chats anesthésiés par ketamine-xylazine. La $[Ca^{2+}]_o$ a été changée à l'aide d'une sonde de microdialyse. La modulation de la $[Ca^{2+}]_o$ a affecté significativement l'hyperpolarisation qui suit les potentiels d'action (AHP) qui est contrôlée par le courant potassique calcium-dépendant, dans tous les neurones. Une augmentation de $[Ca^{2+}]_o$ augmente de façon significative l'amplitude l'AHP, tendis qu'une diminution de $[Ca^{2+}]_o$ diminue l'AHP, en particulier sa composante précoce. La modulation de l'AHP résulte en une modulation notable du patron de décharge intrinsèque et quelques neurones à décharge régulière (RS) ont révélé des décharges en bouffées. Nous suggérons qu'au cours des oscillations spontanées du réseau cortical in vivo, les changements dynamiques des patrons de décharge dépendent en partie de la fluctuation de la $[Ca^{2+}]_o$.

2.2 Abstract

Neocortical neurons can be classified in four major types according to their pattern of discharge: Regular-Spiking (RS), Intrinsically-Bursting (IB), Fast-Rhythmic-Bursting (FRB) and Fast-Spiking (FS). Previously, we have shown that these firing patterns are not fixed and can change as a function of membrane potential and states of vigilance. Other studies have reported that $[Ca^{2+}]_o$ fluctuates as a function of the phase of the cortical slow oscillation. In the present study we investigated how changes in $[Ca^{2+}]_o$ affect the properties of action potentials (APs) and firing patterns in cortical neurons *in vivo*. Intracellular recording were performed in cats anesthetized with ketamine-xylazine while changing $[Ca^{2+}]_o$ with reverse microdialysis. In normal $[Ca^{2+}]_o$, we found an increase of the firing threshold and a decrease of the afterhyperpolarization (AHP) amplitude during the depolarizing phase of the slow oscillation and some neurons also changed their firing pattern as compared with the hyperpolarizing phase. Changes in $[Ca^{2+}]_o$ significantly affected the AP properties in all neurons. The AHP was increased in high calcium condition and decreased in low calcium, in particular the earliest components. Modulation of spike AHP resulted in notable modulation of intrinsic firing pattern and some RS neurons revealed burst firing when $[Ca^{2+}]_o$ was decreased. We suggest that during spontaneous network oscillations *in vivo*, the dynamic changes of firing patterns depend partially from fluctuations of the $[Ca^{2+}]_o$.

2.3 Introduction

In both animals and humans, the slow-wave sleep is characterized by the cyclic alternation of positive and negative EEG waves referred as slow oscillation (<1 Hz) (Steriade *et al.*, 1993b; Steriade *et al.*, 1993d, c; Achermann & Borbely, 1997). During sleep and anesthesia, all cortical neurons are silent and hyperpolarized during the depth-positive EEG waves, whereas during the depth-negative waves, cortical neurons are depolarized and usually fire spikes (Contreras & Steriade, 1995; Steriade *et al.*, 2001; Timofeev *et al.*, 2001). Cortical neurons can generate various firing patterns depending on their morphology, passive properties and active conductances. On the basis of this firing pattern, cortical neurons are classified in four major types: regular spiking (RS), intrinsically bursting (IB), fast-rhythmic-bursting (FRB) and fast-spiking (FS) (McCormick *et al.*, 1985; Gray & McCormick, 1996; Steriade *et al.*, 1998). However, the expression of intrinsic firing pattern expressed by cortical neurons is affected by the presence of network activities or neuromodulators (Wang & McCormick, 1993; Steriade *et al.*, 1998; Timofeev *et al.*, 2000; Steriade *et al.*, 2001; Steriade, 2004). Active network states are associated with increased extracellular potassium concentration ($[K^+]_o$) and decreased $[Ca^{2+}]_o$ (Heinemann *et al.*, 1977). During the cortical slow oscillation, $[Ca^{2+}]_o$ reaches its maximum (about 1.2 mM) during silent network states (depth-positive EEG wave) and decreases by approximately 20% during active network states (depth-negative EEG wave) (Massimini & Amzica, 2001; Crochet *et al.*, 2005).

Neuronal firing is associated with Ca^{2+} influx (Markram *et al.*, 1995; Abel *et al.*, 2004). Rise of intracellular Ca^{2+} concentration ($[Ca^{2+}]_i$) activates Ca^{2+} activated K^+ currents ($I_{K(Ca)}$) that are responsible for the afterhyperpolarizing potential (AHP) following action potentials (APs) (Storm, 1987; Sah & Louise Faber, 2002). In neocortical neurons, one can distinguish three components in the AHP: the fast, the medium and the slow AHP (fAHP, mAHP and sAHP). The fAHP is activated immediately during the AP and lasts several tens of milliseconds (Schwindt *et al.*, 1988); it contributes to the repolarization of APs (Storm, 1987). Although the sAHP is more commonly seen following a train (4–10) of spikes (Lancaster & Nicoll, 1987; Schwindt *et al.*, 1988; Faber *et al.*, 2001), it can follow a single AP in some neurons (Hirst *et al.*, 1985; Sah & McLachlan, 1991). The sAHP is mainly

mediated by calcium-activated potassium channels, but IB neurons also display a sAHP mediated by sodium-activated potassium current (Franceschetti *et al.*, 2003). The sAHP plays a key role in regulating cell firing: (*a*) it limits the firing frequency of the neuron and (*b*) it is responsible for generating the phenomenon of spike-frequency adaptation (McCormick, 1999).

The presence of extracellular Ca^{2+} dynamics and the contribution of $I_{K(Ca)}$ to neuronal output, led us to hypothesis that slow oscillation-dependent fluctuation of $[Ca^{2+}]_o$ in the neocortex could contribute to a dynamic control of intrinsic firing patterns and AP properties. To test this hypothesis, we performed intracellular recordings from cortical neurons *in vivo* in cats anesthetized with ketamine-xylazine; under this condition, cortical activities are dominated by the slow oscillation, like during slow-wave sleep. We also combined intracellular recordings with the reverse-microdialysis technique to change $[Ca^{2+}]_o$.

2.4 Materials and methods

2.4.1 Preparation

Experiments were conducted on 36 adult cats anesthetized with ketamine-xylazine anesthesia (10-15 and 2-3 mg/kg i.m., respectively). The animals were paralyzed with gallamine triethiodide (20 mg/kg) after the EEG showed typical signs of deep general anesthesia, essentially consisting of a slow oscillation (0.5-1 Hz). Supplementary doses of the same anesthetics (5 and 1 mg/kg i.m.) were administered at the slightest changes toward the diminished amplitudes of slow waves. All pressure points and the tissues to be incised were infiltrated with lidocaine (0.5%). The cats were ventilated artificially with the control of end-tidal CO_2 at 3.5-3.7%. The body temperature was maintained at 37-38^{o}C and the heart rate was ~90-100 beats/min. For intracellular recordings, the stability was ensured by the drainage of cisterna magna, hip suspension, bilateral pneumothorax, and by filling the hole made for recordings with a solution of 4% agar. At the end of experiments, the cats were given a lethal dose of intravenous sodium pentobarbital (50 mg/kg). All experimental procedures were performed according to national guidelines and were approved by the committee for animal care of Laval University.

2.4.2 Recording, microdialysis

The intracellular recordings were obtained using glass micropipettes filled with 3 M potassium acetate (DC resistance, 30-70 MΩ). A high-impedance amplifier (bandpass, 10 kHz) with an active bridge circuitry was used to record and inject currents into the cells. Stepping microdrive with minimal steps 0.5 μm (David Kopf Instruments, California, USA) was used to advance the intracellular micropipettes. Parallel recordings of focal field potential were obtained by means of tungsten electrodes inserted at different depths in the vicinity of recording pipettes. All electrical signals were sampled at 20 kHz and digitally stored on Vision (Nicolet, Wisconsin, USA). Offline computer analysis of electrographic recordings was done with IgorPro software (Lake Oswego, Oregon, USA). Statistical analysis was conducted with JMP software (Cary, North Carolina, USA). All numerical values are expressed as a mean ± standard deviation.

The modulation of $[Ca^{2+}]_o$ in the neocortex was achieved using reverse microdialysis method. The membrane of the microdialysis probe (2 mm length, 0.22 mm diameter from EICOM, Kyoto, Japan) was inserted in the cortex and the recording micropipettes were placed at 0.2-0.3 mm apart from the membrane. The microdialysis probe was perfused with the following solutions (concentration in mM): Control (NaCl 124, KCl, 2.5, $NaHCO_3$ 26, NaH_2PO_4 1.25, $MgSO_4$ 2, $MgCl_2$ 1, $CaCl_2$ 1), High calcium (NaCl 124, KCl, 2.5, $NaHCO_3$ 26, NaH_2PO_4 1.25, $MgSO_4$ 2, $MgCl_2$ 0, $CaCl_2$ 5), Calcium free (NaCl 125, KCl, 2.5, $NaHCO_3$ 26, NaH_2PO_4 0, $MgSO_4$ 2, $MgCl_2$ 1, $CaCl_2$ 0, $MnCl_2$ 1). The osmomolarity was adjusted to 300 mOsm. Each dialyzing solution was administrated for 15-30 min. The perfusion velocity was 5 µl/min and the total volume of tubing from the liquid switch to the probe was 12 µl. For other details concerning the microdialysis technique see (Crochet *et al.*, 2005).

2.4.3 Analysis

The initial step of the analysis consisted in averaging the APs of neurons. Averages were obtained from at least 20 to 50 APs. From averaged APs we estimated the firing threshold as the membrane potential at the time point at which the first derivative of the intracellular signal reach the threshold of 10 V/s (Sachdev et al. 2004). This threshold value was chosen because EPSPs have a rising slope slower than 10 V/s and faster rising slopes are reach only by regenerative APs (Crochet *et al.*, 2004) (Fig. 2.1). The exact value of the firing threshold was corrected for pipette offset by subtracting the offset measured when the pipette was withdrawn from the neuron. No effort was made to estimate transmembrane potential, because the values of transmembrane potential are significantly different from the values of membrane potential only during paroxysmal activities (Grenier *et al.*, 2003) and in normal conditions they could include an error of only ~0.5 mV (Henze & Buzsaki, 2001). The spike amplitude was measured as difference in voltage between the firing threshold and the peak of the AP. The spike-width was measured as the time difference between the ascending and descending fluctuations of membrane potential at spikes' half-amplitude. The maximal rising and decaying slopes of spike were taken, respectively, as the maximum and minimum of the first derivative of the AP. The spike-related AHP amplitude was calculated as the difference in voltage between the firing threshold and the maximal hyperpolarization that followed the spike. In addition we measured the mean

firing rates from periods of stable recordings that exceeded 5 min and we noted the depth of recorded neurons from micromanipulator readings.

2.5 Results

2.5.1 Database

We recorded intracellular activities of 103 cortical neurons from 36 cats anesthetized with ketamine-xylazine. All recorded neurons were identified by electrophysiological criteria (McCormick *et al.*, 1985; Gray & McCormick, 1996; Steriade *et al.*, 1998). The intracellular activity of 81 neurons was recorded in control conditions (without $[Ca^{2+}]_o$ change) to study AP and AHP parameters during spontaneous slow oscillations. The activity of the remaining 22 neurons was recorded in 2 or 3 different conditions of $[Ca^{2+}]_o$ to investigate the role of Ca^{2+} influx in the modulation of spike parameters and intrinsic firing pattern.

2.5.2 Activity dependent changes of spike parameters

In ketamine-xylazine anesthetized cats, cortical neurons revealed typically prolonged (>200 ms) hyperpolarizing (silent) states followed by long-lasting (>500 ms) depolarizing (active) states. Most of neocortical neurons fire multiple spikes throughout active states, those shape were apparently different (Fig. 2.2). In control conditions, 56 intracellular recordings were used to compare the parameters of the first spike with those of the last spike during the depolarizing phase of the slow oscillation. The first spontaneous AP occurs when the network activity just switched from silent to active phase, while the last spike occurs at the end of active phase. We found that all measured parameters of APs were affected by network activities (Fig. 2.2, Table 2.1). Following the period of network activity the amplitude of the spike, the amplitude of the AHP, the rising and decaying slopes decreased, the spike width increased, and the firing threshold was more depolarized ($p<0.0001$, paired t-test for each parameter). The amplitude of the AHP of the first spike that fired at the onset of the depolarizing phase was highly correlated with the spike width, maximal rising and decaying slopes, and marginally, but significantly correlated with the firing threshold (Table 2.2). Out of these parameters, the amplitude of AHP of the last spike did not correlate with the firing threshold. There was no significant correlation between AHP and spike amplitudes, nor was there between the mean firing rates and the depth of recorded neurons. The fact that the spike duration, as well as related parameters (maximal rising and

in particular decaying slopes), was correlated with AHP amplitude suggests that neurons with thinner spikes have larger AHP and thus that the intrinsic current mediating fAHP plays a role in controlling spike duration. The decrease in the amplitude of AHP toward the end of active network phase positively correlated with the amplitude of AHP of the first spike ($r=0.54$, $p<0.0001$). The reason for the decrease in AHP amplitude toward the end of the active phase was further investigated.

To characterize the activity dependent modulation of spike AHP we analyzed the parameters of spikes elicited by depolarizing current pulses during silent vs. active network states (n=25, Fig. 2.3). In this set of experiments, a slight negative holding current (-0.2 nA) was injected into neurons to abolish spontaneous firing. Averages of spikes elicited during the active or the silent periods showed that all the studied spike parameters except the AHP amplitude and the firing threshold were not statistically different ($p>0.1$). The firing threshold for spikes elicited during silent states was -49.9 ±4.6 mV and it was -52.7±5.0 mV during active states. Paired Student's t-test reveals statistically significant difference ($p<0.0001$). The AHP amplitude of APs elicited during silent network states was 5.73±2.79 mV and decreased to 3.24±2.70 mV during active states. This difference was also highly significant ($p<0.0001$, Student's paired t-test). The amplitude of AHP affected the expression of firing patterns in some neurons. All the three FRB neurons recorded in this set of experiments revealed a typical FRB firing pattern, consisting in high frequency spike-bursts repeated at gamma frequencies, during active states and fired single spikes with occasional spike doublets during silent states. An example is illustrated Figure 2.3C.

Modulation of AHP by $[Ca^{2+}]_o$

As we mentioned in the introduction, the $[Ca^{2+}]_o$ decreases during active network states, and thus, could decrease the amplitude of AHP mediated by $I_{K(Ca)}$ and modify firing pattern. To test this hypothesis we modified $[Ca^{2+}]_o$ with reversed microdialysis method and recorded intracellular activities from neurons located at 0.2-0.5 mm from the probe. The mean $[Ca^{2+}]_o$ during active periods measured with Ca^{2+} sensitive electrodes placed at ~ 0.2 mm from the probe (n=3) was 1.0±0.1 mM in control, 2.6±0.2 mM in high and 0.6±0.1 mM in low $[Ca^{2+}]_o$ conditions. In these conditions the spike amplitude and the maximal rising slope of spikes were not significantly different (Fig. 2.4, Table 2.3). In high $[Ca^{2+}]_o$

conditions, the width of APs at half amplitude shortened by 0.05±0.02 ms and these differences were significant (Table 2.3). In the same neurons the decay slope significantly decreased by 8.3±3.3 V/s in low $[Ca^{2+}]_o$ conditions, additionally indicating that $I_{K(Ca)}$ could contribute to the control of spike duration. However, the most significant changes were observed with spike AHPs (Table 2.3). The AHP in high Ca^{2+} conditions increased from control by 4.34 mV and it decreased by 2.17 mV in low Ca^{2+} conditions (Fig. 2.4). A decrease in AHP amplitude in low Ca^{2+} condition changed the spontaneous firing pattern. Out of 15 neurons identified as RS in control condition, 4 revealed spontaneous bursts of APs in low Ca^{2+} condition (not shown) or reveal groups of spikes (Fig. 2.4).

$[Ca^{2+}]_o$ modulates intrinsic excitability

To estimate the changes in intrinsic excitability related to the modulation of $[Ca^{2+}]_o$ we applied intracellularly depolarizing current pulses of variable amplitude (range 0.0-2.0 nA, duration 0.3 s) in different Ca^{2+} conditions and counted the number of spikes elicited per current pulse by neurons demonstrating RS firing pattern (n=22, Fig. 2.5). In all the levels of tested currents the increase in $[Ca^{2+}]_o$ to 2.6 mM significantly ($p<0.01$ [Tukey, HSD test]) decreased the number of spikes elicited per pulse. In some neurons (7 out of 22 tested) the lowering of $[Ca^{2+}]_o$ to 0.6 mM markedly increased the number of spikes elicited by current pulses of the same amplitude (Fig. 2.5), however, the statistical comparison for the studied population of neurons did not reveal any significant differences in a large range of depolarizing current pulses. The only significant increase in the number of spikes per current pulse ($p<0.05$) was observed when a current pulses of 1.5 nA or higher intensity were used. Decreasing $[Ca^{2+}]_o$ had another important effect; in 8 out of 22 neurons, the RS firing pattern recorded in control and high Ca^{2+} conditions changed to a bursting pattern (Fig. 2.5, middle and right columns).

2.6 Discussion

In this study we demonstrated that network activities influence multiple parameters of AP generated by neocortical neurons. In particular, the spike related AHP, which was correlated with the firing threshold, spike duration, rising and decaying slopes, was decreased during active periods and the spike duration was increased. Consistently with previous studies in hippocampus (Henze & Buzsaki, 2001) and somatosensory cortex (Sachdev *et al.*, 2004), APs generated at the end of active network states had a higher firing threshold. Since the AHP is mediated by $I_{K(Ca)}$, the major influence in the reduction of AHP amplitude at the end of active periods was probably due to a decreased Ca^{2+} entrance, which might be related to the decrease in $[Ca^{2+}]_o$ during active states (Massimini & Amzica, 2001; Crochet *et al.*, 2005). An increase in the $[K^+]_o$ during active phases of slow oscillation (Amzica & Steriade, 2000) would favour an increase in AHP amplitude, but this was not the case. In keeping with this idea, we found that an artificial increase in $[Ca^{2+}]_o$ via reverse microdialysis method significantly increased the AHP and a decrease in $[Ca^{2+}]_o$ decreased the AHP. Interestingly, the reduction of AHP, either during spontaneous activities or in conditions of artificially reduced $[Ca^{2+}]_o$, turned the RS firing pattern of some neurons into a bursting pattern. Thus, in addition to its effect on passive membrane properties (Destexhe *et al.*, 2003), shunting inhibition (Borg-Graham *et al.*, 1998; Hirsch *et al.*, 1998) and reduction of synaptic efficacy (Crochet *et al.*, 2005), network activity also modulates the discharge properties of neocortical neurons: it affects spike related AHP and subsequently, the intrinsic responsiveness and the firing patterns of neocortical neurons.

2.6.1 Dynamics of intrinsic firing patterns

Neocortical neurons reveal at least four distinct firing patterns: (a) RS, (b) IB, (c) FRB and (d) FS (McCormick *et al.*, 1985; Gray & McCormick, 1996; Steriade *et al.*, 1998). The ability of cortical neurons to generate spikes with a particular pattern is not stable and depends on multiple factors. An intracellular injection of depolarizing current transforms intrinsically-bursting firing pattern to RS one (Wang & McCormick, 1993; Timofeev *et al.*, 2000). Similar effect was observed after bath application of acetylcholine to neocortical

slices maintained *in vitro* (Wang & McCormick, 1993), activation induced by stimulation of mesopontine cholinergic nuclei (Steriade *et al.*, 1993a) or during change in behavioral states, from natural slow-wave sleep to REM sleep (Steriade *et al.*, 2001). Even in the absence of activity in cholinergic structures, the network activity, likely due to its depolarizing effects, decreases the incidence of intrinsically-bursting neurons. The occurrence of cortical intrinsically-bursting neurons is much higher (up to 40-60%) in cortical slices (Yang *et al.*, 1996) or cortical slabs *in vivo* (Timofeev *et al.*, 2000) than in the anesthetized animals (10 %) (Nuñez *et al.*, 1993). The increase in $[K^+]_o$ induces a conversion of some neurons with a RS firing pattern to an IB one (Jensen *et al.*, 1994; Jensen & Yaari, 1997). In this study we have shown that the presence of spontaneous activity as well as lowering $[Ca^{2+}]_o$ convert some neurons displaying RS firing patterns to FRB neurons. Fast-rhythmic-bursting neurons are found mainly *in vivo* (Gray & McCormick, 1996; Steriade *et al.*, 1998; Steriade *et al.*, 2001). In slices maintained *in vitro*, the FRB firing pattern could be induced either by prolonged intracellular stimulation (Kang & Kayano, 1994) or by the use of modified artificial cerebrospinal fluid, which contained physiological levels of $[Ca^{2+}]_o$ (Brumberg *et al.*, 2000). The AHP controls the spike duration as well as the firing pattern of cortical neurons. We found a significant correlation between the amplitude of spike AHP, the spike duration and maximal slope of the spike repolarization (Table 2). The stronger the AHP, the faster the decay and the shorter the spike duration. A strong AHP postponed the generation of consecutive spikes, thus preventing the generation of bursts. Since the AHP is mediated by activation of $I_{K(Ca)}$, the AHP amplitude decreased with a decrease in $[Ca^{2+}]_o$ due either to activity-related fluctuations (Massimini & Amzica, 2001; Crochet *et al.*, 2005) or to artificial changes. Despite the presence of high-threshold Ca^{2+} spikes in neocortical neurons *in vivo* (Paré & Lang, 1998), our results support previous reports that bursts in neocortical neurons are not Ca^{2+} dependent (Mantegazza *et al.*, 1998; Brumberg *et al.*, 2000), if they are not generated by low threshold Ca^{2+} current (de la Peña & Geijo-Barrientos, 1996) and that $I_{K(Ca)}$ is important in the control of burst generation.

2.6.2 Physiological implications

The alterations in the firing pattern of neocortical neurons due to the modulation of $[Ca^{2+}]_o$ during synchronous slow network activities could have at least two important physiological consequences: (a) Sleep is implicated in learning and memory formation (Maquet, 2001; Huber *et al.*, 2004). The synaptic plasticity enhanced or decreased by intrinsic neuronal currents is one of the mechanisms that could contribute to memory formation (Sejnowski & Destexhe, 2000; Steriade & Timofeev, 2003). Intracellularly, the state of slow-wave sleep in neocortical neurons is associated with the generation of long-lasting hyperpolarizing potentials, accompanied by neuronal silence, which are invariantly followed by the neuronal depolarization coupled with intense firing (Steriade *et al.*, 2001; Timofeev *et al.*, 2001). During the active periods, the neocortical synapses are likely at a steady-state of synaptic depression/facilitation, which recovers during silent periods (Galarreta & Hestrin, 1998). The enhancement of bursting during active periods, reported in the present study, would induce steady-state synaptic changes at accelerated rates, thus affecting sleep-related learning and memory processes. In addition to synaptic depression, the effectiveness of synaptic responses will be further reduced due to parallel decrease in $[Ca^{2+}]_o$ and related reduction of synaptic responses (Crochet *et al.*, 2005). (b) The increased intrinsic excitability in conditions of reduced $[Ca^{2+}]_o$ could play a significant role in the maintenance of paroxysmal activities. In hippocampal slices maintained in vitro in 0 mM $[Ca^{2+}]_o$ conditions promote epileptiform discharges (Jefferys & Haas, 1982; Taylor & Dudek, 1982). In neocortex too, electrographic seizures are associated with a marked reduction of $[Ca^{2+}]_o$ to the levels reaching 0.6 mM (Heinemann *et al.*, 1977; Amzica *et al.*, 2002). In these conditions the synaptic responsiveness of cortical neurons is largely impaired (Steriade & Amzica, 1999; Cisse *et al.*, 2004). As a consequence, the synchronization between different neocortical neurons is loose (Neckelmann *et al.*, 1998; Boucetta *et al.*, 2005). Still, the neocortical neurons generate paroxysmal depolarizing shifts, which contain an important intrinsic component (de Curtis *et al.*, 1999; Timofeev & Steriade, 2004). The $I_{K(Ca)}$ plays an important role in the control of PDSs amplitude and duration (Timofeev *et al.*, 2004; Timofeev & Steriade, 2004). Thus, we suggest that enhanced bursting of neuron in the conditions of reduced $[Ca^{2+}]_o$ might contribute to the generation paroxysmal activities.

Taken together, the data presented in this and our previous study (Crochet *et al.*, 2005) suggest that dynamic changes of $[Ca^{2+}]_o$ in neocortex during normal or paroxysmal activities affect both the synaptic and the intrinsic excitability, but tend to maintain a summated excitability at some homeostatic level. An increased intrinsic excitability would be associated with a reduction of synaptic excitability, and an increased synaptic excitability would be associated with a decrease in intrinsic excitability.

2.7 Tables

Table 2.1. Parameters of first and last spikes during active periods.

	Amplitude (mV)	Firing threshold (mV)	AHP amplitude (mV)	Spike width (ms)	Rising slope (v/s)	Decay slope (v/s)
First spike	61.7±8.8	-56.7±5.7	4.67±2.87	0.80±0.28	219.1±65.6	-99.1±38.2
Last spike	56.4±8.7	-53.9±5.7	3.32±2.50	0.88±0.32	181.1±60.3	-85.236.1
Difference	5.3±3.0	2.8±1.5	1.33±0.98	0.08±0.06	38.0±21.8	13.9±8.7

Table 2.2. Correlation (r) and its significance (p) of first and last spike AHPs with other spike parameters during active periods

	First spike AHP (r)	First spike AHP (p)	Last spike AHP (r)	Last spike AHP (p)
First spike amplitude	0.139	0.3067	0.090	0.5079
Last spike amplitude	0.139	0.3059	0.090	0.5073
First spike AHP	1		0.946	<0.0001
Last spike AHP	0.946	<0.0001	1	
First spike width	-0.470	0.0003	-0.432	0.0009
Last spike width	-0.503	<0.0001	-0.471	0.0003
First spike threshold	0.328	0.0135	0.263	0.0502
Last spike threshold	0.290	0.0299	0.228	0.0916
First spike raising slope	0.484	0.0002	0.430	0.0010
Last spike raising slope	0.531	<0.0001	0.469	0.0003
First spike decay slope	-0.499	<0.0001	-0.451	0.0005
Last spike decay slope	-0.553	<0.0001	-0.511	<0.0001

Table 2.3. Statistical significance of differences (p) in action potential parameters in pairs of different Ca^{2+} conditions.

	Spike amplitude (mV)	Spike width (ms)	Rising slope (v/s)	Decaying slope (v/s)	AHP amplitude (mV)
Control-High (n=20)	0.1112	**0.0261**	0.0977	0.2550	**<0.0001**
Control-Low (n=15)	0.0902	0.1427	0.8421	**0.0226**	**<0.0001**
High-Low (n=13)	0.7029	**0.0141**	0.6874	**0.0103**	**<0.0001**

Statistically significant differences are indicated in bold.

2.8 Figures

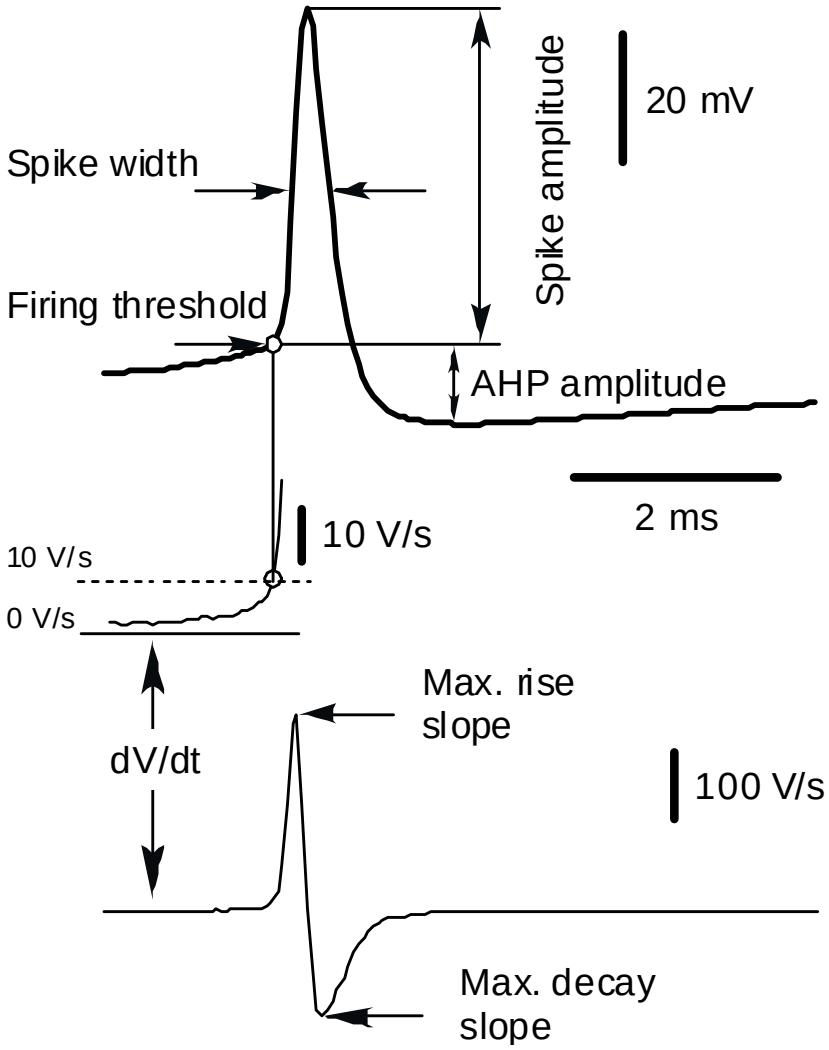

Figure 2.1

Fig. 2.1. Parameters of action potentials measured in the present study.

Upper trace – averaged spike, lower trace – first derivative of the spike. The measured parameters are indicated.

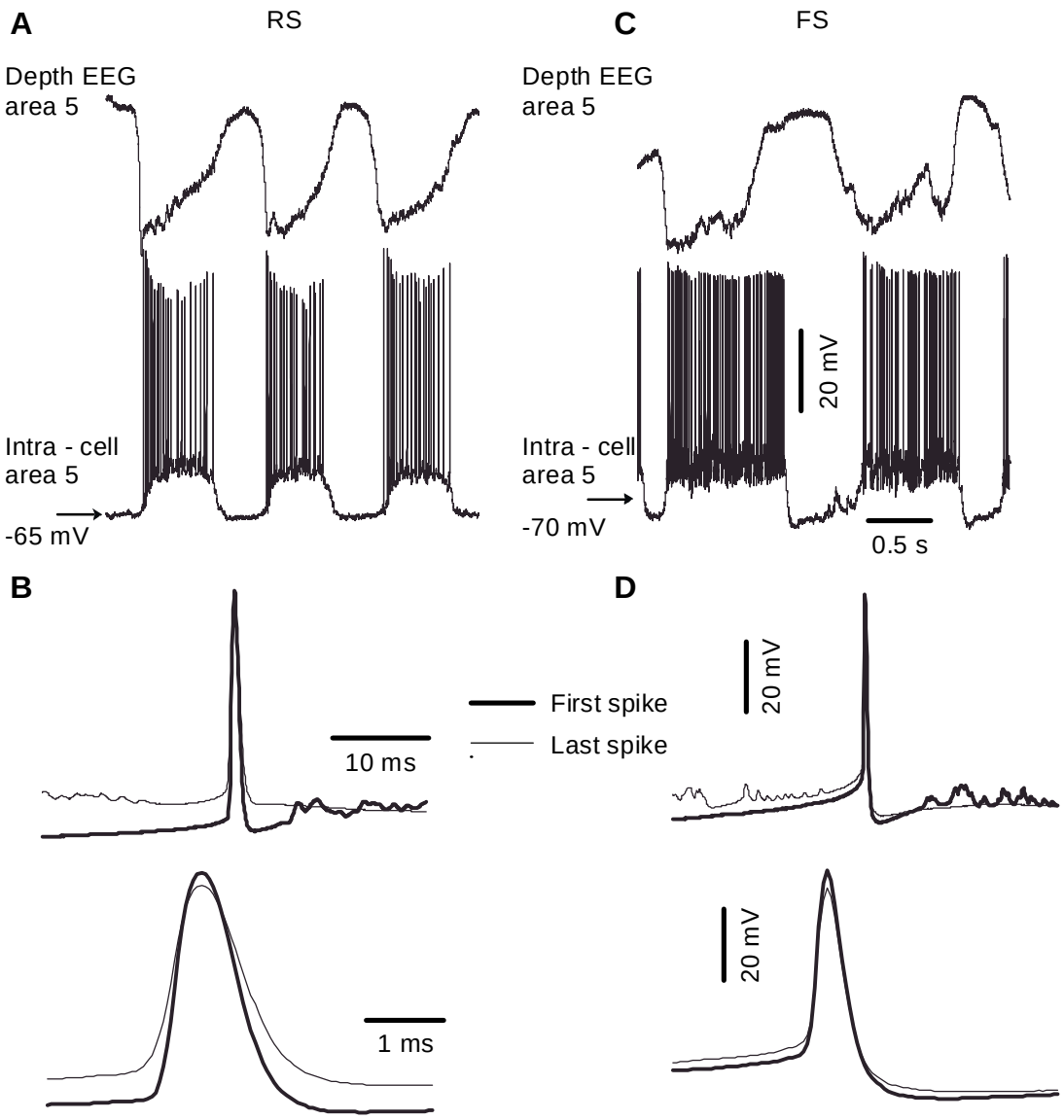
A
RS
Depth EEG
area 5
Intra - cell
area 5
-65 mV
C
FS
Depth EEG
area 5
20 mV
Intra - cell
area 5
-70 mV
0.5 s
B
10 ms
First spike
Last spike
1 ms
D
20 mV
20 mV

Figure 2.2

Figure 2.2: Modulation of spike parameters in neocortical neurons by spontaneous network activities during slow oscillations.

A and **C** – periods of spontaneous field potential and intracellular activity from two different neurons. **A**, regular-spiking (RS) neuron, **C**, fast-spiking (FS) neuron. **B** and **D**, averages of first and last spikes spontaneously occurring during active periods from the same neurons.

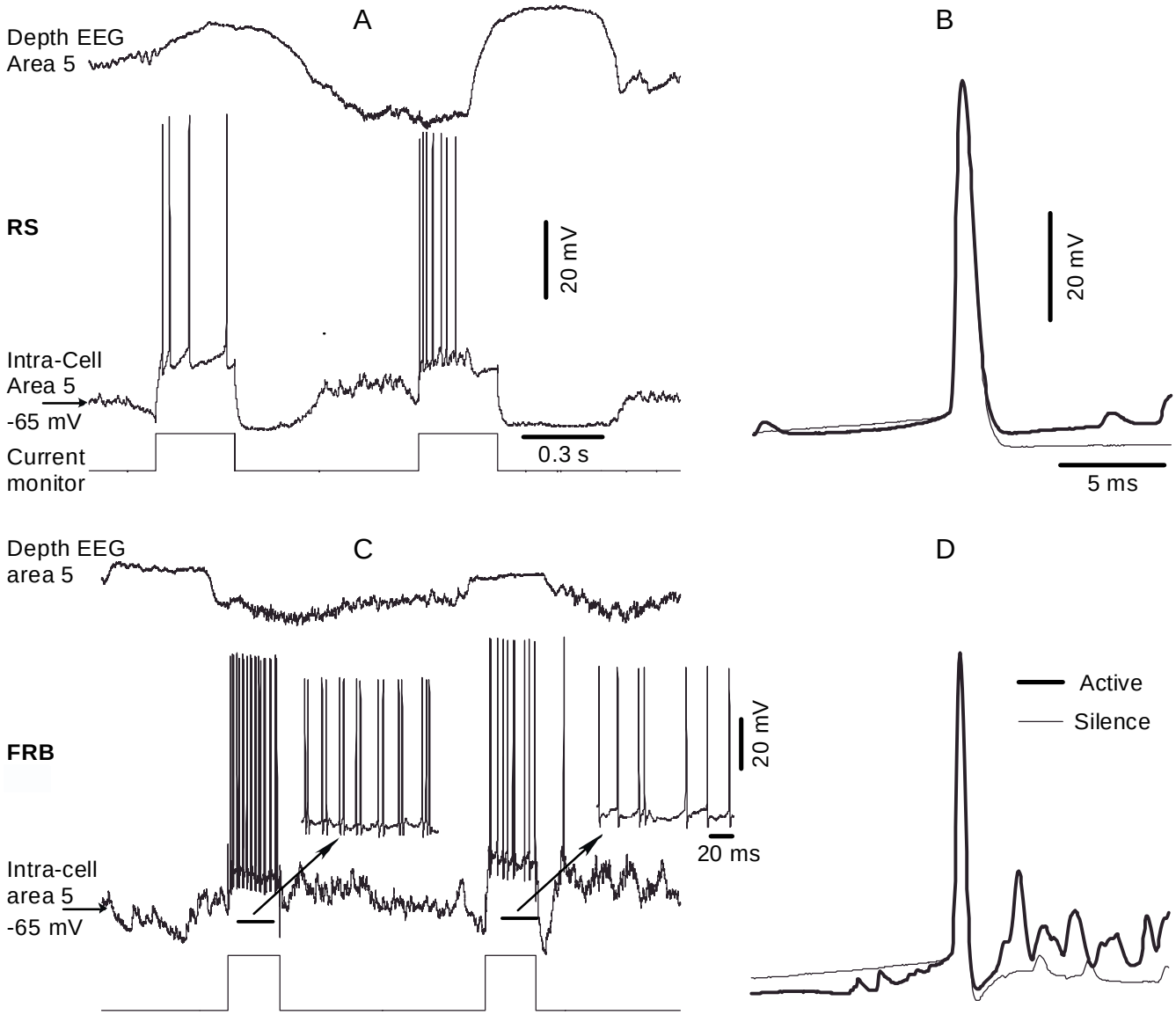
A
Depth EEG
Area 5
RS
20 mV
Intra-Cell
Area 5
-65 mV
Current
monitor
0.3 s
B
20 mV
5 ms
C
Depth EEG
area 5
FRB
20 mV
20 ms
Intra-cell
area 5
-65 mV
D
Active
Silence

Figure 2.3

Figure 2.3: Modulation of spike parameters of cortical neurons during active versus silent network states.

To prevent extensive spontaneous firing, a "-0.2" nA holding current was applied to both neurons shown in panels A and B, and C and D. **A**, depolarizing current pulses of 0.5 nA were applied to RS neuron during active and silent network states. **B**, averages of spikes elicited during active (thick line) and silent (thin line) network states. **C**, depolarizing current pulses of 1.0 nA were applied to the fast-rhythmic-bursting neuron during active and silent network states. Note that FRB pattern of firing was seen only during active network states. **D**, averages of spikes elicited during active (thick line) and silent (thin line) network states. Note in panels B and D that the spike amplitude, duration, rising and decaying phases was similar, but the AHP of spike elicited during active network states are reduced in amplitude.

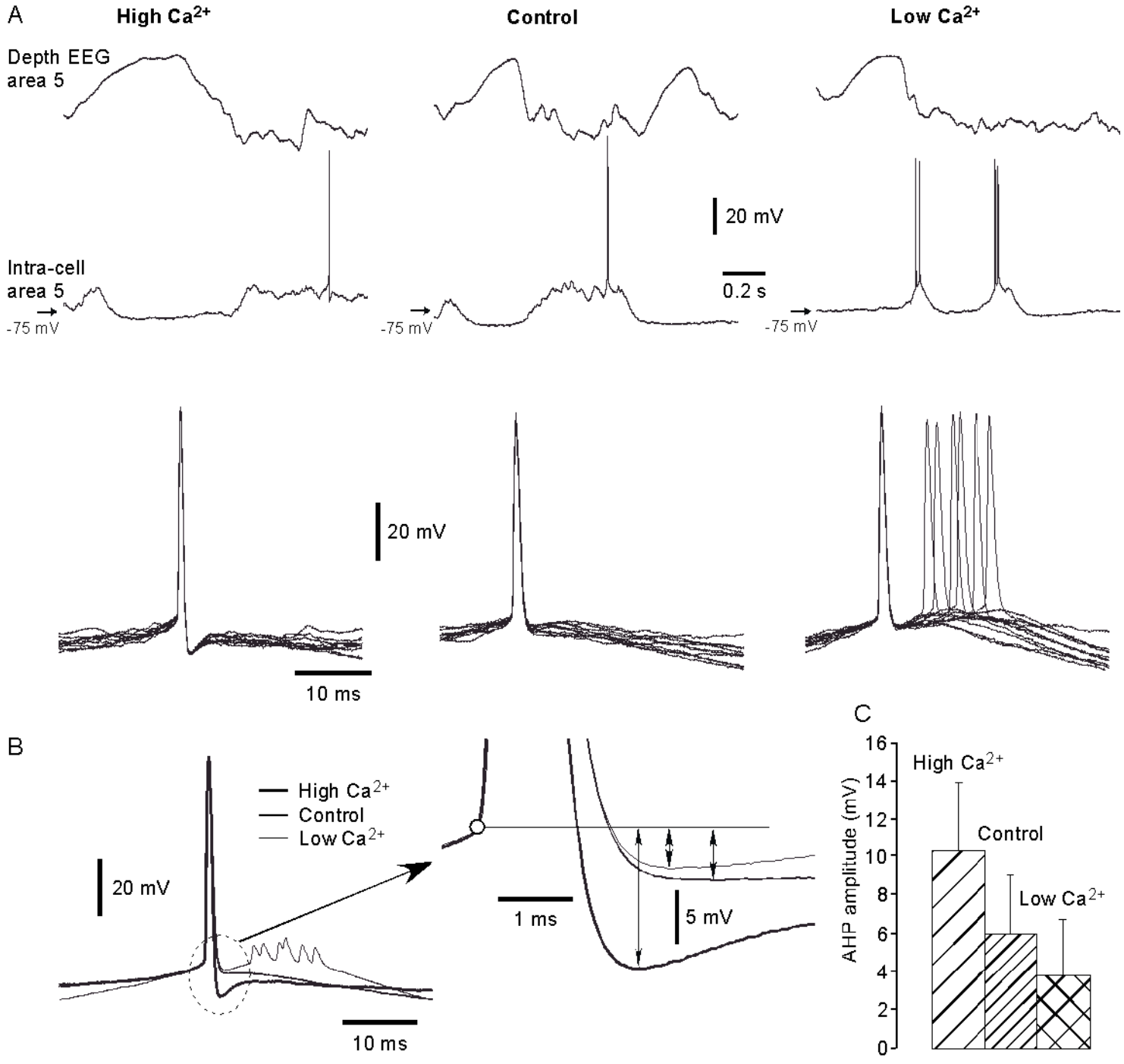
A
High Ca2+
Control
Low Ca2+
Depth EEG
area 5
Intra-cell
area 5
-75 mV
-75 mV
-75 mV
20 mV
0.2 s
20 mV
10 ms
B
High Ca2+
Control
Low Ca2+
20 mV
10 ms
1 ms
5 mV
C
AHP amplitude (mV)
16
14
12
10
8
6
4
2
0
High Ca2+
Control
Low Ca2+

Figure 2.4

Fig. 2.4. Impact of $[Ca^{2+}]_o$ modulation on spontaneous firing of cortical neurons.
A, The same neuron recorded under high, control, and low $[Ca^{2+}]_o$ conditions. Below, superposed spontaneous spikes (n=10) selected during these three different levels of $[Ca^{2+}]_o$. **B**, Averages of spontaneous spikes during these three different $[Ca^{2+}]_o$ conditions. Note the increase of AHP amplitude as $[Ca^{2+}]_o$ is high. **C**, Histograms of mean ± SD AHP amplitude in three different $[Ca^{2+}]_o$ conditions (n=22).

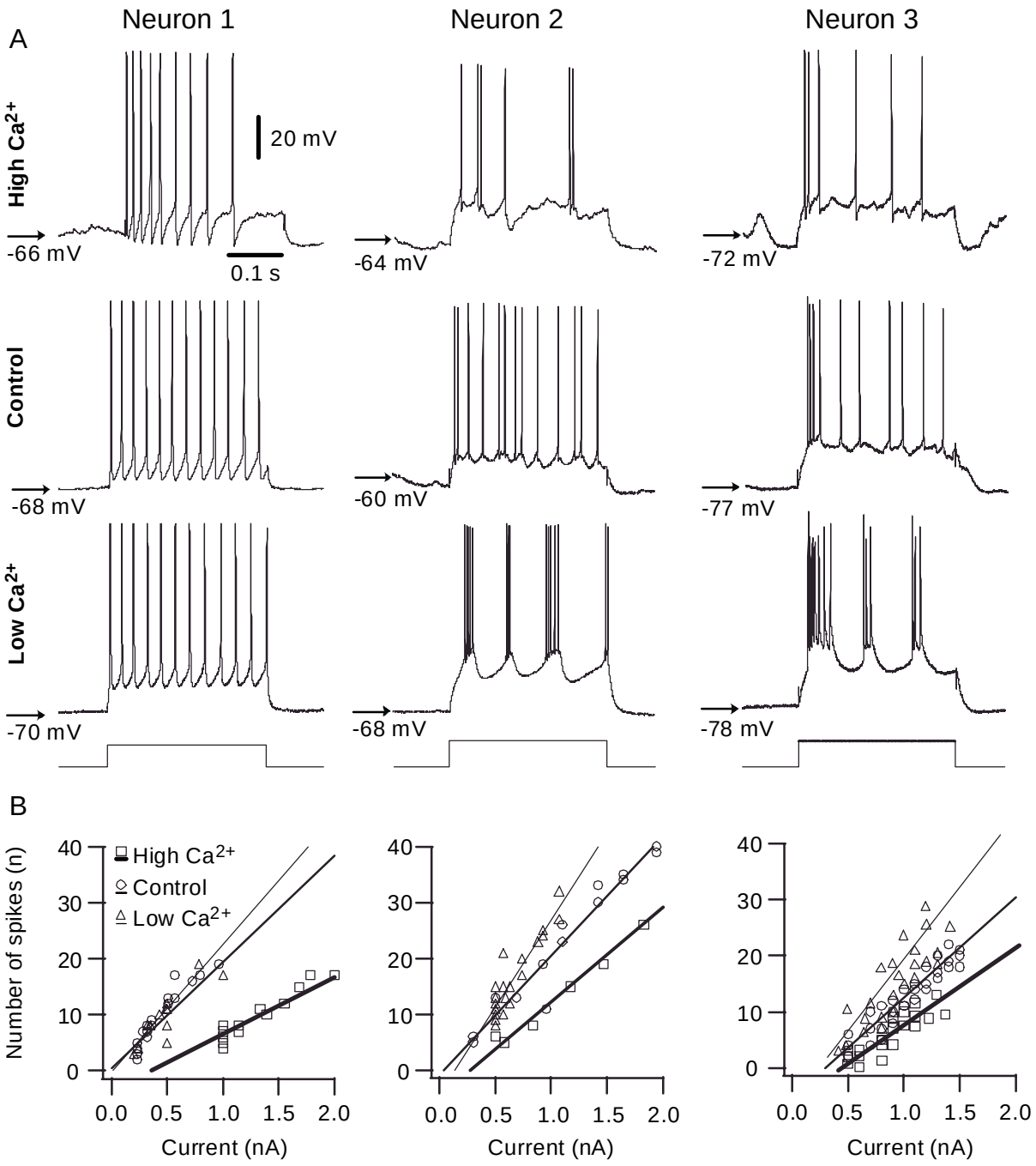
Neuron 1
Neuron 2
Neuron 3
A
High Ca2+
20 mV
0.1 s
-66 mV
-64 mV
-72 mV
Control
-68 mV
-60 mV
-77 mV
Low Ca2+
-70 mV
-68 mV
-78 mV
B
Number of spikes (n)
High Ca2+
Control
Low Ca2+
0
10
20
30
40
0.0
0.5
1.0
1.5
2.0
Current (nA)

Figure 2.5

Figure 2.5: Modulation of $[Ca^{2+}]_o$ affects intrinsic excitability and firing patterns.
A, neuronal excitability was tested by injection of depolarizing current pulses of variable intensity. Examples of responses shown for three different neurons during high, control and low conditions of $[Ca^{2+}]_o$. **B**, plots showing the number of action potentials elicited by intracellularly applied current pulses of different intensity. Note a decrease in the number of action potentials as $[Ca^{2+}]_o$ increases and the bursting response during low $[Ca^{2+}]_o$ conditions for the second (middle column) and third neuron (right column).

2.9 References

Abel, H. J., Lee, J. C., Callaway, J. C. & Foehring, R. C. (2004). Relationships between intracellular calcium and afterhyperpolarizations in neocortical pyramidal neurons. *J Neurophysiol* **91,** 324-335.

Achermann, P. & Borbely, A. A. (1997). Low-frequency (< 1 Hz) oscillations in the human sleep electroencephalogram. *Neuroscience* **81,** 213-222.

Amzica, F., Massimini, M. & Manfridi, A. (2002). Spatial buffering during slow and paroxysmal sleep oscillations in cortical networks of glial cells in vivo. *J Neurosci* **22,** 1042-1053.

Amzica, F. & Steriade, M. (2000). Neuronal and glial membrane potentials during sleep and paroxysmal oscillations in the neocortex. *J Neurosci* **20,** 6648-6665.

Borg-Graham, L. J., Monier, C. & Fregnac, Y. (1998). Visual input evokes transient and strong shunting inhibition in visual cortical neurons. *Nature* **393,** 369-373.

Boucetta, S., Chauvette, S. & Timofeev, I. (2005). Focal generation of paroxysmal fast runs during electrographic seizures. *J Neurophysiol* **submitted**.

Brumberg, J. C., Nowak, L. G. & McCormick, D. A. (2000). Ionic mechanisms underlying repetitive high-frequency burst firing in supragranular cortical neurons. *J Neurosci* **20,** 4829-4843.

Cisse, Y., Crochet, S., Timofeev, I. & Steriade, M. (2004). Synaptic responsiveness of neocortical neurons to callosal volleys during paroxysmal depolarizing shifts. *Neuroscience* **124,** 231-239.

Contreras, D. & Steriade, M. (1995). Cellular basis of EEG slow rhythms: a study of dynamic corticothalamic relationships. *J Neurosci* **15,** 604-622.

Crochet, S., Chauvette, S., Boucetta, S. & Timofeev, I. (2005). Modulation of synaptic transmission in neocortex by network activities. *Eur J Neurosci* **21,** 1030-1044.

Crochet, S., Fuentealba, P., Timofeev, I. & Steriade, M. (2004). Selective amplification of neocortical neuronal output by fast prepotentials in vivo. *Cereb Cortex* **14,** 1110-1121.

de Curtis, M., Radici, C. & Forti, M. (1999). Cellular mechanisms underlying spontaneous interictal spikes in an acute model of focal cortical epileptogenesis. *Neuroscience* **88,** 107-117.

de la Peña, E. & Geijo-Barrientos, E. (1996). Laminar localization, morphology, and physiological properties of pyramidal neurons that have the low-threshold calcium current in the guinea-pig medial frontal cortex. *J Neurosci* **16,** 5301-5311.

Destexhe, A., Rudolph, M. & Pare, D. (2003). The high-conductance state of neocortical neurons in vivo. *Nat Rev Neurosci* **4,** 739-751.

Faber, E. S., Callister, R. J. & Sah, P. (2001). Morphological and electrophysiological properties of principal neurons in the rat lateral amygdala in vitro. *J Neurophysiol* **85,** 714-723.

Franceschetti, S., Lavazza, T., Curia, G., Aracri, P., Panzica, F., Sancini, G., Avanzini, G. & Magistretti, J. (2003). Na+-activated K+ current contributes to postexcitatory hyperpolarization in neocortical intrinsically bursting neurons. *J Neurophysiol* **89,** 2101-2111.

Galarreta, M. & Hestrin, S. (1998). Frequency-dependent synaptic depression and the balance of excitation and inhibition in the neocortex. *Nat Neurosci* **1,** 587-594.

Gray, C. M. & McCormick, D. A. (1996). Chattering cells: superficial pyramidal neurons contributing to the generation of synchronous oscillations in the visual cortex. *Science* **274,** 109-113.

Grenier, F., Timofeev, I., Crochet, S. & Steriade, M. (2003). Spontaneous field potentials influence the activity of neocortical neurons during paroxysmal activities in vivo. *Neuroscience* **119,** 277-291.

Heinemann, U., Lux, H. D. & Gutnick, M. J. (1977). Extracellular free calcium and potassium during paroxsmal activity in the cerebral cortex of the cat. *Exp Brain Res* **27,** 237-243.

Henze, D. A. & Buzsaki, G. (2001). Action potential threshold of hippocampal pyramidal cells in vivo is increased by recent spiking activity. *Neuroscience* **105,** 121-130.

Hirsch, J. A., Alonso, J. M., Reid, R. C. & Martinez, L. M. (1998). Synaptic integration in striate cortical simple cells. *J Neurosci* **18,** 9517-9528.

Hirst, G. D., Johnson, S. M. & van Helden, D. F. (1985). The slow calcium-dependent potassium current in a myenteric neurone of the guinea-pig ileum. *J Physiol* **361,** 315-337.

Huber, R., Ghilardi, M. F., Massimini, M. & Tononi, G. (2004). Local sleep and learning. *Nature* **430,** 78-81.

Jefferys, J. G. & Haas, H. L. (1982). Synchronized bursting of CA1 hippocampal pyramidal cells in the absence of synaptic transmission. *Nature* **300,** 448-450.

Jensen, M. S., Azouz, R. & Yaari, Y. (1994). Variant firing patterns in rat hippocampal pyramidal cells modulated by extracellular potassium. *J Neurophysiol* **71,** 831-839.

Jensen, M. S. & Yaari, Y. (1997). Role of intrinsic burst firing, potassium accumulation, and electrical coupling in the elevated potassium model of hippocampal epilepsy. *J Neurophysiol* **77,** 1224-1233.

Kang, Y. & Kayano, F. (1994). Electrophysiological and morphological characteristics of layer VI pyramidal cells in the cat motor cortex. *J Neurophysiol* **72,** 578-591.

Lancaster, B. & Nicoll, R. A. (1987). Properties of two calcium-activated hyperpolarizations in rat hippocampal neurones. *J Physiol* **389,** 187-203.

Mantegazza, M., Franceschetti, S. & Avanzini, G. (1998). Anemone toxin (ATX II)-induced increase in persistent sodium current: effects on the firing properties of rat neocortical pyramidal neurones. *J Physiol* **507,** 105-116.

Maquet, P. (2001). The role of sleep in learning and memory. *Science* **294,** 1048-1052.

Markram, H., Helm, P. & Sakmann, B. (1995). Dendritic calcium transients evoked by single back-propagating action potentials in rat neocortical pyramidal neurons. *J Physiol* **485,** 1-20.

Massimini, M. & Amzica, F. (2001). Extracellular calcium fluctuations and intracellular potentials in the cortex during the slow sleep oscillation. *J Neurophysiol* **85,** 1346-1350.

McCormick, D. A. (1999). Membrane potential and action potential. In *Fundamental neuroscience*. ed. Zigmond, M. J., Bloom, F. E., Landis, S. C., Roberts, J. L. & Squire, L. R., pp. 129-154. Academic Press, San Diego, London, Boston, New York, Sydney, Tokyo, Toronto.

McCormick, D. A., Connors, B. W., Lighthall, J. W. & Prince, D. A. (1985). Comparative electrophysiology of pyramidal and sparsely spiny stellate neurons of the neocortex. *J Neurophysiol* **54,** 782-806.

Neckelmann, D., Amzica, F. & Steriade, M. (1998). Spike-wave complexes and fast components of cortically generated seizures. III. Synchronizing mechanisms. *J Neurophysiol* **80,** 1480-1494.

Nuñez, A., Amzica, F. & Steriade, M. (1993). Electrophysiology of cat association cortical cells in vitro: Intrinsic properies and synaptic responses. *J Neurophysiol* **70,** 418-430.

Paré, D. & Lang, E. J. (1998). Calcium electrogenesis in neocortical pyramidal neurons in vivo. *Eur J Neurosci* **10,** 3164-3170.

Sachdev, R. N. S., Ebner, F. F. & Wilson, C. J. (2004). Effect of subthreshold up and down states on the whisker-evoked response in somatosensory cortex. *J Neurophysiol* **92,** 3511-3521.

Sah, P. & Louise Faber, E. S. (2002). Channels underlying neuronal calcium-activated potassium currents. *Prog Neurobiol* **66,** 345-353.

Sah, P. & McLachlan, E. M. (1991). Ca(2+)-activated K+ currents underlying the afterhyperpolarization in guinea pig vagal neurons: a role for Ca(2+)-activated Ca2+ release. *Neuron* **7,** 257-264.

Schwindt, P. C., Spain, W. J., Foehring, R. C., Stafstrom, C. E., Chubb, M. C. & Crill, W. E. (1988). Multiple potassium conductances and their functions in neurons from cat sensorimotor cortex in vitro. *J Neurophysiol* **59,** 424-449.

Sejnowski, T. J. & Destexhe, A. (2000). Why do we sleep? *Brain Res* **886,** 208-223.

Steriade, M. (2004). Neocortical cell classes are flexible entities. *Nat Rev Neurosci* **5,** 121-134.

Steriade, M. & Amzica, F. (1999). Intracellular study of excitability in the seizure-prone neocortex in vivo. *J Neurophysiol* **82,** 3108-3122.

Steriade, M., Amzica, F. & Nuñez, A. (1993a). Cholinergic and noradrenergic modulation of the slow (approximately 0.3 Hz) oscillation in neocortical cells. *J Neurophysiol* **70,** 1385-1400.

Steriade, M., Contreras, D., Dossi, R. C. & Nuñez, A. (1993b). The slow (<1 Hz) oscillation in reticular thalamic and thalamo-cortical neurons: scenario of sleep rhythm generation in interacting thalamic and neocortical networks. *J Neurosci* **13,** 3284-3299.

Steriade, M., Nuñez, A. & Amzica, F. (1993c). Intracellular analysis of relations between the slow (<1 Hz) neocortical oscillations and other sleep rhythms of electroencephalogram. *J Neurosci* **13,** 3266-3283.

Steriade, M., Nuñez, A. & Amzica, F. (1993d). A novel slow (<1 Hz) oscillation of neocortical neurons *in vivo* : depolarizing and hyperpolarizing components. *J Neurosci* **13,** 3252-3265.

Steriade, M. & Timofeev, I. (2003). Neuronal plasticity in thalamocortical networks during sleep and waking oscillations. *Neuron* **37,** 563-576.

Steriade, M., Timofeev, I., Dürmüller, N. & Grenier, F. (1998). Dynamic properties of corticothalamic neurons and local cortical interneurons generating fast rhythmic (30-40 Hz) spike bursts. *J Neurophysiol* **79,** 483-490.

Steriade, M., Timofeev, I. & Grenier, F. (2001). Natural waking and sleep states: a view from inside neocortical neurons. *J Neurophysiol* **85,** 1969-1985.

Storm, J. F. (1987). Action potential repolarization and a fast after-hyperpolarization in rat hippocampal pyramidal cells. *J Physiol* **385,** 733-759.

Taylor, C. P. & Dudek, F. E. (1982). Synchronous neural afterdischarges in rat hippocampal slices without active chemical synapses. *Science* **218,** 810-812.

Timofeev, I., Grenier, F., Bazhenov, M., Sejnowski, T. J. & Steriade, M. (2000). Origin of slow cortical oscillations in deafferented cortical slabs. *Cereb Cortex* **10,** 1185-1199.

Timofeev, I., Grenier, F. & Steriade, M. (2001). Disfacilitation and active inhibition in the neocortex during the natural sleep-wake cycle: An intracellular study. *Proc Natl Acad Sci U S A* **98,** 1924-1929.

Timofeev, I., Grenier, F. & Steriade, M. (2004). Contribution of intrinsic neuronal factors in the generation of cortically driven electrographic seizures. *J Neurophysiol* **92,** 1133-1143.

Timofeev, I. & Steriade, M. (2004). Neocortical seizures: initiation, development and cessation. *Neuroscience* **123,** 299-336.

Wang, Z. & McCormick, D. A. (1993). Control of firing mode of corticotectal and corticopontine layer V burst-generating neurons by norepinephrine, acetilcholine, and 1S,3R-ACPD. *J Neurosci* **13,** 2199-2216.

Yang, C. R., Seamans, J. K. & Gorelova, N. (1996). Electrophysiological and morphological properies of layers V-VI principal pyramidal cells in rat prefrontal cortex*in vitro*. *J Neurosci* 16, 1904-1921.

Chapter III

3. Focal generation of paroxysmal fast runs during electrographic seizures

Sofiane Boucetta, Sylvain Chauvette, Maxim Bazhenov and Igor Timofeev. *Submitted to the Journal of Neurophysiology (2005).*

3.1 Résumé

Les crises de type Lennox-Gastaut générées par le cortex sont associées à des décharges de type pointe-onde et polypointes-onde de 2-3 Hz et des ondes paroxysmales rapides (*fast runs)* de 8-15 Hz. Dans cette étude, en utilisant des enregistrements intracellulaires et des potentiels de champ à multisites *in vivo*, et des modèles computationels, nous avons analysé les patrons de synchronisation des ondes paroxysmales rapides durant des crises spontanées enregistrées chez des chats anesthésiés par ketamine-xylazine. Dans différentes expériences, les électrodes d'enregistrement ont été placées soit à courtes distances (< 1 mm) ou à longues distances (jusqu'à 12 mm). Dans la majorité des cas, le commencement et la fin des ondes rapides se produisent presque simultanément dans les différents sites d'enregistrement, ce qui suggère un contrôle extracortical de ces évènements. L'amplitude et la durée des ondes rapides peuvent varier significativement jusqu'à l'abolition totale enregistrée par certaines électrodes. Pendant les ondes rapides, les patrons de synchronisation enregistrés au niveau des différentes électrodes ont été les suivants : (i) synchrone, en phase, (ii) synchrone, avec décalage en phase, (iii) changement, répété en phase/ des transitions avec décalage en phase et (iv) non-synchrone, soit des fréquences légèrement différentes dans les différents sites d'enregistrement, soit l'absence de l'activité oscillatoire dans un des sites d'enregistrement; Tous ces patrons peuvent être enregistrés dans la même paire d'électrode durant différentes crises. Les neurones en bouffées de potentiels d'action (IB) déchargent plus de potentiels d'action par cycle que d'autres neurones, ce qui suggère leur rôle principal dans la génération des ondes paroxysmiques rapides. Une fois commencées, les ondes paroxysmiques rapides sont générées localement avec peu, s'il y en a, de communication entre les foyers corticaux voisins.

3.2 Abstract

A cortically generated Lennox-Gastaut type seizure is associated with spike-wave/polyspike-wave discharges at 2-3 Hz and fast runs at 7-16 Hz. In this study, using multisite field potential and intracellular recordings in vivo and computational models, we analyzed the synchronization patterns of paroxysmal fast runs during spontaneous seizures recorded from cats anesthetized with ketamine-xylazine. In different experiments, the recording electrodes were located either at short distances (<1mm) or at longer distances (up to 12 mm). In the majority of cases, the onset and the offset of fast runs occurred almost simultaneously in different recording sites suggesting extracortical control of these events. The amplitude and duration of fast runs could vary significantly, up to full abolition recorded with some electrodes. Within the fast runs, the patterns of synchronization recorded in different electrodes were as following: (i) synchronous, in phase, (ii) synchronous, with phase shift, (iii) patchy, repeated in phase/phase shift transitions and (iv) non-synchronous, slightly different frequencies in different recording sites or absence of oscillatory activity in one of the recording sites; the synchronous patterns (in phase or with phase shifts) were most common. All these patterns could be recorded in the same pair of electrodes during different seizures. Intrinsically-bursting (IB) neurons fired more spikes per cycle than any other neurons suggesting their leading role in the fast run generation. Once started, the fast runs are generated locally with little, if any, communication between neighboring cortical foci.

3.3 Introduction

Sleep related epilepsy is characterized by seizures developing during periods of slow-wave sleep. Studies on experimental animals point to the intracortical generation of some types of such seizures (Steriade and Contreras 1998). These seizures are characterized by spike-wave (SW) or spike-wave/polyspike-wave (SW/PSW) complexes of 1.5-3 Hz, intermingled with episodes of fast runs at ~7-16 Hz (Neckelmann et al. 1998; Steriade and Contreras 1998; Steriade et al. 1998b; Timofeev et al. 1998). The evolvement of these seizures from the cortically generated slow oscillation, might be shaped by the thalamus (Hughes et al. 2002; Steriade and Contreras 1995; Steriade and Timofeev 2001; Steriade et al. 1998b). The electrographical pattern of these seizures as well as their occurrence during slow-wave sleep resemble the seizures accompanying Lennox-Gastaut syndrome of humans (Halasz 1991; Kotagal 1995; Niedermeyer 1999a, b). The prolonged (more than 2-3 sec) periods of runs of fast EEG spikes were usually associated with tonic components of seizures accompanying Lennox-Gastaut syndrome (Niedermeyer 1999a). The detailed pattern of synchronization as well as the cellular basis of fast runs is not well understood. Previous single-case human study have shown that an increase in the synchronization stops the runs of fast EEG spikes (Ferri et al. 2004). Animal studies showed that (a) the thalamus is not involved in the generation of fast runs (Timofeev et al. 1998), (b) the inhibitory activities in neocortex are impaired during the fast runs (Timofeev et al. 2002), and (c) these changes occur in parallel with decrease in the neuronal input resistance (Matsumoto et al. 1969; Neckelmann et al. 2000; Timofeev et al. 2002) and decrease in the concentration of extracellular Ca^{2+} (Amzica et al. 2002; Heinemann et al. 1977).

During normal (not paroxysmal) brain activities, both the excitatory and inhibitory synaptic interactions provide mechanisms for the synchronization among neighboring recording sites. In a condition of low extracellular Ca^{2+} concentration, impaired inhibitory activities, and low input resistance, the synchronization should be impaired. Thus, we hypothesize that paroxysmal runs of fast EEG spikes are generated locally in a quasi independent manner. The present study supports this hypothesis and provides data on the neuronal basis and patterns of synchronization during fast runs generated within spontaneous electrographic seizures.

3.4 Materials and methods

3.4.1 In vivo experiments

Experiments were conducted on adult cats anesthetized with ketamine-xylazine anesthesia (10-15 and 2-3 mg/kg i.m., respectively). The animals were paralyzed with gallamine triethiodide (20 mg/kg) after the EEG showed typical signs of deep general anesthesia, essentially consisting of a slow oscillation (0.5-1 Hz). Supplementary doses of the same anesthetics (5 and 1 mg/kg) or simply ketamine (5 mg/kg) were administered at the slightest changes toward the diminished amplitudes of slow waves. The cats were ventilated artificially with the control of end-tidal CO_2 at 3.5-3.7%. The body temperature was maintained at 37-38^{o}C and the heart rate was ~90-100 beats/min. For intracellular recordings, the stability was ensured by the drainage of cisterna magna, hip suspension, bilateral pneumothorax, and by filling the hole made for recordings with a solution of 4% agar. At the end of experiments, the cats were given a lethal dose of pentobarbital (50 mg/kg i.v.). All experimental procedures were performed according to national guidelines and were approved by the committee for animal care of Laval University.

Single, dual, triple or quadruple intracellular recordings from suprasylvian association areas 5 and 7 were performed using glass micropipettes filled with a solution of 3 M potassium-acetate (KAc). A high-impedance amplifier with active bridge circuitry was used to record the membrane potential (V_m) and inject current into the neurons. Field potentials were recorded in the vicinity of impaled neurons and also from more distant sites, using bipolar coaxial electrodes, with the ring (pial surface) and the tip (cortical depth) separated by 0.8-1 mm. In 12 cats, arrays of 7 or 8 electrodes, ~1.5 mm apart, were inserted along the suprasylvian gyrus. All electrical signals were sampled at 20 kHz and digitally stored on Vision (Nicolet, Wisconsin, USA). Offline computer analysis of electrographic recordings was done with IgorPro software (Lake Oswego, Oregon, USA). Statistical analysis was conducted with JMP software (Cary, North Carolina, USA). All numerical values are expressed as a mean ± standard deviation.

3.4.2 Computational models

Two cortical models were simulated: 1) a circuit with coupled pyramidal (PY) cell and inhibitory interneuron (IN); 2) a one-dimensional chain of 100 PY neurons and 25 INs. In the network model, the connection fan out was ± 5 neurons for AMPA-mediated PY-PY synapses, ± 1 neuron for AMPA-mediated PY-IN synapses, ± 5 neurons for $GABA_A$-mediated IN-PY synapses. All AMPA- and $GABA_A$-mediated synapses were modeled by first-order activation schemes (Destexhe et al. 1994), and the expressions for the kinetics are given elsewhere (Bazhenov et al. 1998). A simple model of synaptic plasticity (USE=7%, τ=700 msec) was used to describe depression of synaptic connections (Abbott et al. 1997; Galarreta and Hestrin 1998; Timofeev et al. 2000; Tsodyks and Markram 1997). A maximal synaptic conductance was multiplied to depression variable, $D \leq 1$, representing the amount of available ``synaptic resources'': $D = 1 - (1 - D_i(1-U)) \exp(-(t-t_i)/\tau)$, where U=0.07 is the fraction of resources used per action potential, τ = 700 ms the time constant of recovery of the synaptic resources, D_i the value of D immediately before the i_{th} event, and $(t-t_i)$ the time after i_{th} event.

Each PY and IN cell was modeled by two-compartments that included fast Na^+ channels, I_{Na}, and a persistent sodium current, $I_{Na(p)}$, (Alzheimer et al. 1993; Kay et al. 1998) in the axo-somatic and dendritic compartments (Mainen and Sejnowski 1996). A slow voltage-dependent non-inactivating K^+ current, I_{Km}, a slow Ca^{2+} dependent K^+ current, $I_{K(Ca)}$, a high-threshold Ca^{2+} current, I_{Ca}, hyperpolarization-activated depolarizing current I_h were included in the dendritic compartment. A fast delayed rectifier potassium K^+ current, I_K, was present in the axo-somatic compartment. The expressions for the voltage- and Ca^{2+}-dependent transition rates for all other currents are given in (Bazhenov et al. 2004; Timofeev et al. 2000). Reversal potentials for all K^+-mediated currents were calculated using Nernst equation. The extracellular K^+ concentration was continuously updated based on K^+ currents, K^+ pumps, K^+ buffering simulating the glial K^+ uptake system (Bazhenov et al. 2004). The glial buffering was modeled by first order kinetics (Kager et al. 2000). The firing properties of this two compartment model depend on the coupling conductance between compartments (g=1/R, where R is resistance between comartments) and the ratio of dendritic area to axo-somatic area. The ratio, r, controls the firing patterns in the model

(Mainen and Sejnowski 1996). We used a model of a regular-spiking neuron for PY cells (r = 165) and a model of a fast spiking neuron for IN cells (r = 50). The firing patterns of these cell types in response to DC pulses of different amplitude are shown in (Rulkov et al., 2004; Fig. 3B).

3.5 Results

3.5.1 In vivo experiments

3.5.1.1 Experimental model and database

We performed various experiments to study different aspects of thalamocortical physiology. During these experiments, some of the cats displayed electrographic seizures. In these animals we stopped the initially thought experiment and changed experimental approach to address hypothesis described in the introduction the present study. We recorded electrophysiological activities from 87 cats initially anesthetized with ketamine-xylazine. As a mean, supplementary doses of anesthesia were administrated every two hours. In 41 cats, an initial anesthesia was followed by additional doses of ketamine. Similar to other studies (Steriade and Contreras 1995), in these experiments ~30 % of cats (12 cats out of 41) developed spontaneous paroxysmal discharges. Adding ketamine-xylazine as supplementary anesthetic resulted in the generation of electrographic seizures in ~75% of cats (35 out of 46). Usually, the seizures started after administration of the third-fourth supplementary dose. These seizures, consisting of SW complexes at 2–4 Hz or SW/PSW complexes associated with fast runs at 7–16 Hz, were developed from sleep-like slow rhythm. In total, we analyzed 224 electrographic seizures recorded with field potential electrodes. In parallel with EEG recording, we recorded intracellular activities of 157 neurons. This includes 8 simultaneous quadruple, 15 triple and 22 dual records. In 11 neurons, we recorded more than 20 seizures. An example of typical seizure is shown in Fig. 3.1 A in which the first 5 sec show a normal slow oscillation. The beginning of electrographic seizure was associated with ampler EEG waves and ampler intracellularly recorded depolarizing potentials repeated at frequencies 1.0-3.0 Hz. In some of the neurons the enhanced depolarizing potentials were associated with an increased firing (as in neuron 1 and neuron 4 in Fig. 3.1). After several cycles of spike-wave/polyspike-wave discharges the activity switched to runs of paroxysmal spikes (7-16 Hz) during which the long-lasting depth-positive EEG waves and associated intracellular hyperpolarizing potentials were absent. The fast runs appeared as a prolongation of polyspike-wave complexes. In this study, the polyspike discharges exceeding 1 sec were considered as runs of fast EEG

spikes. The total duration of seizures was between 10 and 120 s (37.2±22.2 s, mean±SD, Fig. 3.1 C). We analyzed 252 periods of fast runs, which lasted between 1 and 30 s (4.9±5.7 s, Fig. 3.1 C). Out of these, 174 periods lasted for less than 5 sec. Each electrographic seizure recorded in these experimental conditions could have several periods of fast runs (1-8, mean 2.4±1.4, Fig. 3.1 C) and spike-wave complexes. Below, we will focus on the generation of paroxysmal runs of fast spikes.

3.5.1.2 Multisite distant recordings during fast runs

Using multisite recordings, we evaluated the patterns of synchronization between the field potentials and intracellular activities during fast runs. Within the fast runs, the patterns of synchronization recorded with different electrodes were as following: (a) synchronous, in phase, (b) synchronous, with phase shift (one recording lead preceded or followed the activity in reference electrode), (c) "patchy", repeated in phase/phase shift transitions, and (d) non-synchronous, different frequencies in different recording sites or absence of rhythmic activities at one of the recording sites (see Fig. 3.4C). All these patterns could be recorded in the same pair of electrodes during different seizures. Some of these patterns are illustrated in Fig. 1 where the field potential and quadruple intracellular recordings were used. In this experiment, the electrodes were located in the suprasylvian gyrus: the most anterior intracellular electrode (Intra-cell 1) was located in the anterior part of area 5, the other electrodes were equally spaced with a distance between neighboring electrodes about 4 mm, and the most posterior electrode (Intra-cell 4) was located at the most posterior part of area 21. The seizure contained three periods of fast runs (2 of them are shown at a higher time resolution in the Fig. 3.1A). To estimate the patterns of synchrony we used the maximum of depth negativity of field potential as the reference time (see vertical black lines in the expended parts of Fig. 3.1 A). During the *first* period of fast runs the maximal depolarization of neurons 1, 2, and 3 preceded the maximal field potential depth negativity and the maximal depolarization of neuron 4 followed the field potential (see black lines in Fig. 3.1 A and B). The onset of each oscillatory cycle occurred first at the electrode Intra-cell 2 (see blue dotted lines in Fig. 3.1) during all the cycles of this period of fast runs (Fig. 3.1 B). During the *second* period of fast runs the most rostrally located neuron (Intra-cell 1) was always the first in the generation of each oscillatory cycle. The onset of depolarization in the neuron 2, estimated as 10% of amplitude between the

most hyperpolarized and the most depolarized (spikes excluded) values of the oscillatory cycle, occurred coincidentally with the spike in the neuron 1; the onset of depolarization in the neuron 3 was delayed and the delay fluctuated in 20-30 milliseconds range. The oscillatory activity in the neuron 4 was dumped and the neuron 4 revealed a patchy pattern of activity: there was a phase shifts during each several cycles. Generally, the frequency of activity during the same period of relatively short (<5 sec) fast runs remained similar in different recording sites, but the phase-shifts were very variable during different epochs of the fast runs. Thus, the multisite intracellular and field potential recordings revealed that runs of fast spikes behave as quasi-independent oscillators.

To characterize the patterns of synchronization during the fast runs we performed cross-correlation analysis. As expected, during the spike-wave/polyspike-wave complexes, the cross-correlation between intracellular activities and EEG was generally negative since active periods were characterized by the neuronal depolarization and depth-negative EEG waves, and during depth-positive EEG waves the neurons were hyperpolarized (Fig. 3.2). The cross-correlation between pairs of neurons was positive (not shown). The fast runs were characterized by variable patterns of synchronization. In the majority of cases (70 %), the delay between the two recording leads was stable throughout the period of fast runs. As shown in the example in Fig. 3.2 B, the Intra-cell 1 preceded the EEG by about 35 ms during the first period of fast runs. During the second period of fast runs, the intracellular activities of this neuron preceded the EEG during initial period of fast oscillations and it was synchronous in phase oscillation during the second period of fast runs. The second neuron (Intra-cell 2) and EEG had stable relation during fast runs and the maximum of neuronal excitation preceded the EEG with delay of about 10 ms during both periods of fast runs (Fig. 3.2 B). The relation between the two neurons occurred in a similar way. During the spike-wave/polyspike-wave complexes both neurons oscillated in phase, with very little variability in the phase shifts. During the first period of fast runs the phase-shift was high and the neurons oscillated with the phase-shift approaching 180^{o}. During the second period of fast runs, the synchronization had a patchy pattern. At the beginning, the neuron 2 preceded the neuron 1 by about 50 ms, but during the second part of the same train of fast EEG spikes, the neuron 2 preceded the neuron 1 by only about 10 ms (not shown).

Although in the vast majority of cases the periods of fast runs occurred almost simultaneously in all recording leads along the suprasylvian gyrus, on some occasions, the pattern was different. The Fig. 3.3 shows an example in which the seizure started from the fast run generated in the anterior part of suprasylvian cortex (EEG 7). The correlation between the anterior and posterior electrodes had small values (Fig. 3.3B, 3.1). Progressively, this activity involved more posterior regions of suprasylvian gyrus and the oscillation with frequency 11 Hz becomes dominant on all 7 EEG leads with a high value of correlation accompanied by a small propagation of activity in posterior-anterior direction (Fig. 3.3 B, 3.2). Another period of the fast runs, during the same seizure, started almost simultaneously in all EEG electrodes (frequency 8.5 Hz, see the middle expanded part in Fig. 3.3 A), and the correlation between all electrodes was high with a marked anterior-posterior propagation (Fig. 3.3 B, 3.3). At the end of the seizure the runs of fast spikes (9.5 Hz) were dominant in the posterior part of suprasylvian gyrus, while the anterior suprasylvian gyrus displayed frequency around 4 Hz, therefore the anterior-posterior correlation was low (Fig. 3.3 B, 3.4).

Thus, our multisite recordings demonstrated that in the majority of cases the onset and the end of runs of fast spikes occurred almost simultaneously at different locations, but either the frequency of oscillation or the phase shifts between different locations were dissimilar in each period of the fast runs, and even the dominating pattern of activity could switch during the same epoch of fast runs.

3.5.1.3 Divergence of synchronizing patterns during fast runs

As we have shown above with distant multisite recordings, the phase shift during the same run of fast spikes could be very variable when it is recorded with two or more electrodes located at distances larger than several millimeters. In long-lasting recordings (longer than 10 min), we analyzed the patterns of synchronization during fast runs between neurons and field potential recorded at about 1 mm apart (Fig. 3.4). We found that each pair of records (cell-EEG) had preferred phase relationship, but on some occasions, it revealed significant variations in the pattern of synchronization. Similar to distant recordings, in the majority of cases, the paroxysmal oscillation was synchronous, but each period of fast runs had a particular phase shift (Fig. 3.1, cell 1, 2, 3, Fig. 3.2, cell 2 and Fig. 3.3 periods 2, 3). Even in close recordings the pattern of synchronization during fast runs within the same

seizure could vary, and during one period of fast runs, the oscillation in two electrodes could be synchronous (0 time lag), while during another period the oscillation in two electrodes could be of different frequencies (Fig. 3.4). As an extreme case, we recorded large amplitude EEG fast runs and absence of such or similar oscillation in a closely located neuron (n=5), while the previous or following periods of fast runs showed synchronous oscillations in both electrodes (not shown). During 218 periods of fast runs we analyzed the pattern of synchronization between activities recorded with intracellular and nearby field potential electrodes (Fig. 3.4, C). We found that in only 20 % of cases the oscillation was in phase (the neuron fired during ascending phase or maximum of the EEG depth-negative wave). However, the synchronous patterns with or without different delays were recorded in 70% of cases. In 22 % of cases the activity was not synchronous: either two sites revealed oscillation with different frequencies or record showed arrhythmic activity (Fig. 3.4, C). In 8% of cases the activity was patchy; there were two or more changes in the pattern of synchronization (see examples in Fig. 1, intra-cell 4, second period and Fig. 3.2 Intra-cell 1, second period).

We systematically analyzed the spatial synchronization of fast runs within suprasylvialn gyrus of cats. For this analysis we have chosen only periods of fast runs that revealed consistent delays of coherent activity over 10 or more consecutive cycles with variability of crosscorrelation maximums not exceeding 2 milliseconds (Fig. 3.5). We analyzed separately pairs of EEG recordings and pairs of intracellular recordings obtained at different distances. In most of cases, the activity in the more anterior electrodes preceded the activity in the more posterior electrodes. We found that the fast run activity could propagate with maximal velocity reaching 10 m/s; however, the mean velocity was estimated as 2.13±0.38 m/s from pairs of EEG electrodes and 2.23±0.60 m/s from pairs of cells, indicating the presence of similar delays detected with two different methods of recordings. During consecutive fast runs the same pair of either EEG or intracellular recordings could reveal propagation from -5 m/s (posterior to anterior) to 8 m/s (anterior to posterior). Thus, each period of fast runs was characterized by unique propagation velocity and direction of propagation. However, the recordings from closely located neurons (<0.2 mm lateral distance) revealed that the coherent oscillation between two neurons could be

delayed by up to 20 ms. Thus, similar to studies in desinhibited slices, if propagation of activity takes place its varied manifold (Chervin et al. 1988).

The frequency of oscillation during the prolonged periods (>10 sec) of fast runs usually underwent a progressive decrease. To estimate the duration of a cycle during different periods of the same fast run, we obtained autocorrelations for consecutive periods lasting 5 sec (Fig. 3.6 A). In the extreme cases, the duration of oscillatory periods decreased almost twice, from 65 ms to 100 ms (Fig. 3.6 B).

In a sample of 115 periods of fast runs that lasted 5 sec or longer we analyzed the duration of oscillatory cycles (Fig.3.6). The frequency of oscillations composing fast runs decreased as the fast run progressed (Fig. 3.6 B). At the beginning of the prolonged fast runs the mean frequency of oscillation was 13.8±2.0 Hz and at the end it was slightly but significantly 11.3±2.1 Hz (paired t-test, p=0.007). The decrease in frequency by cycle was 0.036±0.016 Hz. Since the frequency decrease in a range of several cycles was low, we computed autocorrelations (Fig. 3.6 C) to evaluate (a) mean frequency of oscillation, measured by the time of the second peak occurrence, and (b) rhythm coefficient, measured as the amplitude of the second peak of autocorrelation, being 1 when all cycles had identical frequency and 0 when all cycles had different frequency. The duration of cycles varied from 62 ms to 124 ms (16 Hz to 8 Hz, Fig. 3.6, E 1) with the mean frequency 12.0±1.4 Hz. The autocorrelation obtained from the field potential recordings during fast runs was very high, and for 75% of cases it was above 0.8, suggesting a high periodicity of cycles (Fig. 3.6 E 2). The intracellular traces revealed slightly lower values of correlation (Fig. 3.6 D 2, E 2). This was likely because the variability of cycle duration for one neuron was larger than for field potential recordings; field potentials reflect the averaged activity of a set of neurons and glial cells and thus, they are much less sensitive to the variability in individual cycles of individual cells. As we reported above, the cycle duration in both the intracellular and the EEG recordings was usually similar (Fig. 3.6 D 1, 2). However, during some period of fast runs the difference could be as large as a double of the frequency.

3.5.1.4 Membrane potential during fast runs

The membrane potential during spike and wave components of seizures had a bimodal distribution and exposed two relatively stable states. In the neuron shown in the

(Fig. 3.7, A) the neuron was hyperpolarized to -80 mV during EEG wave component and it was depolarized to -55 mV during EEG spike component as revealed by the histogram of membrane potential distribution (Fig. 3.7, B). During fast runs the membrane potential oscillated continuously and only one peak could be detected from the histogram of membrane potential distribution (Fig. 3.7, B). The peak value of membrane potential histogram was in between the peak values of membrane potential during de- and hyperpolarized states. The histograms membrane potential distribution mode values for depolarized states, hyperpolarized states and fast runs (Fig. 3.7, C) for 50 neurons demonstrate that only some neurons during fast runs could be either much depolarized (above -50 mV, n=4) or much hyperpolarized (below -75 mV, n=4). The majority of neurons had the modal membrane potential values between that of de- and hyperpolarized states during spike-wave complexes. The membrane potential during fast runs was by 9.11±1.13 mV ($p<0.0001$) more hyperpolarized than during the depolarized components of seizures. There was significant correlation relations ($r=0.57$, $p<0.0001$) between the membrane potential during fast runs and depolarizing component of seizures.

3.5.1.5 Intrinsic neuronal properties and fast runs

All neurons that were recorded during both electrographic seizures and periods outside seizures (n=102), were classified by electrophysiological criteria as regular-spiking, fast-rhythmic-bursting, intrinsically-bursting (IB) and fast spiking (Connors and Gutnick 1990; Gray and McCormick 1996; Steriade et al. 1998a). The electrophysiological classification of neurons was performed during periods of normal (not paroxysmal) activity. In this set of experiments we identified 70.6 % of neurons as regular-spiking, 11.8 % as fast-rhythmic-bursting, 11.8 % as IB and the remaining 6 neurons were fast spiking. In each of these neurons we calculated the mean number of spikes per cycle generated during fast runs (Fig. 3.8). At least 100 cycles were counted to obtain a mean number of spikes generated by each neuron. Since in many instances the amplitude of spikes was significantly reduced as compared to spikes occurring outside seizures, we counted only spikes that were at least a half of amplitude of a mean spike recorded during normal activities. For example, in the displayed period in figure 6, the cell 1 had 3 spikes during each cycle, the cell 2 had 1 spike during 6 cycles and 2 spikes during one cycle and cell 3 had 1 spike during each cycle. Some neurons revealed a large variability in the number of

spikes per cycle, which could fluctuate from 1 to 6 (Fig. 3.1, Intra – cell 1). Statistically, we found however that the number of spikes per cycle generated by IB and fast-rhythmic-bursting neurons was significantly higher (Tukey-Kramer HSD [honestly significant difference] test) than the number of spikes generated by other types of neurons (Fig. 3.8).

Since, in all recorded combinations, we observed either repeatable phase shifts or absence of synchrony, we hypothesized that fast paroxysmal runs are generated locally. We used a highly simplified network model to demonstrate how extremely variable phase relations can indeed develop between synaptically coupled, oscillating neurons.

3.5.2 Computational model

3.5.2.1 Oscillations in small excitatory-inhibitory cortical circuits

We have previously shown that increases in $[K^+]_o$ could, in principle, lead to slow 2-3 Hz oscillations and fast runs (Bazhenov et al. 2004). Here we explore phase relations between neurons in different oscillatory states. We start from single neuron analysis and then we show effect of synaptic interaction on network synchronization. An external stimulus (DC pulse of 10 sec duration) applied to a single cortical pyramidal (PY) neuron induced a high-frequency spiking in this cell (Fig. 3.9). A flow of K^+ ions to the extracellular milieu overpowered effects of K^+ pump and glial buffering, and led to $[K^+]_o$ increase (see insert in Fig. 3.9 B). After stimulus termination, a neuron sustained periodic bursting in 2-4 Hz frequency range. For each cycle of oscillations the slow membrane potential depolarization between bursts (due to combined effects of I_h, $I_{K(Ca)}$ deactivation, and high $[K^+]_o$ that depolarized reversal potentials of all K^+ currents) activated the persistent sodium current and led to the new burst onset (see details in (Bazhenov et al. 2004)). Each burst started with a few spikes followed by spike inactivation and a depolarizing plateau that lasted 50-100 msec (see insert in Fig. 3.9 A). Progressive increase of the intracellular Ca^{2+} concentration during depolarized state increased activation of the Ca^{2+} dependent K^+ current and the neuron switched back to the hyperpolarized state. Since K^+ reversal potentials remained below -80 mV even when $[K^+]_o$ elevation was maximal during slow bursting, the neuron stayed hyperpolarized below normal resting potential (-65 mV) between bursts. Deactivation of $I_{K(Ca)}$ determined the length of the hyperpolarized state and ultimately the frequency of slow bursting. During slow bursting, $[K^+]_o$ gradually

decreased and 5-6 sec later, bursting was replaced by faster oscillations at 10-15 Hz range. Decrease of $[K^+]_o$ restored "normal" hyperpolarized K^+ reversal potentials. This increased hyperpolarizing "force", so the neuron did not stay "locked" in depolarized state after burst onset, but quickly repolarized back to the resting potential. Such brief depolarization led to only minimal activation of the Ca^{2+} dependent K^+ current, so the next spike (or short burst of spikes) occurred with much smaller delay. Therefore, the frequency of oscillations increased and, on average, the neuron stayed at more depolarized level of membrane potential than in slow bursting mode. Fast oscillations lasted 20-25 sec and eventually terminated when $[K^+]_o$ decreased below a level, which was necessary to maintain spiking. Thus the change of the $[K^+]_o$ can account for transitions between slow and fast paroxysmal oscillations and silent state in the cortical neuron model.

To study effect of $[K^+]_o$ increase on the circuit dynamics, we included inhibitory interneuron (IN) receiving excitatory (AMPA-type) connection from PY cell and sending back inhibitory ($GABA_A$-type) synapse. Strength of PY-IN synapse was adjusted so that IN remained silent during tonic firing of PY neuron (Fig. 3.9 B). When PY neuron started to burst, the excitatory drive from PY to IN cell was sufficient to trigger periodic IN spiking. In agreement with in vivo data (Timofeev et al. 2002), IN spiking stopped when PY neuron switched from slow bursting to the tonic firing. Two main factors contributed to the absence of IN spiking during fast runs. First, steady-state depression of excitatory coupling between PY and IN neurons was stronger during fast runs; during slow bursting short-term depression was significantly reduced by the end of hyperpolarized (interburst) state. Second, during slow bursting a first few spikes at the burst onset occurred at highest frequency, therefore promoting EPSPs summation.

3.5.2.2 Network oscillations

To study synchrony of population oscillations during different oscillatory regimes, we simulated network model of 100 PY neurons and 25 INs. Upon DC stimulus termination, all the neurons displayed slow bursting followed by fast spiking. Because of random variability of the model parameters across neurons and different initial conditions, the neurons fired independently when synaptic coupling was turned off (Fig. 3.10 A, top). Slow bursting lasted less than 4 sec. When excitatory/inhibitory coupling between neurons was included, the slow paroxysmal bursting lasted much longer (~10 sec) and became

synchronized across neurons (Fig. 3.10 A, bottom). Fig. 3.10 B shows cross-correlation between neighbor PY cells in the network; during slow paroxysmal oscillations these neurons fired with minimal phase delays. In agreement with single neuron study, progressive change of $[K^+]_o$ triggered transition from slow to fast oscillations. In most cases neighbor neurons displayed this transition nearly simultaneously; however we found a few large clusters with very different transition times (compare neurons #1-50 and #51-100 in Fig. 3.10 A, bottom). Including long-range connections between PY neurons would likely increase the global synchrony of transitions between epochs of slow and fast oscillations. To test this hypothesis we included random long-range connections between PY neurons and varied probability of long-range coupling *P*. When $P > 0.02$-0.03, transition from slow bursting to fast runs occurred almost simultaneously with less than 200 msec variability across all neurons in the network (not shown). Including long-range connections with such low probability did not produce, however, any systematic effect on phase relations between neurons during fast oscillations.

In contrast to the slow bursting mode, during fast runs the degree of synchrony between neurons (even in close proximity) was significantly reduced. Typically, neighbor neurons fired with a phase shift which was consistent for a few cycles of network oscillations thus suggesting local spike propagation. Different cell pairs displayed phase delays of different signs (propagation in different directions). Phase relations between neurons could change from in-phase to out-phase oscillations or vice versa either gradually (see, e.g., cross-correlation plot for PY35 and PY36 in Fig. 3.10 B) or suddenly (see, e.g., cross-correlation plot for PY35 and PY38 in Fig. 3.10 B). These modeling results suggest that synaptic coupling may explain synchrony of slow bursting oscillations. During fast runs, however, local synaptic excitation influences phase relations between neighbor neurons but is not sufficient to arrange steady network synchronization. Random long-range connections increase synchrony of transitions between slow bursting and fast runs but can not enhance synchrony of fast oscillations on cycle-to-cycle basis.

3.6 Discussion

In the present study, we analyzed the spatio-temporal properties of runs of fast spikes recorded during spontaneous seizures in cats anesthetized with ketamine-xylazine and in computational models. We found that (a) the runs of fast EEG spikes with frequency 7-16 Hz accompanied most of neocortical seizures; (b) the patterns of synchrony during fast runs were as following (i) synchronous, in phase, (ii) synchronous, with phase shift, (iii) patchy, repeated in phase/phase shift transitions and (iv) non-synchronous, slightly different frequencies in different recording sites or absence of oscillatory activity in one of the recording sites; the synchronous patterns were most common; (c) the runs of fast spikes appeared as quasi-independent oscillators even in neighboring cortical locations suggesting their focal origin; (d) for synchronous fast runs there was a tendency for propagation in anterior-posterior direction with velocity 2.1-2.2 m/s; (e) the membrane potential during fast runs was by ~9 mV less depolarized as compared to the depolarizing components of spike-wave complexes.

3.6.1 Experimental model of paroxysmal activity

Most of the cats anesthetized with ketamine-xylazine anesthesia, followed by supplementary doses of ketamine-xylazine developed paroxysmal activities consisting of spike-wave discharges at 1-3 Hz and runs of fast spikes at 7-16 Hz. These seizures are generated neocortically as (a) they could be obtained in athalamic cats (Steriade and Contreras 1998), (b) small neocortical slabs (Timofeev et al. 1998) or (c) in the undercut cortex (Topolnik et al. 2003), and (d) most of thalamocortical neurons do not fire during this type of seizures (Pinault et al. 1998; Steriade and Contreras 1995; Timofeev et al. 1998). The cause of these seizures is unclear. A combination of two major factors could account for the development of those paroxysmal activities.

(a) *Slow oscillations.* As previously suggested, spontaneously occurring, compound seizures consisting of spike-wave complexes at 2–4 Hz and fast runs at 7–16 Hz, developed without discontinuity from the slow (mainly 0.5–0.9 Hz), cortically generated oscillation (Steriade and Contreras 1995; Steriade et al. 1998b). Long-lasting periods of disfacilitation accompanying sleep oscillations could likely activate a large number of intrinsic and synaptic factors leading to the development of seizures (see (Timofeev and Steriade 2004)

for the detailed discussion). However, the occurrence of seizures during sleep is far lower than the occurrence of seizures in cats anesthetized with ketamine-xylazine.

(b) *Effects of ketamine-xylazine.* Ketamine at anesthetic doses blocks NMDA dependent synaptic events (MacDonald et al. 1991). An activation of NMDA receptors contributes, but is not essential in the generation of paroxysmal discharges (Barkai et al. 1994; Traub et al. 1996). Thus, the NMDA-dependent Ca^{2+} contribution in the generation of paroxysmal discharges in our experiments was impaired, which should decrease the propensity to the seizure generation and not to be a seizure promoting factor. Additional blockage of N-cholinoreceptors by ketamine (Rudolph and Antkowiak 2004) might have some impact, because, the blockage of these receptors should remove their depolarizing action on thalamocortical neurons (McCormick 1992), low-threshold spike cortical interneurons (Xiang et al. 1998), and should reduce the efficacy of excitatory synapses formed by thalamocortical neurons on cortical neurons (Gil et al. 1997).

Xylazine is the agonist of alpha-2 adrenoreceptors, heavily present in the neocortex (Nicholas et al. 1993), likely, on presynaptic terminals (Hedler et al. 1981). Administration of low doses of xylazine favors the development of seizures (Joy et al. 1983). The role of thalamus in the effects of xylazine on those seizures remains unclear. It has been proposed that administration of xylazine promotes oscillatory behavior of thalamocortical system via agonistic action on alpha-2 receptors (Buzsaki et al. 1991), but clonidine, a potent agonist of alpha-2 receptors inhibited action potential generation of thalamocortical neurons in a near dose-dependent manner (Funke et al. 1993), and finally norepinephrine application to slices, depolarize thalamocortical neurons, suppressed their burst firing, and promoted the occurrence of single spike activity (McCormick and Prince 1988). Thus, we suggest that xylazine actions in neocortex could be essential factor in the generation of paroxysmal activity induced by ketamine-xylazine anesthesia.

3.6.2 Synaptic interactions and synchronization during seizures

The amplitude of field potentials during spike-wave components of electrographic seizures is higher than the amplitude of slow oscillation (Figs. 3.2 and 3.4). This suggests that the focal synchronization during seizures is higher than during the normal brain activities. The long-range synchronization during seizures is reduced (Neckelmann et al. 1998). Our modeling data demonstrate that seizure-like activity could be obtained in a

single cortical neuron (Fig. 3.9), if some extracellular conditions (primarily increased $[K]_o$) are present. These results question the role of synaptic interactions in the generation of seizures. Multiple data suggest that synaptic activities mediated by chemical synapses during seizures play a little role. (a) Paroxysmal activities are associated with decreased $[Ca^{2+}]_o$ (Amzica et al. 2002; Heinemann et al. 1977), and as a consequence, the effectiveness of synaptic strength decreases, but the intrinsic neuronal excitability increases (Hille 2001). (b) The use of low or even 0 mM $[Ca^{2+}]_o$ in vitro results in the development of epileptiform discharges (Bikson et al. 1999; Leschinger et al. 1993; Pan and Stringer 1997). (c) The synaptic responsiveness during electrographic seizures in vivo decreases (Cisse et al. 2004; Steriade and Amzica 1999), (d) the long-range synchronization during seizures, particularly during fast runs, is low or absent (Fig. 3.4), and finally (e) the neuronal firing dramatically reduces toward the end of the seizure, while intracellular and field potential activities are ampler as compared to the beginning of the seizure (Bazhenov et al. 2004; Timofeev and Steriade 2004). In a condition of reduced efficiency of chemical synaptic transmission, the focal neuronal synchronization could be achieved either via electrical coupling between different groups of neurons (Galarreta and Hestrin 1999; Gibson et al. 1999; Perez Velazquez and Carlen 2000; Schmitz et al. 2001), glial cells (Amzica et al. 2002), or via ephaptic interactions (Grenier et al. 2003; Taylor and Dudek 1982, 1984a, b). These mechanisms have very reduced, if any, efficacy for the long-range synchronization. During fast runs, the activity of fast spiking interneurons is significantly reduced (Timofeev et al. 2002), and consequently the efficiency of synchronization via electrically coupled interneuronal network (Galarreta and Hestrin 1999; Gibson et al. 1999; Perez Velazquez and Carlen 2000) is diminished; the amplitude of field potentials is also reduced (Figs. 3.1-3.5) and as a result, its synchronizing efficiency is impaired. As consequence, the runs of fast EEG spikes are accompanied with a remarkable loss of synchrony.

Commonly, the onset and the end of fast runs occurred almost simultaneously at a large cortical distances (Figs. 3.1, 3.2). The model suggests that long-range excitatory connections between pyramidal cells may account for this synchrony if the density of long-range connections is high enough. Another possibility includes existence of some synchronizing input arriving to the different cortical loci and droving both the onset and the end of fast runs. The source of this input is unknown. Theoretically, the thalamocortical

neurons from non-specific nuclei, which project to wide cortical areas, could provide such a synchronous drive. However, the majority of thalamocortical neurons are silent during cortically generated seizures (Pinault et al. 1998; Steriade and Contreras 1995; Timofeev et al. 1998) and that would limit the implementation of such a mechanism. The other possibility is that the activating pathways would direct the switch to and from fast runs. Indeed, the fast spiking neurons fire many spikes during EEG spike-wave complexes and become silent during the fast runs (Timofeev et al. 2002). One of the possibilities is that cholinergic activities would activate muscarinic receptors on fast-spiking interneurons (Xiang et al. 1998), which would stop their firing and switch spike-wave discharges to the fast runs. The model suggests that the global change of extracellular K^+ concentration may play a role in transitions between fast and slow oscillatory modes. K^+ diffusion in the extracellular space tends to even K^+ concentration between remote foci, thus, the concentration change may serve as a global signal for state transitions. At the same time, K^+ diffusion is too slow to synchronize spiking of individual neurons during fast runs.

Our finding that both IB and fast-rhythmic-bursting neurons fired more spikes during fast runs than the other types of neurons (Fig. 3.8), imply that both types of bursting neurons could generate the fast runs. The intrinsic tuning of intraburst frequency for fast-rhythmic-bursting neurons is in the range from 20 Hz to 60 Hz (Gray and McCormick 1996; Steriade et al. 1998a), thus their frequency is much higher than the frequency of paroxysmal fast runs (Fig. 3.8), and their leading role in the generation of fast runs is doubtful. The intraburst frequency of IB neurons in vivo during normal network activities is around 8 Hz (Nuñez et al. 1993) (see also Fig. 3.8), which is close to the frequency of fast runs. Seizure related changes in extracellular Ca^{2+} and K^+ concentration (Heinemann et al. 1977) could slightly modulate the intraburst frequency of IB neurons and thus to cover all range of fast run frequencies. Thus, we suggest that cortical IB neurons could play a role of pacemakers during paroxysmal fast runs.

We conclude that the runs of fast EEG spikes, which accompany cortically generated seizures, are generated as quasi-independent oscillators, with very little synaptic communication within cortical network. Our data suggest that the onset and the end of fast runs have global (possibly extracortical) origin.

3.7 Figures

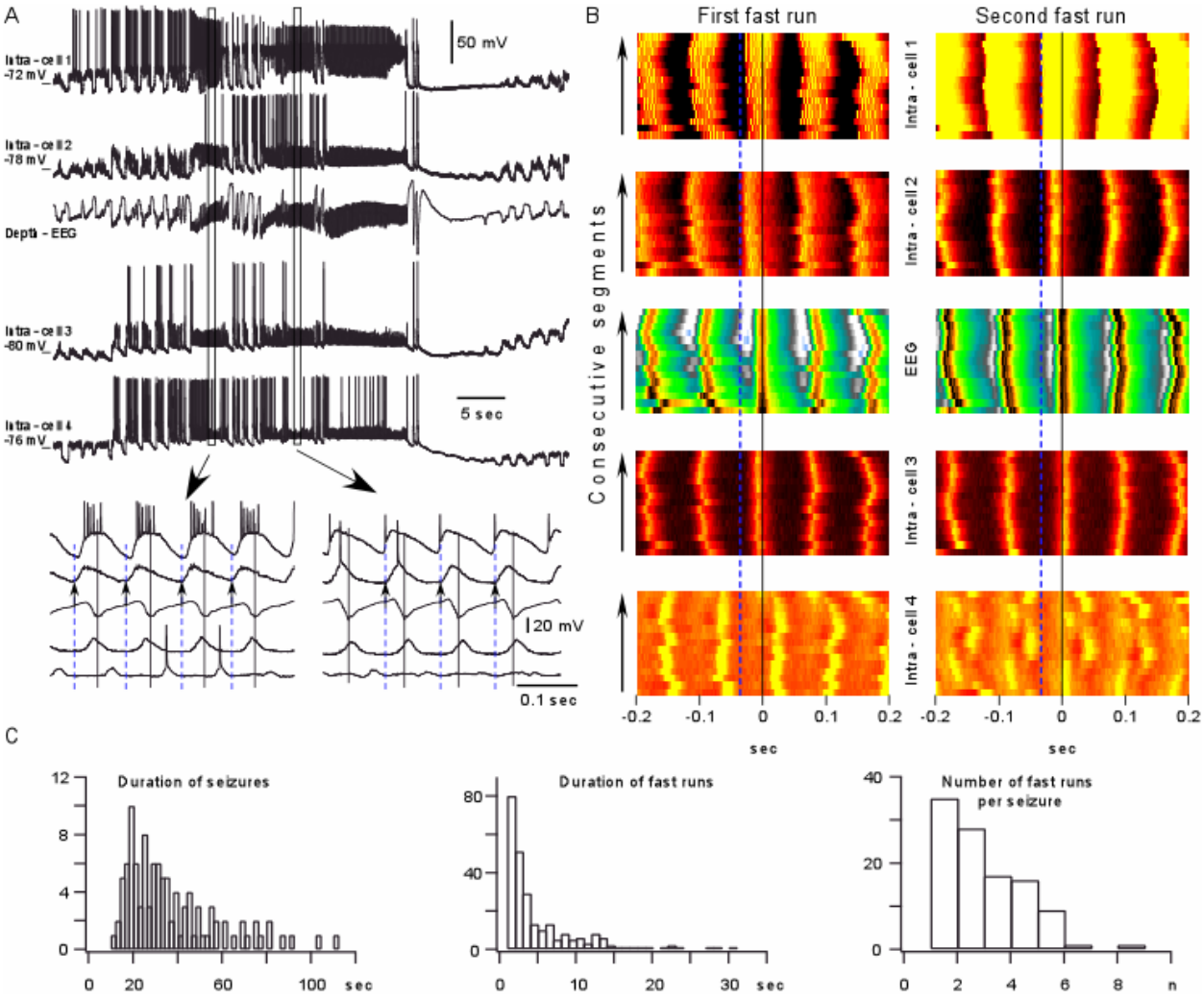

Figure 3.1

Figure 3.1: Synchronization of field potential and intracellular activities during paroxysmal fast runs.

A. Simultaneous depth-EEG and quadruple intracellular recordings. The electrodes were equally distributed from anterior to posterior parts of suprasylvian gyrus. The intra-cell 1 was in the anterior part of area 5 and the intra-cell 4 was in the posterior part of area 21. Encircled fragments are expanded below as indicated by arrows. **B.** Fifteen cycles during the first and the second fast run are color coded (dark brown: -70 mV, yellow: -50 mV). The maximum of field potential depth negativity is taken as zero time. Note that in both periods, the first maximum of depolarization in neuron 1 and 2 preceded the maximum in the field potential, the neuron 3 slightly preceded the field potential during the first shown period and followed the field during the second period and finally the neuron 4 followed the field with constant delay during the first period and showed "patchy" pattern during the second period, during which, some cycles had similar delays, the next group of cycles was either not involved in the activity or had another delay in respect to the field. **C.** Summary data showing histograms of distribution of seizures duration, individual fast run duration and the number of fast runs per seizure.

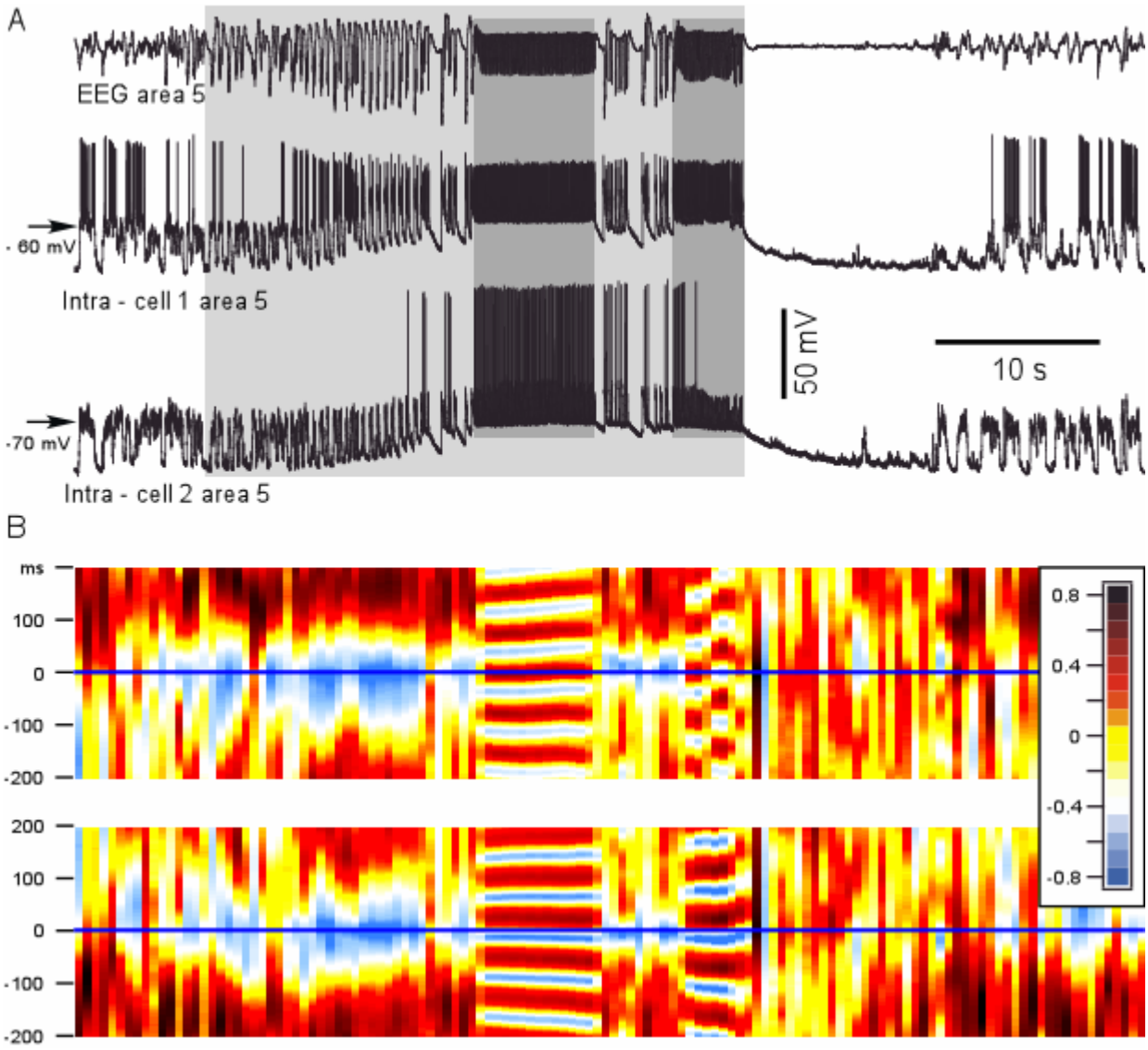
A
EEG area 5
- 60 mV
Intra - cell 1 area 5
50 mV
10 s
-70 mV
Intra - cell 2 area 5
B
ms
100
0
-100
-200
200
100
0
-100
-200
0.8
0.4
0
-0.4
-0.8

Figure 3.2

Figure 3.2: Dynamics of cross-correlation during paroxysmal fast runs.

A. Depth-EEG and dual intracellular recording during a seizure containing two periods of fast runs. **B**, the consecutive cross-correlations between EEG and neurons. The running correlogram was calculated as following: for a time interval 1.0 s the correlation function between two channels was calculated with correlation length ±0.2 s. Frame was then moved with a step 0.5 s, correlation calculated, color coded, plotted, and so on. Each of correlated periods is represented as single color strip in the bottom panels. Note that during spike-wave discharges the correlation between neuron and EEG was negative, as expected. During the first period of fast runs, the neuron 1 had reversed phase relations with EEG, while during the second period of fast runs the neuron revealed a patchy pattern. It oscillated several cycles in phase and another several cycles in counter phase; the neuron 2 oscillated in phase with the EEG during both spike-wave complexes and during both periods of fast runs.

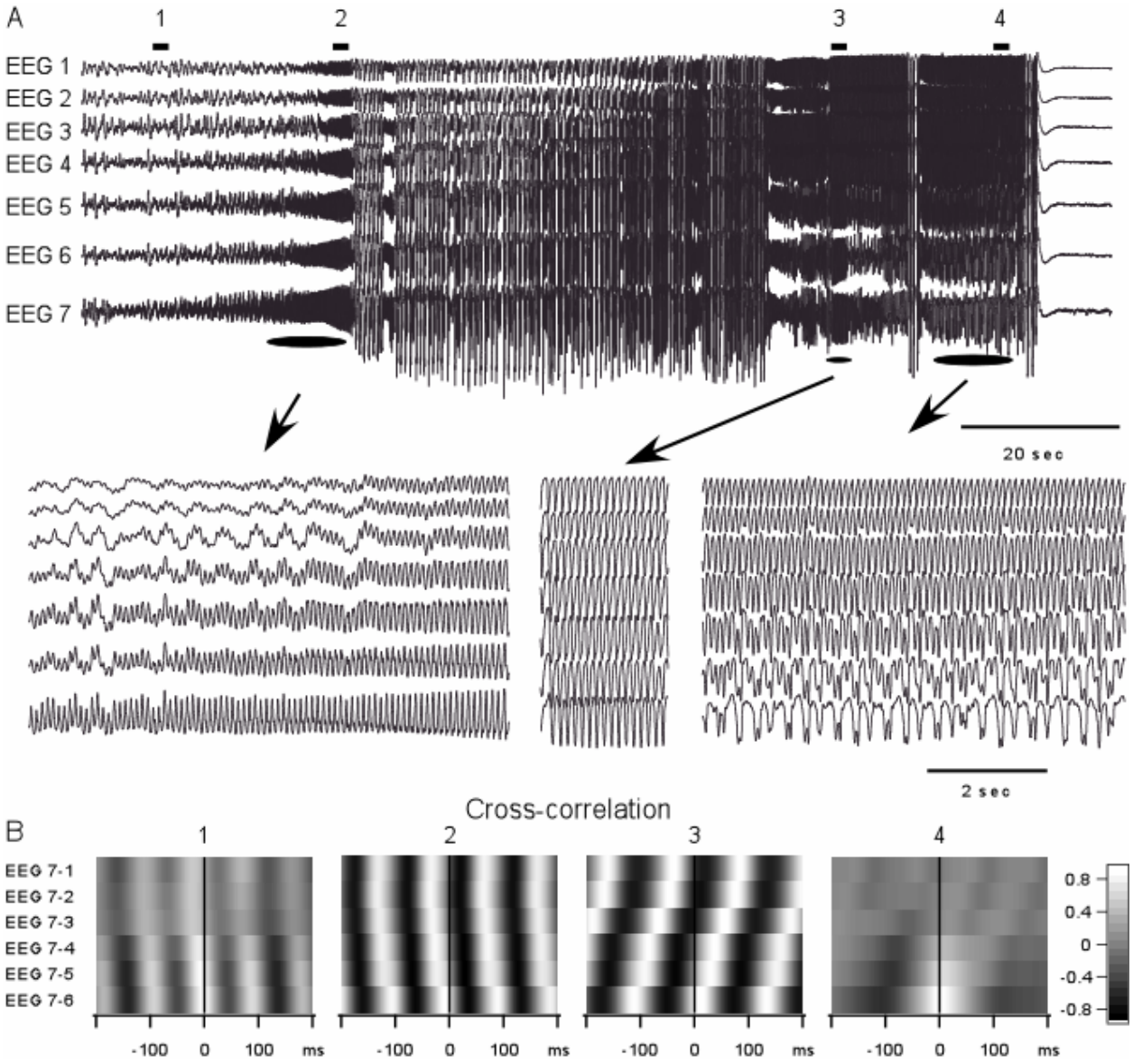
A
1
2
3
4
EEG 1
EEG 2
EEG 3
EEG 4
EEG 5
EEG 6
EEG 7
20 sec
2 sec
Cross-correlation
B
1
2
3
4
EEG 7-1
EEG 7-2
EEG 7-3
EEG 7-4
EEG 7-5
EEG 7-6
-100
0
100
ms
0.8
0.4
0
-0.4
-0.8

Figure 3.3

Figure 3.3: Progressive involvement and variability of synchronous patterns during fast runs.

A. Seven depth-EEG recordings were obtained from suprasylvian gyrus with inter-electrode distance of 1.5 mm. The seizure started with the runs of fast spikes recorded with electrode 7 (most anterior), the other electrodes reveal a progressive involvement of surpasylvian gyrus in the fast run. After several spike-wave/polyspike-wave complexes, the next period of fast runs was accompanied with perfect synchrony over suprasylvian gyrus. At the end of the seizure, the oscillatory activity with frequency around 10 Hz was found at electrode 1 and progressively declined to the electrode 7. **B.** Correlation analysis. Cross-correlations were obtained from periods of 2 seconds as indicated by horizontal bars and numbers in the panel A. Electrode 7 was taken as reference. At the beginning (1) and at the end (4) of seizure, the correlation between anterior and posterior electrodes was low. During periods indicated as 2 and 3 the correlation between different electrodes was high; the activity was propagating, but the propagation occurred in two different directions.

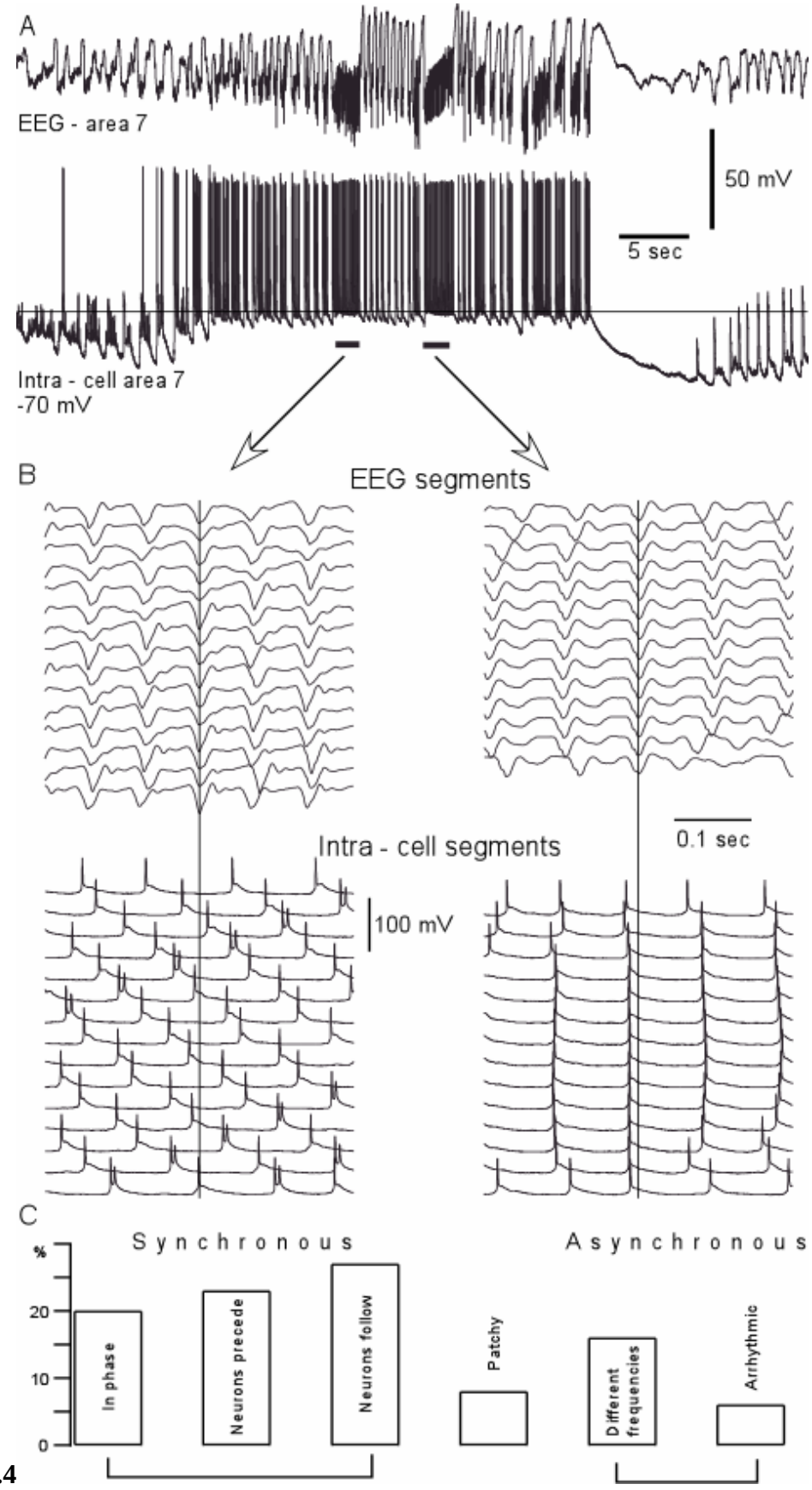
A
EEG - area 7
50 mV
5 sec
Intra - cell area 7
-70 mV
B
EEG segments
Intra - cell segments
0.1 sec
100 mV
C
Synchronous
Asynchronous
%
20
10
0
In phase
Neurons precede
Neurons follow
Patchy
Different frequencies
Arrhythmic

Figure 3.4

Figure 3.4: Variability in neuron – field synchronization during fast runs.

A. Depth-EEG and simultaneous intracellular recordings during an electrographic seizure. The distance between field potential electrode and intracellularly recorded neuron was 2 mm. **B.** A superposition of field potential (upper panels) and intracellular recordings (lower panels) during fast runs for the two consecutive periods of fast runs. Note the different frequencies of oscillations in the EEG and intracellularly recorded neuron during the first period and in phase synchronization during the second period. **C.** the distribution of patterns of synchronization for 312 periods of fast runs. The synchronous patterns (in phase or with phase shift) constituted 70 % of cases. Arrhythmic stands for periods of fast runs recorded at one electrode, while the activity in another electrode was not rhythmic.

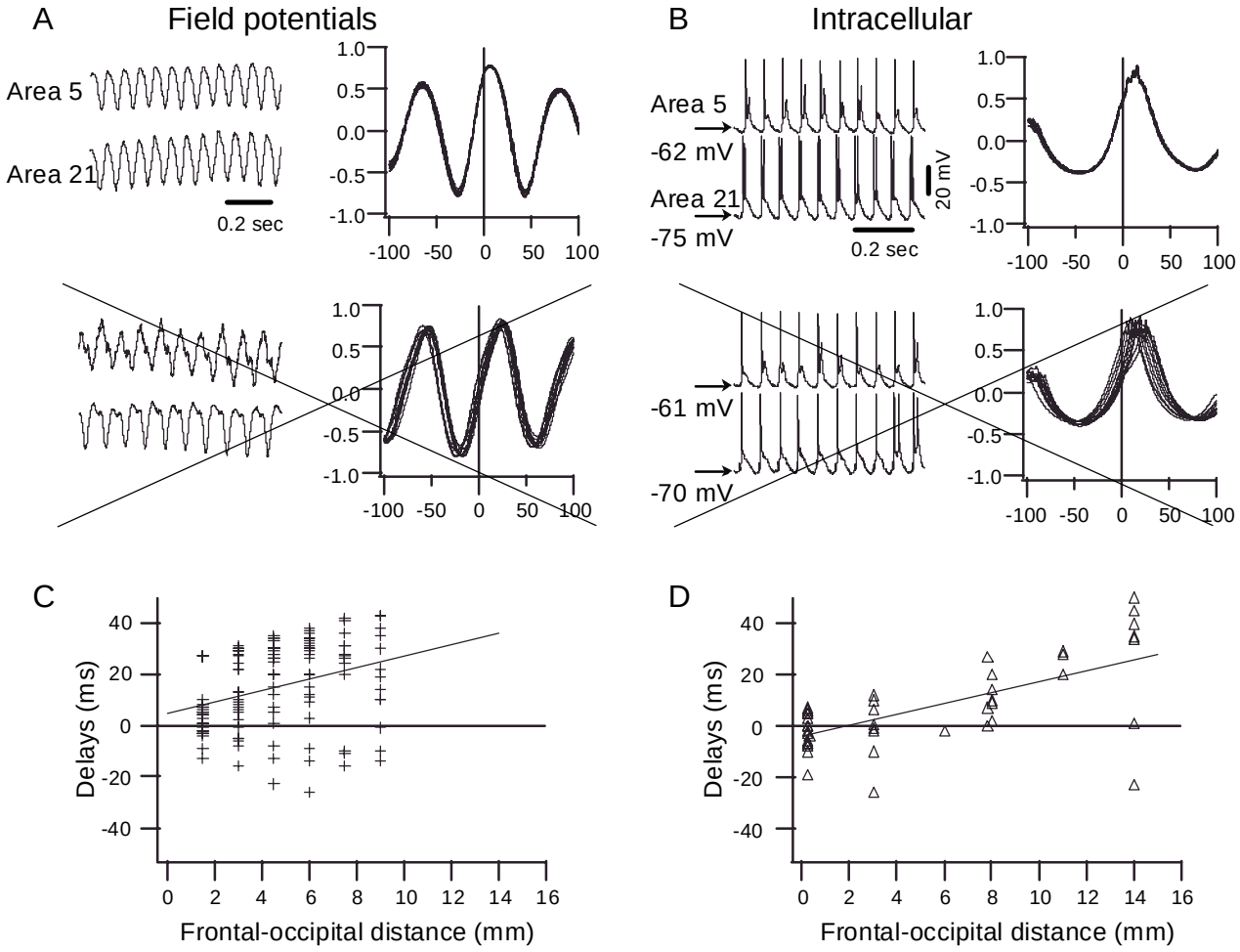
A
Field potentials
Area 5
Area 21
0.2 sec
B
Intracellular
Area 5
-62 mV
Area 21
-75 mV
0.2 sec
20 mV
-61 mV
-70 mV
C
D
Delays (ms)
Frontal-occipital distance (mm)

Figure 3.5

Figure 3.5: Propagation of fast run activity during coherent oscillations.

A. Upper left – a fragment of field potential recordings during fast runs; upper right – cross-correlation for 10 consecutive cycles of highly coherent activity. Lower panels – examples of field potential activity and cross-correlation in which the frequency of activity was slightly different in the two electrodes. Such periods were not included in the analysis of propagation shown in **C**. **B** and **D**. The same arrangement as in **A** and **C**, but for dual intracellular recordings.

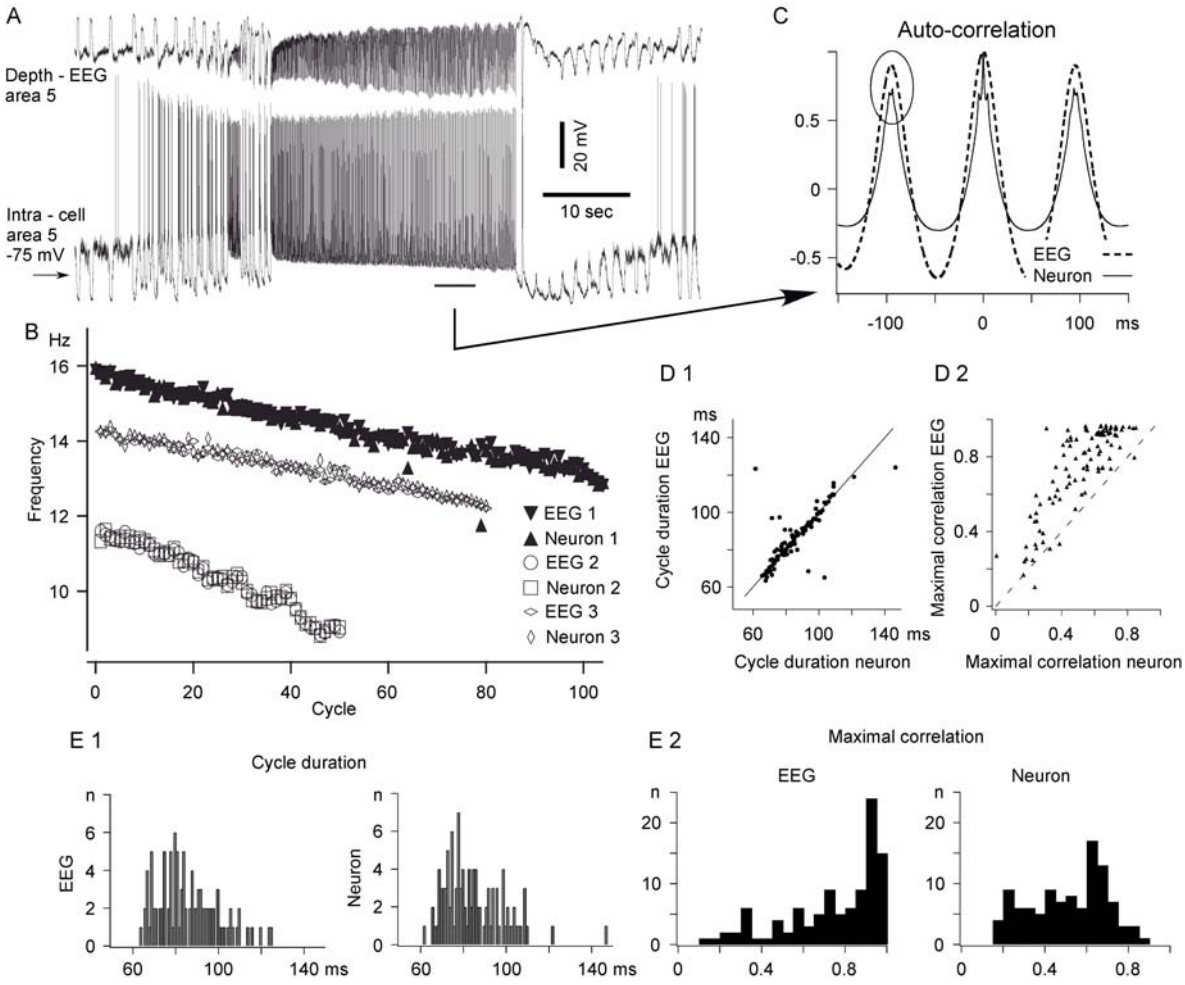
A
Depth - EEG
area 5
Intra - cell
area 5
-75 mV
20 mV
10 sec
C
Auto-correlation
EEG
Neuron
ms
B
Hz
Frequency
Cycle
EEG 1
Neuron 1
EEG 2
Neuron 2
EEG 3
Neuron 3
D 1
Cycle duration EEG
Cycle duration neuron
D 2
Maximal correlation EEG
Maximal correlation neuron
E 1
Cycle duration
EEG
Neuron
E 2
Maximal correlation
EEG
Neuron

Figure 3.6

Figure 3.6: Frequency of fast runs and their modulation during seizure.

A. An example of electrographic seizure containing a prolonged period of fast runs.

B. Instantaneous frequency of oscillation during fast runs: filed symbols for field potential and neuron shown in panel A, empty symbols - examples from two other recordings. Note a progressive decrease in the frequency of the fast run. **C**. Autocorrelation of EEG and intracellular activities from 5 sec period indicated in the panel **A**. Note, lower values of maximal correlation obtained from intracellular traces as compared to EEG traces. **D 1**. The frequency relation between EEG and intracellular recordings. and **D 2**. Maximal autocorrelation relation between EEG and intracellular recordings. Note that in the majority of cases the frequency of fast runs at EEG and intracellular levels was similar. In the vast majority of cases the amplitude of autocorrelation for EEG traces was higher then for intracellular traces. **E 1**. Histograms of cycle duration for EEG (left) and intracellular recordings (right). **E 2**. Maximal correlation values for EEG (left) and intracellular (right) recordings.

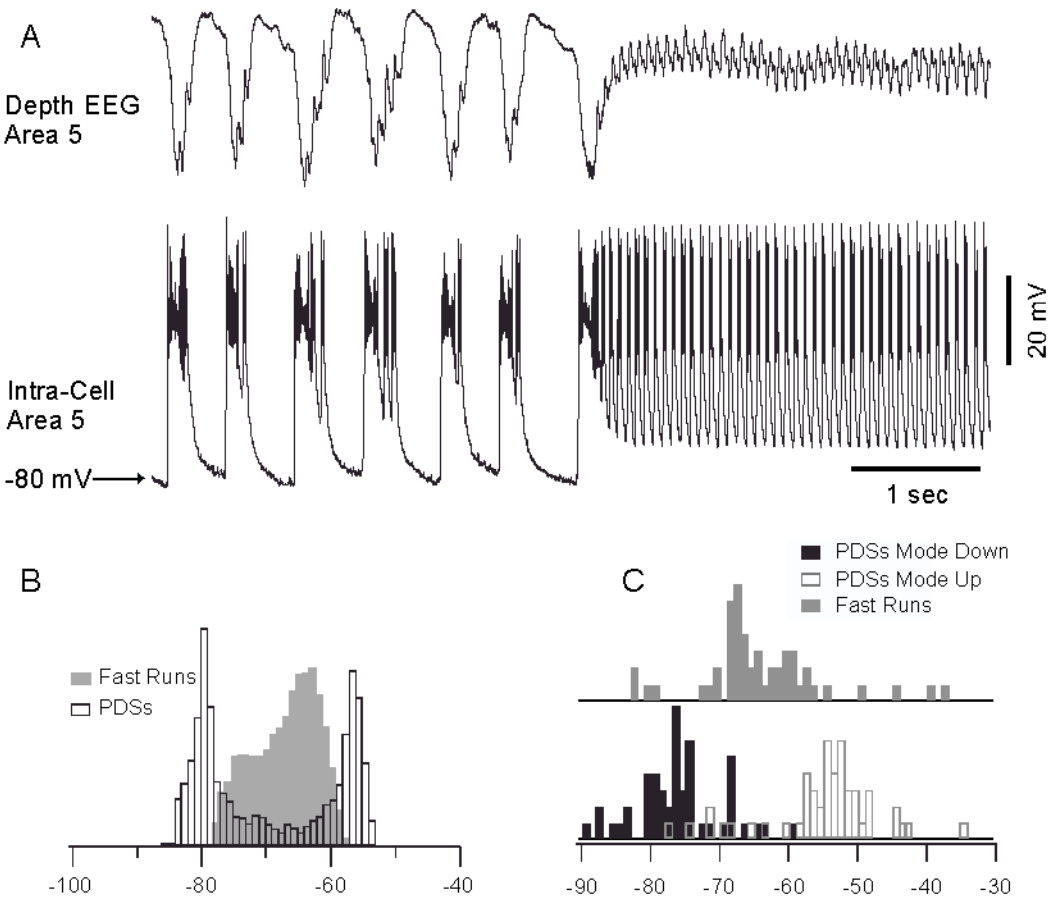
A
Depth EEG
Area 5
Intra-Cell
Area 5
-80 mV
20 mV
1 sec
B
Fast Runs
PDSs
-100
-80
-60
-40
C
PDSs Mode Down
PDSs Mode Up
Fast Runs
-90
-80
-70
-60
-50
-40
-30

Figure 3.7

Figure 3.7: Membrane potential of cortical neurons during spike-wave and fast run components of seizures.

A. Field potential and intracellular recordings during a fragment of electrographic seizure containing spike-wave complexes and a fast run period. **B**. Histogram of membrane potential during spike-waves (transparent bars) and fast run (grey bars) from the neuron shown in **A**. Note the presence of two peaks during spike-wave complexes and one peak during fast runs. **C**. Distribution of membrane potential modes for hyperpolarizing (black bars),

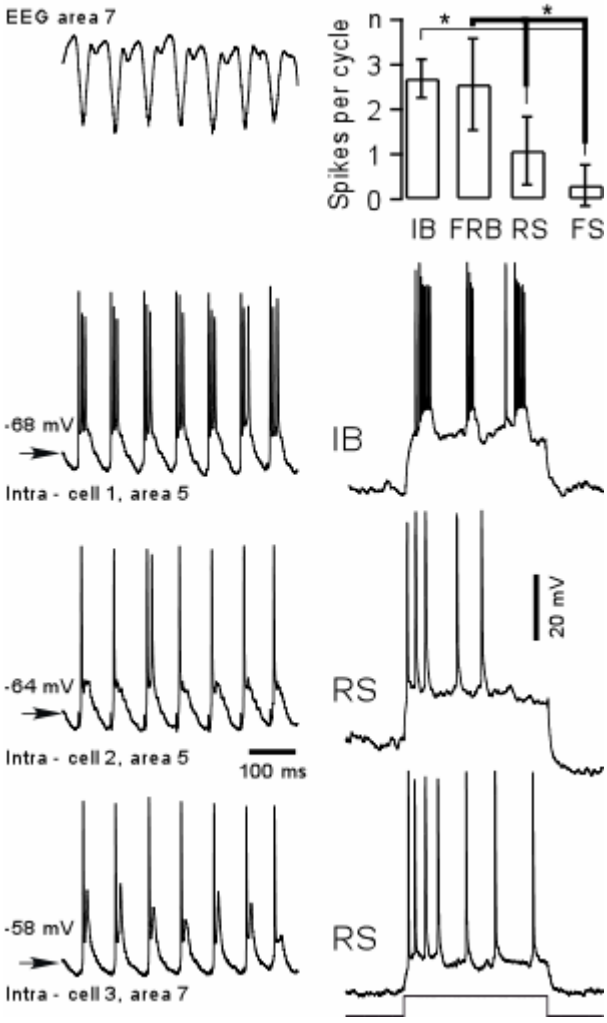
EEG area 7
Spikes per cycle
n
3
2
1
0
*
*
IB FRB RS FS
-68 mV
Intra - cell 1, area 5
IB
-64 mV
Intra - cell 2, area 5
100 ms
20 mV
RS
-58 mV
Intra - cell 3, area 7
RS

Figure 3.8

Figure 3.8: Discharge patterns of variable electrophysiological types of neurons during fast runs.

Left column – field potential and simultaneous triple intracellular recording during a period of fast run. Histogram at upper right corner displays a mean number of spikes generated by neurons of different electrophysiological types during each cycle of paroxysmal fast runs. Electrophysiological identification of neurons from left column is indicated at right. IB – intrinsically-bursting, FRB – fast-rhythmic-bursting, RS – regular spiking neuron and FS fast – spiking neurons. Statistically significant difference (alpha 0.01) is indicated by asterisks.

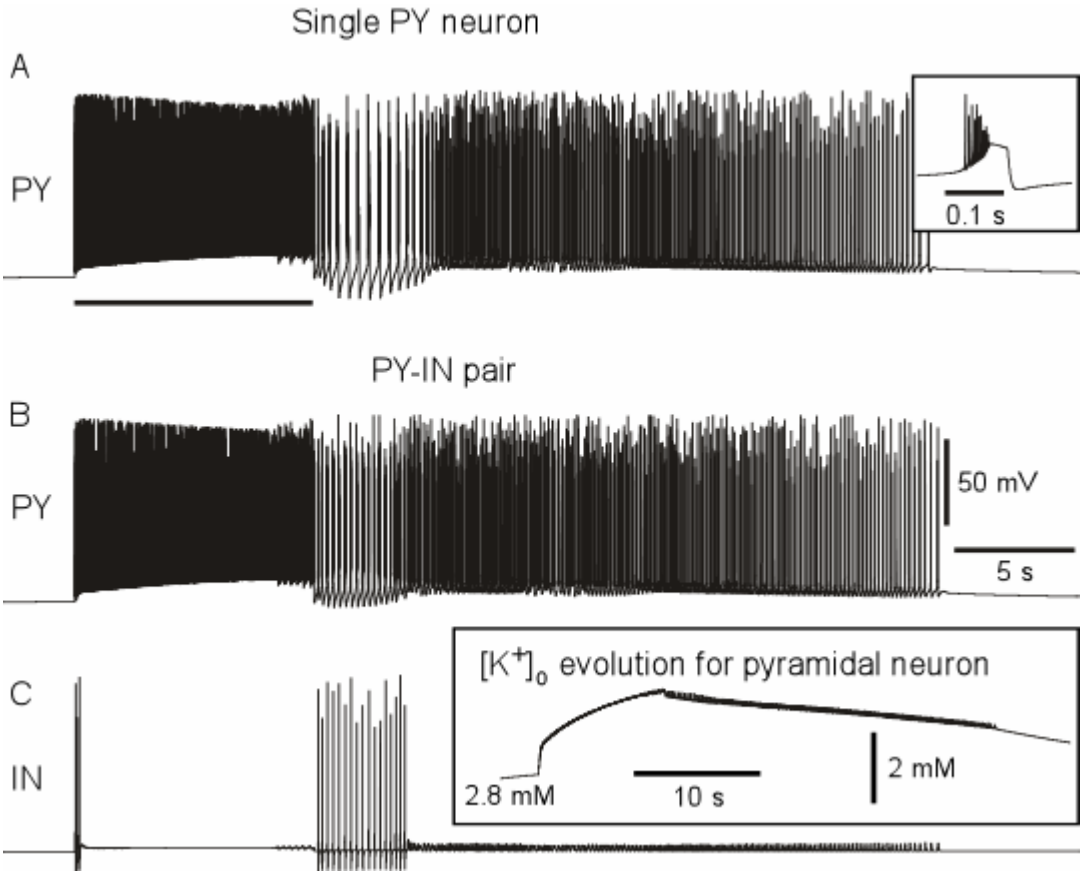
Single PY neuron
A
PY
0.1 s
PY-IN pair
B
PY
50 mV
5 s
C
IN
[K+]o evolution for pyramidal neuron
2.8 mM
10 s
2 mM

Figure 3.9

Figure 3.9: Modeled neuron oscillatory activity induced by a current pulse.

DC pulse (10 sec in duration, bar) was applied to the model PY neuron. Following high frequency firing, $[K^+]_o$ increased and maintained oscillations in PY neuron after DC pulse was removed. (A) Single neuron. Insert shows typical burst of spikes. (B) Reciprocally connected PY-IN pair. Insert shows $[K^+]_o$ evolution for PY neuron. Change of the $[K^+]_o$ induced transition from slow (2-3 Hz) to fast (10-15 Hz) oscillations. Bursts of spikes (but not tonic spiking) in PY neuron induced spikes in the inhibitory interneuron.

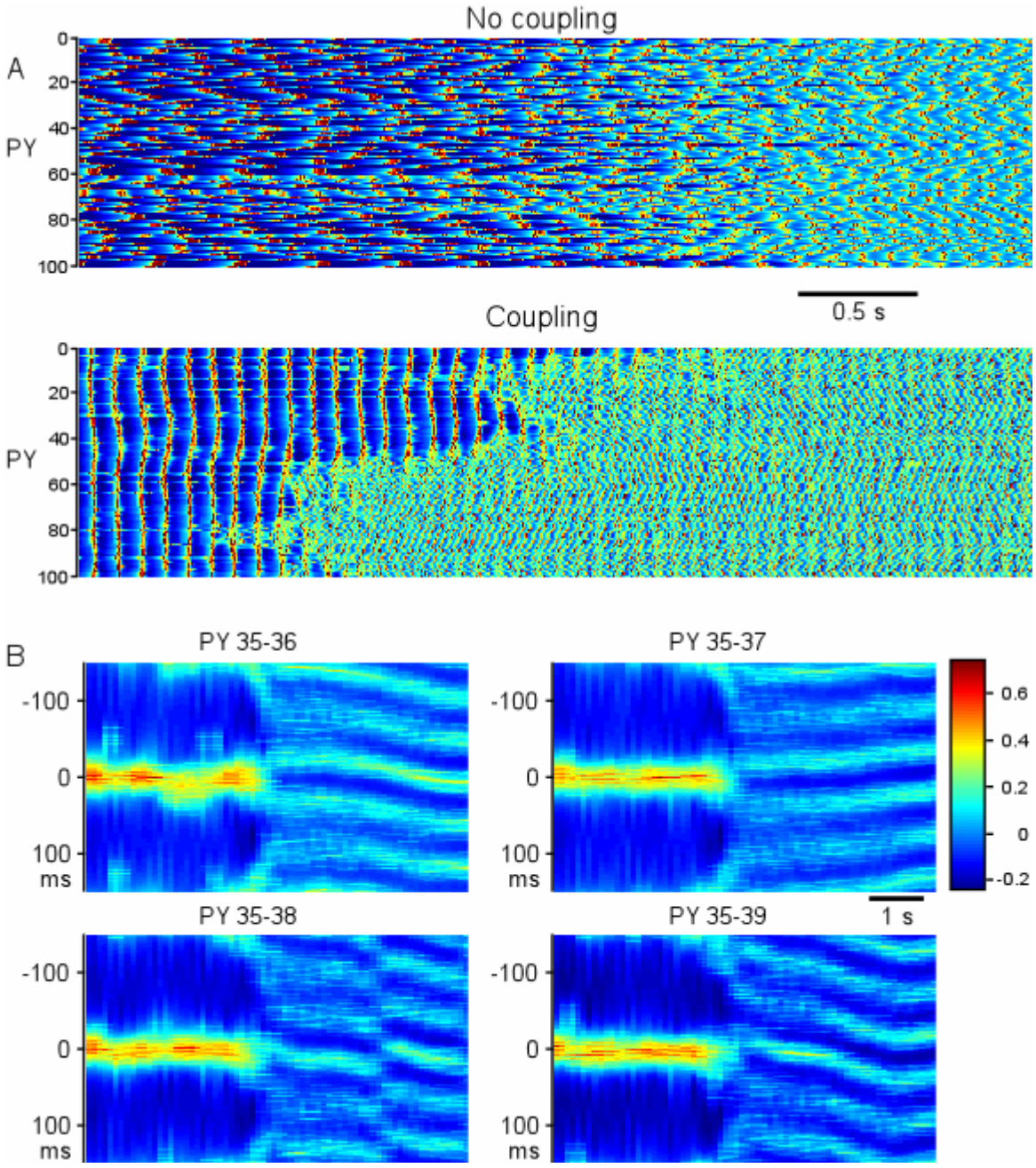
No coupling
A
PY
0
20
40
60
80
100
0.5 s
Coupling
PY
0
20
40
60
80
100
B
PY 35-36
PY 35-37
PY 35-38
PY 35-39
-100
0
100
ms
1 s
0.6
0.4
0.2
0
-0.2

Figure 3.10

Figure 3.10: Oscillations in the network model (100 PY and 25 IN neurons).

DC stimulus was presented for 10 sec (from t=8 sec to t=18 sec) to all PY neurons and was followed by slow bursting and then by fast oscillations. (A) Network activity near the transition from slow bursting to fast runs. Top, no coupling ($g_{PY\text{-}PY}$=0, $g_{PY\text{-}IN}$=0, $g_{IN\text{-}PY}$=0), time interval from t=19 sec to t=26 sec. Bottom, coupled network ($g_{PY\text{-}PY}$=0.07 μS, $g_{PY\text{-}IN}$=0.07 μS, $g_{IN\text{-}PY}$=0.05 μS), time interval from t=26 sec to t=33 sec. (B) Cross-correlations (sliding window, 500 msec duration, 100 msec time steps) between one PY neuron (PY35, shown by arrow in panel A) and its neighbors (PY36-PY39). Vertical arrows indicate transition from slow bursting to fast runs. Oscillations were highly synchronized with zero phase shift in the bursting mode. During fast run, oscillations in the neighbor PY cells displayed variable phase shift (local activity propagation) with sudden phase changes.

3.8 References

1 **Abbott LF, Varela JA, Sen K and Nelson SB**. Synaptic depression and cortical gain control. *Science* 275: 220-224, 1997.

2 **Alzheimer C, Schwindt PC and Crill WE**. Modal gating of Na+ channels as a mechanism of persistent Na+ current in pyramidal neurons from rat and cat sensorimotor cortex. *J Neurosci* 13: 660-673, 1993.

3 **Amzica F, Massimini M and Manfridi A**. Spatial buffering during slow and paroxysmal sleep oscillations in cortical networks of glial cells in vivo. *J Neurosci* 22: 1042-1053, 2002.

4 **Barkai E, Grossman Y and Gutnick MJ**. Long-term changes in neocortical activity after chemical kindling with systemic pentylenetetrazole: an in vitro study. *J Neurophysiol* 72: 72-83, 1994.

5 **Bazhenov M, Timofeev I, Steriade M and Sejnowski TJ**. Computational models of thalamocortical augmenting responses. *J Neurosci* 18: 6444-6465, 1998.

6 **Bazhenov M, Timofeev I, Steriade M and Sejnowski TJ**. Potassium model for slow (2-3 Hz) in vivo neocortical paroxysmal oscillations. *J Neurophysiol* 92: 1116-1132, 2004.

7 **Bikson M, Ghai RS, Baraban SC and Durand DM**. Modulation of burst frequency, duration, and amplitude in the zero-Ca(2+) model of epileptiform activity. *J Neurophysiol* 82: 2262-2270, 1999.

8 **Buzsaki G, Kennedy B, Solt VB and Ziegler M**. Noradrenergic Control of Thalamic Oscillation: the Role of alpha-2 Receptors. *Eur J Neurosci* 3: 222-229, 1991.

9 **Chervin RD, Pierce PA and Connors BW**. Periodicity and directionality in the propagation of epileptiform discharges across neocortex. *J Neurophysiol* 60: 1695-1713, 1988.

10 **Cisse Y, Crochet S, Timofeev I and Steriade M**. Synaptic responsiveness of neocortical neurons to callosal volleys during paroxysmal depolarizing shifts. *Neuroscience* 124: 231-239, 2004.

11 **Connors BW and Gutnick MJ**. Intrinsic firing patterns of divers neocortical neurons. *Trends Neurosci.* 13: 99-104, 1990.

12 **Destexhe A, Mainen ZF and Sejnowski TJ**. Synthesis of models for excitable membranes, synaptic transmission and neuromodulation using a common kinetic formalism. *J Comput Neurosci* 1: 195-230, 1994.

13 **Ferri R, Stam CJ, Lanuzza B, Cosentino FI, Elia M, Musumeci SA and Pennisi G**. Different EEG frequency band synchronization during nocturnal frontal lobe seizures. *Clin Neurophysiol* 115: 1202-1211, 2004.

14 **Funke K, Pape HC and Eysel UT**. Noradrenergic modulation of retinogeniculate transmission in the cat. *J Physiol* 463: 169-191, 1993.

15 **Galarreta M and Hestrin S**. Frequency-dependent synaptic depression and the balance of excitation and inhibition in the neocortex. *Nat Neurosci* 1: 587-594, 1998.

16 **Galarreta M and Hestrin S**. A network of fast-spiking cells in the neocortex connected by electrical synapses. *Nature* 402: 72-75, 1999.

17 **Gibson JR, Beierlein M and Connors BW**. Two networks of electrically coupled inhibitory neurons in neocortex. *Nature* 402: 75-79, 1999.

18 **Gil Z, Connors BW and Amitai Y**. Differential regulation of neocortical synapses by neuromodulators and activity. *Neuron* 19: 679-686, 1997.

19 **Gray CM and McCormick DA**. Chattering cells: superficial pyramidal neurons contributing to the generation of synchronous oscillations in the visual cortex. *Science* 274: 109-113, 1996.

20 **Grenier F, Timofeev I, Crochet S and Steriade M**. Spontaneous field potentials influence the activity of neocortical neurons during paroxysmal activities in vivo. *Neuroscience* 119: 277-291, 2003.

21 **Halasz P**. Runs of rapid spikes in sleep: a characteristic EEG expression of generalized malignant epileptic encephalopathies. A conceptual review with new pharmacological data. *Epilepsy Res Suppl* 2: 49-71, 1991.

22 **Hedler L, Stamm G, Weitzell R and Starke K**. Functional characterization of central alpha-adrenoceptors by yohimbine diastereomers. *Eur J Pharmacol* 70: 43-52, 1981.

23 **Heinemann U, Lux HD and Gutnick MJ**. Extracellular free calcium and potassium during paroxsmal activity in the cerebral cortex of the cat. *Exp Brain Res* 27: 237-243, 1977.

24 **Hille B**. *Ionic channels of excitable membranes*. Sunderland, Massachusetts: Sinauer Associates INC, 2001.

25 **Hughes SW, Cope DW, Blethyn KL and Crunelli V**. Cellular mechanisms of the slow (<1 Hz) oscillation in thalamocortical neurons in vitro. *Neuron* 33: 947-958, 2002.

26 **Joy RM, Stark LG and Albertson TE**. Dose-dependent proconvulsant and anticonvulsant actions of the alpha 2 adrenergic agonist, xylazine, on kindled seizures in the rat. *Pharmacol Biochem Behav* 19: 345-350, 1983.

27 **Kager H, Wadman WJ and Somjen GG**. Simulated seizures and spreading depression in a neuron model incorporating interstitial space and ion concentrations. *J Neurophysiol* 84: 495-512, 2000.

28 **Kay AR, Sugimori M and Llinas R**. Kinetic and stochastic properties of a persistent sodium current in mature guinea pig cerebellar Purkinje cells. *J Neurophysiol* 80: 1167-1179, 1998.

29 **Kotagal P**. Multifocal independent Spike syndrome: relationship to hypsarrhythmia and the slow spike-wave (Lennox-Gastaut) syndrome. *Clin Electroencephalogr* 26: 23-29, 1995.

30 **Leschinger A, Stabel J, Igelmund P and Heinemann U**. Pharmacological and electrographic properties of epileptiform activity induced by elevated K+ and lowered Ca2+ and Mg2+ concentration in rat hippocampal slices. *Exp Brain Res* 96: 230-240, 1993.

31 **Mainen ZF and Sejnowski TJ**. Influence of dendritic structure on firing pattern in model neocortical neurons. *Nature* 382: 363-366, 1996.

32 **Matsumoto H, Ayala GF and Gumnit RJ**. Effects of intracellularly injected currents on the PDS and the hyperpolarizing after-potential in neurons within an epileptic focus. *Electroencephalogr Clin Neurophysiol* 26: 120., 1969.

33 **McCormick DA**. Neurotransmitter actions in the thalamus and cerebral cortex and their role in neuromodulation of thalamocortical activity. *Prog Neurobiol* 39: 337-388, 1992.

34 **McCormick DA and Prince DA**. Noradrenergic modulation of firing pattern in guinea pig and cat thalamic neurons, in vitro. *J Neurophysiol* 59: 978-996, 1988.

35 **Neckelmann D, Amzica F and Steriade M**. Spike-wave complexes and fast components of cortically generated seizures. III. Synchronizing mechanisms. *J Neurophysiol* 80: 1480-1494, 1998.

36 **Neckelmann D, Amzica F and Steriade M**. Changes in neuronal conductance during different components of cortically generated spike-wave seizures. *Neuroscience* 96: 475-485, 2000.

37 **Nicholas AP, Pieribone V and Hokfelt T**. Distributions of mRNAs for alpha-2 adrenergic receptor subtypes in rat brain: an in situ hybridization study. *J Comp Neurol* 328: 575-594, 1993.

38 **Niedermeyer E**. Abnormal EEG patterns: epileptic and paroxysmal. In: *Electroencephalography: Basic Principles, Clinical Applications, and Related Fields*, edited by Niedermeyer E and Lopes de Silva F. Baltimor MD: Williams & Wilkins, 1999a, p. 235-260.

39 **Niedermeyer E**. Epileptic seizure disorders. In: *Electroencephalography: Basic Principles, Clinical Applications, and Related Fields*, edited by Niedermeyer E and Lopes de Silva F. Baltimor MD: Williams & Wilkins, 1999b, p. 476-585.

40 **Nuñez A, Amzica F and Steriade M**. Electrophysiology of cat association cortical cells in vitro: Intrinsic properies and synaptic responses. *J Neurophysiol* 70: 418-430, 1993.

41 **Pan E and Stringer JL**. Role of potassium and calcium in the generation of cellular bursts in the dentate gyrus. *J Neurophysiol* 77: 2293-2299, 1997.

42 **Perez Velazquez JL and Carlen PL**. Gap junctions, synchrony and seizures. *Trends Neurosci* 23: 68-74, 2000.

43 **Pinault D, Leresche N, Charpier S, Deniau JM, Marescaux C, Vergnes M and Crunelli V**. Intracellular recordings in thalamic neurones during spontaneous spike and wave discharges in rats with absence epilepsy. *J Physiol* 509: 449-456, 1998.

44 **Rudolph U and Antkowiak B**. Molecular and neuronal substrates for general anesthetics. *Nat Rev Neurosci* 5: 709-720, 2004.

45 **Schmitz D, Schuchmann S, Fisahn A, Draguhn A, Buhl EH, Petrasch-Parwez E, Dermietzel R, Heinemann U and Traub RD**. Axo-axonal coupling. a novel mechanism for ultrafast neuronal communication. *Neuron* 31: 831-840, 2001.

46 **Steriade M and Contreras D**. Relations between cortical and thalamic cellular events during transition from sleep patterns to paroxysmal activity. *J Neurosci* 15: 623-642, 1995.

47 **Steriade M and Contreras D**. Spike-wave complexes and fast components of cortically generated seizures. I. Role of neocortex and thalamus. *J Neurophysiol* 80: 1439-1455, 1998.

48 **Steriade M and Amzica F**. Intracellular study of excitability in the seizure-prone neocortex in vivo. *J Neurophysiol* 82: 3108-3122, 1999.

49 **Steriade M and Timofeev I**. Corticothalamic operations through prevalent inhibition of thalamocortical neurons. *Thalamus & related systems* 1: 225-236, 2001.

50 **Steriade M, Timofeev I, Dürmüller N and Grenier F**. Dynamic properties of corticothalamic neurons and local cortical interneurons generating fast rhythmic (30-40 Hz) spike bursts. *J Neurophysiol* 79: 483-490, 1998a.

51 **Steriade M, Amzica F, Neckelmann D and Timofeev I**. Spike-wave complexes and fast components of cortically generated seizures. II. Extra- and intracellular patterns. *J Neurophysiol* 80: 1456-1479, 1998b.

52 **Taylor CP and Dudek FE**. Synchronous neural afterdischarges in rat hippocampal slices without active chemical synapses. *Science* 218: 810-812, 1982.

53 **Taylor CP and Dudek FE**. Excitation of hippocampal pyramidal cells by an electrical field effect. *J Neurophysiol* 52: 126-142, 1984a.

54 **Taylor CP and Dudek FE**. Synchronization without active chemical synapses during hippocampal afterdischarges. *J Neurophysiol* 52: 143-155, 1984b.

55 **Timofeev I and Steriade M**. Neocortical seizures: initiation, development and cessation. *Neuroscience* 123: 299-336, 2004.

56 **Timofeev I, Grenier F and Steriade M**. Spike-wave complexes and fast components of cortically generated seizures. IV. Paroxysmal fast runs in cortical and thalamic neurons. *J Neurophysiol* 80: 1495-1513, 1998.

57 **Timofeev I, Grenier F and Steriade M**. The role of chloride-dependent inhibition and the activity of fast-spiking neurons during cortical spike-wave seizures. *Neuroscience* 114: 1115-1132, 2002.

58 **Timofeev I, Grenier F, Bazhenov M, Sejnowski TJ and Steriade M**. Origin of slow cortical oscillations in deafferented cortical slabs. *Cereb Cortex* 10: 1185-1199, 2000.

59 **Topolnik L, Steriade M and Timofeev I**. Partial cortical deafferentation promotes development of paroxysmal activity. *Cereb Cortex* 13: 883-893, 2003.

60 **Traub RD, Borck C, Colling SB and Jefferys JG**. On the structure of ictal events in vitro. *Epilepsia* 37: 879-891, 1996.

61 **Tsodyks MV and Markram H**. The neural code between neocortical pyramidal neurons depends on neurotransmitter release probability. *Proc Natl Acad Sci U S A* 94: 719-723, 1997.

62 **Xiang Z, Huguenard JR and Prince DA**. Cholinergic switching within neocortical inhibitory networks. *Science* 281: 985-988, 1998.

4. General Conclusion

In contrast to the obsolete ideas that, during slow-wave sleep, there is a global resting in cortex, neurons in neocortical areas display unexpectedly high levels of spontaneous activity and the intracortical dialogue is maintained. The slow oscillation during slow-wave sleep is initiated, maintained, and terminated through the interplay of intrinsic currents and synaptic interaction. Thus, this slow oscillation represents a spontaneous event during which cortical neurons are alternated between silent and active states for a fraction of a second. This striking change in neuronal activity and excitability involve most of the cortex and repeats hundreds of times during a sleep episode. The active and silent states are accompanied with changes in extracellular correlation of endogenous ions. The modulation of extracellular concentration of certain ions affects the intrinsic and synaptic activity. As it is mentioned above in this thesis, the Ca^{2+} modulation during slow oscillation has a major impact on behavior and responsiveness of these neurons in both intrinsic and synaptic levels. The change of $[Ca^{2+}]_o$ has an opposite effect on the intrinsic and synaptic neuronal responses. At synaptic level, the increase of $[Ca^{2+}]_o$ provoke an increase in synaptic efficiency and a decrease of $[Ca^{2+}]_o$ leads to a decrease in synaptic efficiency due to Ca^{2+} effects on release probability (Crochet et al., 2005). In contrast, the increase of $[Ca^{2+}]_o$ leads an decrease in intrinsic excitability and the decrease of $[Ca^{2+}]_o$ results in an increase in intrinsic excitability, via Ca^{2+} effects on Ca^{2+}-activated K^+ conductance and its impact on spike AHP (see chapter II). Thus, under physiological conditions, where the level of synaptic activity can change quickly, modulation of somatic voltage-gated conductances may be a potent mechanism to regulate excitability.

The modulation of extracellular concentration of ions has also the impact during paroxysmal activity; this modulation mediates the switch from normal activity to paroxysmal fast activity and within paroxysmal discharges from spike-wave complexes to runs of fast spikes. The decrease in $[Ca^{2+}]_o$ during seizures (Heinemann et al., 1977; Amzica et al., 2002) has decreases the long-range synchronization between different cortical foci via reduction of synaptic efficiency, but enhances intrinsic excitability, which help to maintain paroxysmal network excitability. Thus paroxysmal activity is characterized by large amplitude PDSs containing a significant intrinsic component

(Timofeev et al., 2004) and loose synchrony (see chapter III) because the synaptic excitability was impaired.

Finally, most of electrophysiological studies address issues of (i) intrinsic neuronal mechanisms, (ii) synaptic interactions and (iii) network phenomena. However, multiple extracellular factors such as fluctuation of endogenous ion concentration or effects of extracellular field potentials produced by neighboring neuronal pulls are often ignored. Considering these factors in the understanding of brain functions would often provide missing links mediating cellular mechanisms of normal and paroxysmal brain activity.

5. Bibliography

1. **Abbott LF, Varela JA, Sen K and Nelson SB**. Synaptic depression and cortical gain control. *Science* 275: 220-224, 1997.

2. **Achermann P and Borbely AA**. Low-frequency (< 1 Hz) oscillations in the human sleep electroencephalogram. *Neuroscience* 81: 213-222, 1997.

3. **Adams PR, Constanti A, Brown DA and Clark RB**. Intracellular Ca2+ activates a fast voltage-sensitive K+ current in vertebrate sympathetic neurones. *Nature* 296: 746-749, 1982.

4. **Amzica F and Massimini M**. Glial and neuronal interactions during slow wave and paroxysmal activities in the neocortex. *Cereb Cortex* 12: 1101-1113, 2002.

5. **Amzica F, Massimini M and Manfridi A**. Spatial buffering during slow and paroxysmal sleep oscillations in cortical networks of glial cells in vivo. *J Neurosci* 22: 1042-1053, 2002.

6. **Amzica F and Steriade M**. Disconnection of intracortical synaptic linkages disrupts synchronization of a slow oscillation. *J Neurosci* 15: 4658-4677, 1995a.

7. **Amzica F and Steriade M**. Short- and long-range neuronal synchronization of the slow (< 1 Hz) cortical oscillation. *J Neurophysiol* 73: 20-38, 1995b.

8. **Amzica F and Steriade M**. The K-complex: its slow (<1-Hz) rhythmicity and relation to delta waves. *Neurology* 49: 952-959, 1997.

9. **Amzica F and Steriade M**. Cellular substrates and laminar profile of sleep K-complex. *Neuroscience* 82: 671-686, 1998a.

10. **Amzica F and Steriade M**. Electrophysiological correlates of sleep delta waves. *Electroencephalogr Clin Neurophysiol* 107: 69-83, 1998b.

11. **Brumberg JC, Nowak LG and McCormick DA**. Ionic mechanisms underlying repetitive high-frequency burst firing in supragranular cortical neurons. *J Neurosci* 20: 4829-4843, 2000.

12. **Cohen I, Navarro V, Clemenceau S, Baulac M and Miles R**. On the origin of interictal activity in human temporal lobe epilepsy in vitro. *Science* 298: 1418-1421, 2002.

13. **Connors BW and Gutnick MJ**. Intrinsic firing patterns of diverse neocortical neurons. *Trends Neurosci* 13: 99-104, 1990.

14. **Contreras D and Steriade M**. Cellular basis of EEG slow rhythms: a study of dynamic corticothalamic relationships. *J Neurosci* 15: 604-622, 1995.

15. **Contreras D, Timofeev I and Steriade M**. Mechanisms of long-lasting hyperpolarizations underlying slow sleep oscillations in cat corticothalamic networks. *J Physiol* 494 (Pt 1): 251-264, 1996.

16. **Cragg BG**. The density of synapses and neurones in the motor and visual areas of the cerebral cortex. *J Anat* 101: 639-654, 1967.

17. **Crochet S, Chauvette S, Boucetta S and Timofeev I**. Modulation of synaptic transmission in neocortex by network activities. *Eur J Neurosci* 21: 1030-1044, 2005.

18. **Cudmore RH and Turrigiano GG**. Long-term potentiation of intrinsic excitability in LV visual cortical neurons. *J Neurophysiol* 92: 341-348, 2004.

19. **DeFelipe J and Farinas I**. The pyramidal neuron of the cerebral cortex: morphological and chemical characteristics of the synaptic inputs. *Prog Neurobiol* 39: 563-607, 1992.

20. **Desai NS, Rutherford LC and Turrigiano GG**. Plasticity in the intrinsic excitability of cortical pyramidal neurons. *Nat Neurosci* 2: 515-520, 1999.

21. **Dichter MA and Ayala GF**. Cellular mechanisms of epilepsy: a status report. *Science* 237: 157-164, 1987.

22. **Faber ES, Callister RJ and Sah P**. Morphological and electrophysiological properties of principal neurons in the rat lateral amygdala in vitro. *J Neurophysiol* 85: 714-723, 2001.

23. **Fisher RS, Webber WR, Lesser RP, Arroyo S and Uematsu S**. High-frequency EEG activity at the start of seizures. *J Clin Neurophysiol* 9: 441-448, 1992.

24. **Fujiwara-Tsukamoto Y, Isomura Y, Nambu A and Takada M**. Excitatory GABA input directly drives seizure-like rhythmic synchronization in mature hippocampal CA1 pyramidal cells. *Neuroscience* 119: 265-275, 2003.

25. **Galarreta M and Hestrin S**. Frequency-dependent synaptic depression and the balance of excitation and inhibition in the neocortex. *Nat Neurosci* 1: 587-594, 1998.

26. **Gray CM and McCormick DA**. Chattering cells: superficial pyramidal neurons contributing to the generation of synchronous oscillations in the visual cortex. *Science* 274: 109-113, 1996.

27. **Grenier F, Timofeev I and Steriade M**. Neocortical very fast oscillations (ripples, 80-200 Hz) during seizures: intracellular correlates. *J Neurophysiol* 89: 841-852, 2003.

28. **Gruner JE, Hirsch JC and Sotelo C**. Ultrastructural features of the isolated suprasylvian gyrus in the cat. *J Comp Neurol* 154: 1-27, 1974.

29. **Halasz P**. Runs of rapid spikes in sleep: a characteristic EEG expression of generalized malignant epileptic encephalopathies. A conceptual review with new pharmacological data. *Epilepsy Res Suppl* 2: 49-71, 1991.

30. **Heinemann U, Lux HD and Gutnick MJ**. Extracellular free calcium and potassium during paroxsmal activity in the cerebral cortex of the cat. *Exp Brain Res* 27: 237-243, 1977.

31. **Hille B**. *Ionic channels of excitable membranes*. Sunderland, Massachusetts: Sinauer Associates INC, 2001.

32. **Hirst GD, Johnson SM and van Helden DF**. The slow calcium-dependent potassium current in a myenteric neurone of the guinea-pig ileum. *J Physiol* 361: 315-337, 1985.

33. **Johnston D and Brown TH**. Control theory applied to neural networks illuminates synaptic basis of interictal epileptiform activity. *Adv Neurol* 44: 263-274, 1986.

34. **Katz B**. *The release of neuronal transmitter substances*. Springfield, Illinois: Thomas, 1969.

35. **Kotagal P**. Multifocal independent Spike syndrome: relationship to hypsarrhythmia and the slow spike-wave (Lennox-Gastaut) syndrome. *Clin Electroencephalogr* 26: 23-29, 1995.

36. **Lancaster B and Nicoll RA**. Properties of two calcium-activated hyperpolarizations in rat hippocampal neurones. *J Physiol* 389: 187-203, 1987.

37. **Macleod GT, Marin L, Charlton MP and Atwood HL**. Synaptic vesicles: test for a role in presynaptic calcium regulation. *J Neurosci* 24: 2496-2505, 2004.

38. **Massimini M and Amzica F**. Extracellular calcium fluctuations and intracellular potentials in the cortex during the slow sleep oscillation. *J Neurophysiol* 85: 1346-1350, 2001.

39. **McCormick DA, Connors BW, Lighthall JW and Prince DA**. Comparative electrophysiology of pyramidal and sparsely spiny stellate neurons of the neocortex. *J Neurophysiol* 54: 782-806, 1985.

40. **Neckelmann D, Amzica F and Steriade M**. Spike-wave complexes and fast components of cortically generated seizures. III. Synchronizing mechanisms. *J Neurophysiol* 80: 1480-1494, 1998.

41. **Nelson SB and Turrigiano GG**. Synaptic depression: a key player in the cortical balancing act. *Nat Neurosci* 1: 539-541, 1998.

42. **Nicoll RA**. The coupling of neurotransmitter receptors to ion channels in the brain. *Science* 241: 545-551, 1988.

43. **Niedermeyer**. Abnormal EEG patterns: epileptic and paroxysmal. In: *Electroencephalography: Basic Principles, Clinical Applications, and Related Fields*, edited by Niedermeyer E LdSFBM: Williams and Wilkins, 1999a, p. 235-260.

44. **Niedermeyer**. Epileptic seizure disorders. In: *Electroencephalography: Basic Principles, Clinical Applications, and Related Fields*, edited by Niedermeyer E LdSFBM: Williams and Wilkins, 1999b, p. 476-585.

45. **Pare D and Lang EJ**. Calcium electrogenesis in neocortical pyramidal neurons in vivo. *Eur J Neurosci* 10: 3164-3170, 1998.

46. **Pennefather P, Goh, J.W**. Relationship between calcium load and the decay of IAHP in bullfrog ganglion neurons. *Soc. Neurosci*, Abstr, 1988.

47. **Pennefather P, Lancaster B, Adams PR and Nicoll RA**. Two distinct Ca-dependent K currents in bullfrog sympathetic ganglion cells. *Proc Natl Acad Sci U S A* 82: 3040-3044, 1985.

48. **Rutecki PA**. Neuronal excitability: voltage-dependent currents and synaptic transmission. *J Clin Neurophysiol* 9: 195-211, 1992.

49. **Sah P**. Role of calcium influx and buffering in the kinetics of Ca(2+)-activated K+ current in rat vagal motoneurons. *J Neurophysiol* 68: 2237-2247, 1992.

50. **Sah P**. Ca(2+)-activated K+ currents in neurones: types, physiological roles and modulation. *Trends Neurosci* 19: 150-154, 1996.

51. **Sah P and Faber ES**. Channels underlying neuronal calcium-activated potassium currents. *Prog Neurobiol* 66: 345-353, 2002.

52. **Sah P and McLachlan EM**. Ca(2+)-activated K+ currents underlying the afterhyperpolarization in guinea pig vagal neurons: a role for Ca(2+)-activated Ca2+ release. *Neuron* 7: 257-264, 1991.

53. **Sah P and McLachlan EM**. Potassium currents contributing to action potential repolarization and the afterhyperpolarization in rat vagal motoneurons. *J Neurophysiol* 68: 1834-1841, 1992.

54. **Sammaritano M, Gigli GL and Gotman J**. Interictal spiking during wakefulness and sleep and the localization of foci in temporal lobe epilepsy. *Neurology* 41: 290-297, 1991.

55. **Sanchez-Vives MV and McCormick DA**. Cellular and network mechanisms of rhythmic recurrent activity in neocortex. *Nat Neurosci* 3: 1027-1034, 2000.

56. **Schwindt PC and Crill WE**. Amplification of synaptic current by persistent sodium conductance in apical dendrite of neocortical neurons. *J Neurophysiol* 74: 2220-2224, 1995.

57. **Schwindt PC, Spain WJ, Foehring RC, Stafstrom CE, Chubb MC and Crill WE**. Multiple potassium conductances and their functions in neurons from cat sensorimotor cortex in vitro. *J Neurophysiol* 59: 424-449, 1988.

58. **Shao LR, Halvorsrud R, Borg-Graham L and Storm JF**. The role of BK-type Ca2+-dependent K+ channels in spike broadening during repetitive firing in rat hippocampal pyramidal cells. *J Physiol* 521 Pt 1: 135-146, 1999.

59. **Simon NR, Manshanden I and Lopes da Silva FH**. A MEG study of sleep. *Brain Res* 860: 64-76, 2000.

60. **Steriade M**. Interneuronal epileptic discharges related to spike-and-wave cortical seizures in behaving monkeys. *Electroencephalogr Clin Neurophysiol* 37: 247-263, 1974.

61. **Steriade M and Amzica F**. Coalescence of sleep rhythms and their chronology in corticothalamic networks. *Sleep Res Online* 1: 1-10, 1998.

62. **Steriade M, Amzica F and Contreras D**. Cortical and thalamic cellular correlates of electroencephalographic burst-suppression. *Electroencephalogr Clin Neurophysiol* 90: 1-16, 1994a.

63. **Steriade M, Amzica F, Neckelmann D and Timofeev I**. Spike-wave complexes and fast components of cortically generated seizures. II. Extra- and intracellular patterns. *J Neurophysiol* 80: 1456-1479, 1998a.

64. **Steriade M and Contreras D**. Relations between cortical and thalamic cellular events during transition from sleep patterns to paroxysmal activity. *J Neurosci* 15: 623-642, 1995.

65. **Steriade M and Contreras D**. Spike-wave complexes and fast components of cortically generated seizures. I. Role of neocortex and thalamus. *J Neurophysiol* 80: 1439-1455, 1998.

66. **Steriade M, Contreras D and Amzica F**. Synchronized sleep oscillations and their paroxysmal developments. *Trends Neurosci* 17: 199-208, 1994b.

67. **Steriade M, Contreras D, Amzica F and Timofeev I**. Synchronization of fast (30-40 Hz) spontaneous oscillations in intrathalamic and thalamocortical networks. *J Neurosci* 16: 2788-2808, 1996.

68. **Steriade M, Nunez A and Amzica F**. Intracellular analysis of relations between the slow (< 1 Hz) neocortical oscillation and other sleep rhythms of the electroencephalogram. *J Neurosci* 13: 3266-3283, 1993a.

69. **Steriade M, Nunez A and Amzica F**. A novel slow (< 1 Hz) oscillation of neocortical neurons in vivo: depolarizing and hyperpolarizing components. *J Neurosci* 13: 3252-3265, 1993b.

70. **Steriade M, Timofeev I, Durmuller N and Grenier F**. Dynamic properties of corticothalamic neurons and local cortical interneurons generating fast rhythmic (30-40 Hz) spike bursts. *J Neurophysiol* 79: 483-490, 1998b.

71. **Steriade M, Timofeev I and Grenier F**. Natural waking and sleep states: a view from inside neocortical neurons. *J Neurophysiol* 85: 1969-1985, 2001.

72. **Storm JF**. Action potential repolarization and a fast after-hyperpolarization in rat hippocampal pyramidal cells. *J Physiol* 385: 733-759, 1987.

73. **Storm JF**. Potassium currents in hippocampal pyramidal cells. *Prog Brain Res* 83: 161-187, 1990.

74. **Szentagothai J**. The use of degeneration methods in the investigation of short neuronal connections. In: *Degeneration Patterns in the Nervous System*, edited by Singer MS, P. Amsterdam: Progress in Brain Research, Elsevier, 1965, p. 1-32.

75. **Tasker JG and Dudek FE**. Electrophysiology of GABA-mediated synaptic transmission and possible roles in epilepsy. *Neurochem Res* 16: 251-262, 1991.

76. **Thomson AM, West DC, Hahn J and Deuchars J**. Single axon IPSPs elicited in pyramidal cells by three classes of interneurones in slices of rat neocortex. *J Physiol* 496 (Pt 1): 81-102, 1996.

77. **Timofeev I, Bazhenov M, Sejnowski T and Steriade M**. Cortical hyperpolarization-activated depolarizing current takes part in the generation of focal paroxysmal activities. *Proc Natl Acad Sci U S A* 99: 9533-9537, 2002a.

78. **Timofeev I, Grenier F, Bazhenov M, Sejnowski TJ and Steriade M**. Origin of slow cortical oscillations in deafferented cortical slabs. *Cereb Cortex* 10: 1185-1199, 2000a.

79. **Timofeev I, Grenier F and Steriade M**. Spike-wave complexes and fast components of cortically generated seizures. IV. Paroxysmal fast runs in cortical and thalamic neurons. *J Neurophysiol* 80: 1495-1513, 1998.

80. **Timofeev I, Grenier F and Steriade M**. Impact of intrinsic properties and synaptic factors on the activity of neocortical networks in vivo. *J Physiol Paris* 94: 343-355, 2000b.

81. **Timofeev I, Grenier F and Steriade M**. Disfacilitation and active inhibition in the neocortex during the natural sleep-wake cycle: an intracellular study. *Proc Natl Acad Sci U S A* 98: 1924-1929, 2001.

82. **Timofeev I, Grenier F and Steriade M**. The role of chloride-dependent inhibition and the activity of fast-spiking neurons during cortical spike-wave electrographic seizures. *Neuroscience* 114: 1115-1132, 2002b.

83. **Timofeev I, Grenier F and Steriade M**. Contribution of intrinsic neuronal factors in the generation of cortically driven electrographic seizures. *J Neurophysiol* 92: 1133-1143, 2004.

84. **Timofeev I and Steriade M**. Low-frequency rhythms in the thalamus of intact-cortex and decorticated cats. *J Neurophysiol* 76: 4152-4168, 1996.

85. **Timofeev I and Steriade M**. Neocortical seizures: initiation, development and cessation. *Neuroscience* 123: 299-336, 2004.

86. **Topolnik L, Steriade M and Timofeev I**. Hyperexcitability of intact neurons underlies acute development of trauma-related electrographic seizures in cats in vivo. *Eur J Neurosci* 18: 486-496, 2003a.

87. **Topolnik L, Steriade M and Timofeev I**. Partial cortical deafferentation promotes development of paroxysmal activity. *Cereb Cortex* 13: 883-893, 2003b.

88. **Traub RD, Buhl EH, Gloveli T and Whittington MA**. Fast rhythmic bursting can be induced in layer 2/3 cortical neurons by enhancing persistent Na+ conductance or by blocking BK channels. *J Neurophysiol* 89: 909-921, 2003.

89. **Ward AA, Jr. and Schmidt RP**. Some properties of single epileptic neurons. *Arch Neurol* 5: 308-313, 1961.

90. **Xiong ZQ, Saggau P and Stringer JL**. Activity-dependent intracellular acidification correlates with the duration of seizure activity. *J Neurosci* 20: 1290-1296, 2000.